The Jordan Journal of Earth and Environmental Sciences (JJEES)

JJEES is an international peer-reviewed research journal, issued by the Deanship of Academic Research and Graduate Studies, the Hashemite University, in corporation with, the Jordanian Scientific Research Support Fund, the Ministry of Higher Education and Scientific Research.

EDITORIAL BOARD

Editor-in-Chief

Professor Abdul Rahim A. Hamdan
The Hashemite University

Editorial board

- **Professor Abdulkader M. Abed**
  University of Jordan
- **Professor Hani N. Khoury**
  University of Jordan
- **Professor Zuhair H. El-Isa**
  University of Jordan
- **Professor Sameh Gharaibeh**
  Yarmouk University
- **Professor Ahmad Abu Hilal**
  Yarmouk University
- **Professor Issa Makhlouf**
  The Hashemite University
- **Professor Tayel M. El-Hasan**
  Mu'tah University

THE INTERNATIONAL ADVISORY BOARD

- **Prof. Sayed Abdul Rahman,**
  Cairo University, Egypt.
- **Prof. Abdullah Al-Amri,**
  King Saud University, Saudi Arabia.
- **Prof. Waleed Al-Zubair,**
  Arabian Gulf University, Bahrain.
- **Prof. Ute Austermann-Haun,**
  Fachhochschule Lippe und Hoexter, Germany.
- **Prof. Ibrahim Banat,**
  University of Ulster, UK.
- **Prof. Matthias Barjenbruch,**
  Technisch Universitat Berlin, Germany.
- **Prof. Mohamed Boukhary,**
  Ain Shams University, Egypt.
- **Prof. Mohammad El-Sharkawy,**
  Cairo University, Egypt.
- **Prof. Venugopalan Ittekkot**.
  Center for Tropical Marine Ecology, Bremen, Germany.
- **Prof. Christopher Kendall,**
  University of North Carolina, U.S.A.
- **Prof. Elias Salameh,**
  University of Jordan, Jordan.
- **Prof. V. Subramanian,**
  Jawaharlal Nehru University, India.
- **Prof. Omar Rimawy,**
  University of Jordan, Jordan.
- **Prof. Hakam Mustafa,**
  Yarmouk University, Jordan.
- **Dr. Michael Crosby,**
  The National Science Board, National Science Foundation, Virginia, U.S.A.
- **Dr. Brian Turner,**
  Durham University, U.K..
- **Dr. Friedhelm Krupp,**
  Senckenberg Research Institute and Natural History Museum, Germany.
- **Dr. Richard Lim,**
  University of Technology, Australia.

EDITORIAL BOARD SUPPORT TEAM

Language Editor	**Publishing Layout**
Dr.Qusai Al-Debyan	MCPD. Osama AlShareet

SUBMISSION ADDRESS:

Professor **Abdul Rahim A. Hamdan**
Deanship of Academic Research and Higher Studies
Hashemite University, P.O. Box 330127, Postal Code 13133, Zarqa, Jordan.

Phone: +962-5-3903333 ext. 4151
E-Mail: jjees@hu.edu.jo , hamdan@hu.edu.jo

Hashemite Kingdom of Jordan

Hashemite University

Jordan Journal of Earth and Environmental Sciences

JJEES

An International Peer-Reviewed Scientific

Special Publication 2

http:// jjees.hu.edu.jo/

ISSN 1995-6681

JJEES

Jordan Journal of Earth and Environmental Sciences

Editorial Preface

It is my great pleasure to introduce the first special publication of the Jordan Journal of Earth and Environmental Sciences (JJEES), dealing with eight selected papers that have been presented in the International Conference on Materials in Jordan.

I have read the papers of this issue with lively interest, with real enjoyment, and with close attention and appreciation of its accurate and discreet coverage of materials in Jordan.

This special publication is intended to help the participants as well as colleagues in material sciences of different disciplines to work together on their common or interrelated problems and to use their work ideas and information presented at the conference. This document will be useful to many materials scientists.

Without the warm support and patient assistance of the editorial board this work could not have been completed. They cheerfully helped me in this publication.

Many special thanks go to MCPD. Osama Al-Shareet from the Computer Center, who prepared this special issue for the printer with great skill.

Editor-in-Chief,
JJEES,
Professor Abdul Rahim A. Hamdan,
Dept. of Earth and Environmental Sciences,
The Hashemite University,
Zarqa, Jordan.

The International Conference on Materials in Jordan
Humboldt Kolleg
9-11 April 2011

Conference Preface

The 1st International Conference on Materials in Jordan (ICMJ) was held in Amman between 4-6 March 2009 following the successful "Materials Workshop" organized by the Jordanian Club of Humboldt Fellows (JCHF) at Goethe Institute/Amman on 12.4.2008. The 2nd Materials Int. Workshop (Humboldt Kolleg) took place in Amman between 10-12 April 2010. Like other Kollegs, the 2nd Int Conf. on Materials in Jordan (Humboldt Kolleg) was held between 9-11 April 2011 with the main co-hosting universities being the GJU and PSUT.

This ICMJ was mainly organized by the JCHF in addition to a large body of national organizers involved: Jordan Atomic Energy Commission (JAEC), German-Jordanian University (GJU), Mu'tah University (MU), Yarmouk University (YU), Jordan University of Science and Technology (JUST), Al al-Bayt University (AaBU), University of Jordan (UJ), Hashemite University (HY). This participation reflects the interest and belief for the achievements to be an outcome of these activities. As a product of this conference and workshops several of our Ph.D. students are completing their studies abroad and scientists are enjoying joint research projects with Int. researchers.

The executive committee of the JCHF that organized the Conference consists of:
Prof. Dr Yaseen Al-Soud / Al al-Bayt University; Secretary General
Prof. Dr. Ahmad Al Ajlouni / JUST; Vice President
Prof. Dr. Marwan S. Mousa / Mu'tah University, President of JCHF

The leadership and guidance by HE Prof Dr. Khaled Toukan, Minister of Energy and Mineral Resources and chairman of the conference, valuable assistance by the GJU, scientific guidance by Dr Nelli Wanderka from Berlin, full support by HE the ambassador of Germany in Jordan Dr. Joachim Heidorn and the First Secretary and the Cultural Attachee of the Embassy Mr Carsten Fischer were all valuable for the success of the conference.

Prof. Dr. Wajih M. Owais Minister of Higher Education and Scientific Research (MoHESR) gave great support to the conference. The financial support by King Abdullah II for Development, Jordan Kuwait Bank, Jordan Ahli Bank, Abdul Hameed Shoman Foundation in addition to the crucial financial support from the Alexander von Humboldt Foundation in Germany enabled us to cover most of the financial expenses for the event. The conference co-hosting by PSUT and the support extended by its president were important to achieve goals of the conference.

The conference was patronized and opened by HE Prof. Dr. Wajih M. Owais MoHESR. The sessions were held at PSUT with attendance of 365 people. HE Prof. Dr. Khaled Toukan the chairman of the conference emphasized the importance that the conf. aims to open avenues of cooperation between academic research institutions, industry, scientific societies and governmental agencies.

Following the opening of the conference the Key Note Speaker Dr. Nelli Wanderka gave a scientific talk about the joint scientific work between Germany and Jordan titled “Modification of Mo-Si alloy microstructure by small additions of Zr”. This was followed by 11 sessions of talks and a poster session. The talks concentrated on modern techniques by Americans, Germans and other participating scientists. Geopolymers session was very interesting in addition to presentations on materials like Uranium, Zeolite, Kaoline, Zircon, Oil Shale, Potassium Chloride from the Dead Sea, natural materials in German industry, nanowire arrays, electron sources development, limestone Ash Mortars of castles in Jordan.

A full day of research on Pharmacy and Pharmaceutical materials was held with the Humboldtian Prof. Luay Rashan organizing that highly exciting day with wide participation from scientists coming from several countries like Jordan, Iraq, Czec, Germany, France Egypt, and Morocco.

The Jordanian National TV gave coverage of the opening, talks and Humboldt Kolleg. Most of the Jordanian newspapers and Petra News Agency covered the conference with articles, pictures and interviews.

It was an honor to the kolleg by dedicating the Conference to Dr. Gisella Janetzke, ex-deputy Secretary General of AvH Foundation after dedicated 30 years of service towards world friendship, cooperation and academic exchange. Dr Janetzke gave a talk about the foundation and held a session with scientists to explain means and ways to apply for the AvH fellowships. A fruitful working meeting was held on April 10th at the Marriot hotel Amman prior to the conference banquet, discussed means of strengthening cooperation. The meeting was attended by Dr. Janteske, Ms. Dine Hayat, Minister Prof. Wajih Owais, Minister Prof. Khaled Toukan, JCHF, DAAD, German Scientists, Germany Embassy, Presidents and Vice Presidents of Jordanian Public Universities. Following the conference, visits were arranged for delegations interested in joint collaborations with various Jordanian universities.

Prof. Dr. Marwan S. Mousa
Director of 2 ICMJ (Humboldt Kolleg)
President of the Jordanian Club of Humboldt Fellows
President of Jordanian Physics Society
Prof. of Materials
Dept. of Physics
Mu'tah University
Al-Karak, Jordan
email: mmousa@mutah.edu.jo, marwansmousa@yahoo.com

The International Conference on Materials in Jordan
9-11 April 2011
Princess Sumaya University For Technology
Amman, Jordan.

Conference Organizing Committee:

1- HE Prof. Dr. Khalid Toukan, Minister of Energy and Mineral Resources, Chairman of the Jordanian Atomic Energy Commission (Chairman of the Conference)
2- Prof. Dr. Labib Khadra, President of German Jordanian University GJU (Co-Chairman of the Conference).
3- Prof. Dr. Marwan S. Mousa, President of Jordanian Club of Humboldt Fellows (Director of the Conference)
4- Dr. Nelia Wanderka, Helmholtz-Center Berlin for Materials and Energy

Conference Advisory Committee:

1- Prof. Dr. Sultan Abu Orabi, President of Yarmouk Univ. (YU) (Humboldt Fellow)
2- Prof. Dr. Abdelrahim Hunaiti, President of Mu'tah Univ. (MU) (Humboldt Fellow)
3- Prof. Dr. Nabil Shawagfeh, President of Al al Bayt Univ. (AABU)
4- Prof. Dr. Issa Batarseh, President of Princess Sumaya Univ. for Technology (PSUT)
5- Dr. Khaled Shreideh, Sec. General of Higher Council for Science and Technology (HCST)
6- Prof. Dr. Abdul Rahim Hamdan, Vice President of Hashemite Univ. (HU)
7- Prof. Dr. Ziad Al-Saad, General Director of Jordan Dept. of Antiquaties (Humboldt Fellow)
8- Prof. Dr. Abdelhadi Soudi, President of Magreb Club of Humboldt Fellows, Rabat, Morocco (Humboldt Fellow)
9- Eng. Samir Abdul Rahim, Assistant GM – Plants Operational Manager, Jordan Abyad Fertilizers & Chemicals

Conference Scientific Committee:

1- Prof. Dr. Marwan S. Mousa (Mu'tah University)
2- Prof. Dr. Hani Nicola Khouri (Jordan University)
3- Prof. Dr. Abdul Rahim Hamdan (Hashemite University)
4- Prof. Dr. Nizar Abu Jaber (German-Jordanian University)
5- Prof. Dr. Ibrahim Abu Al-Jarayesh (Yarmouk University)
6- Prof. Dr. Abdul Haleem Wreikat (Jordanian Atomic Energy Commission)
7- Dr. Ned Xoubi (Jordanian Atomic Energy Commission)
8- Prof. Dr. Awni Hallak (Jordanian Atomic Energy Commission)
9- Prof. Dr. Khaled Khleifat (Mu'tah University)
10- Prof. Dr. Ahmad M Al-Ajlouni, Jordan University of Science and Technology
11- Prof. Dr. Yaseen Al-Sou'd (Al al-Bayt University)
12- Prof. Dr. Sami Mahmood Jordan University)
13- Prof. Dr. Eqab Rabei (Al al-Bayt University)
14- Prof. Dr. Sawsan Al-Oran (Jordan University)
15- Prof. Dr. Laila Abu Hassan (Jordan University)
16- Prof. Dr. Mahmoud Alawi (Jordan University)
17- Dr. Yaser Yousef (Yarmouk University)
18- Dr. Amjad Fahoum (Yarmouk University)
19- Dr. Khaldoun Tarawneh (Princess Sumaya Univ. for Technology)
20- Dr. Hussein Allaboun (Jordanian Atomic Energy Commission)
21- Dr. Laith Darabee (Jordanian Atomic Energy Commission)
22- Prof. Dr. Saed Dabaneh (Al Balqa Applied University and JNRC)
23- Prof. Dr. Tayel El-Hasan (Mu'tah University)
24- Prof. Dr. Mousa Abu Arabai (Jordan University of Science and Technology)
25- Prof. Dr. Mohammad El-Khateeb (Jordan University of Science and Technology)
26- Prof. Dr. Issa Makhlouf (Hashemite University)
27- Prof. Dr. Luay Rashan (Applied Science University)

28- Dr. Mousa Gougazeh, Tafila Technical University)
29- Dr Jamal Alali (Aqaba Petroleum for Oil Shale)
30- Dr Khalid Al-Nawayseh, Arab Potash Co.
31- Eng. Zeid Matouk (Abyad Fertilizers & Chemicals Co.)
32- Prof. Dr. Mufeed Batarseh (Mu'tah University)
33- Prof. Dr. Mahmoud Ajour (Philadelphia University)
34- Dr. Lamia El-Khouri (Yarmouk University)
35- Dr. Sherin Sarayreh (Al-Hussein Bin Talal University)
36- Dr. Bothina Hamad (Jordan University)
37- Prof. Dr. Mohamed AlShare (Mu'tah University)
38- Dr. Khaled Nawafleh (Mu'tah University)
39- Dr. Andreas Fischer (Feodor Lynen Research Fellow, Mu'tah University)
40- Mr. Cyrus Salimi Asl (DAAD Coordination Office in Jordan)

Conference Int. Scientific Committee:

1- Dr. Nelia Wanderka (Helmholtz-Center Berlin for Materials and Energy)
2- Prof. Dr. Thomas Kelly (Cameca, Madison, Wisconsin, USA)
3- Prof. Dr. Simon Ringer (University of Sydney, Australia)
4- Prof. Dr. Gregory Thomson (University of Alabama, USA)
5- Prof. Dr. Jan Wastiels (Vrije Univ. Brussel, Belgium)
6- Prof. Dr. Peter Langer (University of Rostock, Germany)
7- Prof. Dr. Frederic Danoix (University of Rouen, France)
8- Prof. Dr. Majda Sekkal-Rahal (University Sidi Bel Abbas, Algeria)
9- Prof. Dr. Mohamed Ellouze (Sfax University, Tunis)
10- Prof. Dr. Fawzi Lakrad (University Hassan II Casablanca, Morocco)
11- Prof. Dr. Hadef Redjem (University Oum El Bouaghi, Algeria)
12- Prof. Dr. Marian Jaskula (Jagiellonian University, Cracow, Poland)
13- Prof. Dr. Ibrahim Zeid (Monoufia University, Egypt)
14- Prof. Dr. Abdelaziz Khlaifat (Weatherford Oil Tool ME Ltd, Dubai, UAE)

Proceedings Guest Editors:

1- Prof. Dr. Marwan S Mousa (Mu'tah University) : marwansmousa@yahoo.com
2- Prof. Dr. Hani Nicola Khouri (Jordan University) : khouryhn@yu.edu.jo
3- Prof. Dr. Abdul Rahim Hamdan (Hashemite University): hamdan@hu.edu

JJEES

Volume 4, (Special Publication, Number 2), Jan. 2012
ISSN 1995-6681
Pages 1- 6

Jordan Journal of Earth and Environmental Sciences

Rehabilitation of Al-Shawbak Castle Using El-Lajjun Bituminous Limestone Ash Mortars and Plasters.

Nafeth A.Abdel Hadi[a,*], Monther A. Abdel Hadi[b]

[a] *Department. Of Civil Engineering ,Al Balqa Applied University*

[b] *Department. Of Civil Engineering,Amman Ahliyya University, E-mail: mabdelhadi@ammanu.edu.jo*

Abstract

Al-Shawbak castle mortars and plasters were characterized through physical, mechanical and chemical analysis. The studied masonry and plaster mortars have shown intensive weathering and erosion features, low compressive strength, and high absorption and disintegration behavior when soaked in water. Limy ash has been prepared from the El-Lajjun bituminous limestone by direct combustion at 950 ^{0}C in an attempt to rehabilitate Al-Shawbak castle. The ash has been mixed with sand and water to prepare self cementitious mortar material that gain strength at normal ambient temperature. The laboratory tests have been selected with respect to construction needs in various remedial works in archeological sites to replace weathered and eroded masonry and plaster mortars.

The limy ash mortar has similar color, chemical and mineralogical composition similar to the tested ancient mortar and plaster samples. The mortar has a higher compressive strength and resistively to disintegration under saturation conditions. The ash mortars could be used to rehabilitate various damaged archeological parts of AL-Shawbak Castle.

Keywords: Rehabilitation, Al-Shawbak Castle, El-Lajjun, Bituminous Limestone, Ash Mortars.

1. Introduction

Al-Shawbak castle, an important historical and archeological site, located in the southern part of Jordan (Fig. 1a) and built in the first half of the eleventh century at the Crusader time (Brown, 1988).). Random parts of the castle were subjected to sever damage over the past 800 years due to earthquakes, weathering processes, denudations and erosion, hence the castle became under immanent danger.

The creativity of the ancient cultures is reflected in the stability of the major parts of these ruins against weathering and earthquakes of various intensities over the past centuries (Amrat, 1992)

Natural sculpted limestone and dimension silicified limestone blocks of various sizes were used as building materials in long and high stable walls, arches, domes in addition to the other architectural features in the castle. Materials similar to the masonry and plaster mortars that were used during the construction of the castle could be prepared and used in recent remedial and restoration activities in Al- Shawbak castle.

Huge quantities of solid waste ash are expected to be produced through utilization of bituminous limestone as an energy source through direct combustion in thermal power stations.

Fig. 1a Location map shows Al Shobak area. (www.atlastours.net)

This ash can be utilized as a self cementitious material when mixed with water at normal ambient temperature and hence transferring the friable ash wastes into useful material in various construction activities. Various mortars utilizing limy ash and glass sand will be prepared from El-Lajjun oil shale deposit which is located 110 km southwest of Amman, Roman legionary camp (Parker, 1985), to be

---

[*] Corresponding author :e-mail: nafeth22@yahoo.com

compared with masonry and plaster mortars that were used during the construction of the castle.

All studies conducted so far were limited to the description of the monument ignoring the intrinsic value of its restoration.

The following study aims to rehabilitate Al-Shawbak castle using limy ash mortars. It concentrates on determining the physical, chemical, and mechanical properties of the masonry and plaster mortars that were used during the construction of the castle. The results are expected to reveal the possibility of utilizing the limy ash from El-Lajjun area as a self cementing material in restoration and remedial work in the weathered, eroded and collapsed portions of the castle.

2. The studied Area

Al-Shawbak Castle is a Crusader, Ayyubid, Mamluk castle of the 12 th and 13 th centuries, located in southern Jordan, 120 Km. south of Karak and 35 km. north of the fabulous Nabataean city of Petra. In 509 A.H/ 1115 AD Baldwin I, founder of the Latin kingdom of Jerusalem, led a major expedition into the region south east of the dead sea. He crossed Wadi Araba and marched to the fertile, wooded district of Al-Shawbak. There a top a steep mountain overlooking a well-watered valley, Baldwin erected a huge castle, which he named " la Carc de Montreal") (fig. 1b).

Fig. 1b. Al-Shoubak Castle, general view.

The construction of the castle of Al-Shawbak, along with smaller ones in and around Petra, al-Habis and Wa'airah, gave the Crusaders a loose control over the territory between the Dead Sea and the Gulf of Aqaba, and had the further advantage of hindering both the commercial and military connection between Syria, Egypt and the Hejaz. Al-Shawbak fell to the soldiers of Saladin in 584 A.H / 1188 A.D. And was refortified several times by both the Ayyubids (1174-1250) and the Mamluks (1250-1517). The castle was occupied throughout the late Ottoman period (18th -19th centuries) (Brown, 1988)

Considerable remains of all these periods fill the interior numerous Arabic inscriptions in Naskhi (cursive) script record the various reconstructions of the castle.

3. Materials and Methods

Random mortar samples from different locations in the castle where collected. fig. (2) illustrates the sample locations. Whitish, grayish and reddish mortars were used in ancient building activities.

a-Wall mortar(northern part)
b-Arch mortar
c- wall mortar(southern part)
d-Entrance mortar

Fig. 2.The sampling sites of mortars from Al-Shoubak Castle

The samples were labeled M1...M17 (Table 1)

Table 1.Physical, mechanical and total dissolved salts for the mortar samples

Sample No.	T.D.S Mg/l	Color	SG	Absorption %	Comp. strength Kg/cm2	Gradation %		
						Sand	Silt	clay
M1	160	Yellow	2.02	21.70	-	81.6	13.1	5.3
M2	112	White	2.10	29.04	-	62.6	31.6	5.8
M3	367	=	1.80	41.07	12.3	66.7	23.3	10
M4	2730	=	1.62	22.02	-	61.3	26.5	12.2
M5	4610	Grey	2.07	35.11	15.6	61.9	27.3	10.8
M6	1250	White	1.91	40.93	22.1	52.2	31	16.8
M7	8256	=	1.71	47.42	29.29	36.4	57.8	5.8
M8	1148	=	1.88	43.48	19.29	82	14	4
M9	-	=	1.95	38.39	-	44.2	49.9	5.9
M10	-	=	1.85	35.68	37.83	54.1	37.3	8.6
M11	-	Grey	1.89	37.08	18.53	54.1	37.3	8.6
M12	-	White	2.08	39.27	18.78	76.7	15.2	8.1
M13	120	White	1.70	45.30	6.12	73.9	17	9.1
M14	-	Grey	1.91	44.12	-	69.1	21.6	9.3
M15	-	White	2.08	38.99	5.8	55.1	38.6	6.3
M16	-	Grey	1.65	42.46	-	-	-	-
M17	-	White	2.16	36.10	-	47.4	39.3	13.3

Red, brown, gray mortar samples were collected as slices from some locations in which these mortars were used as a plaster. The samples were labeled P1, P2, P3, P4, P5, and P6 (Table 2).

Table 2. Physical, mechanical and total dissolved salts for plaster samples

Sample No.	Color	Specific Gravity	Absorption %	Porosity %	Gradation %		
					Sand	Silt	Clay
P1	White	2.35	17.86	29.5	-	-	-
P2	Red & white	2.21	23.06	33.8	-	--	--
P3	Brown	-	-	--	-	-	-
P4	White-Brown	-	-	--	7.8	50.2	42
P5	Grey	1.95	35.7	41.0	-	-	-
P6	Creamy-white	1.86	17.10	24.0	-	-	-

The thickness of the ancient mortars is variable and range from 2-4 cm. It was very difficult to get enough bulk samples to determine the compressive and tensile strength on standard dimensional samples. Therefore, Point Load

Strength Index was used to estimate the compressive strength of some bulk ancient mortars.

Various mortars utilizing limy ash from El-Lajjun area and glass sand were prepared. These mortars were analyzed using necessary chemical, mineralogical and physical testing. Porosity, specific gravity, moisture content, compressive strength, and absorption tests were carried out for the ancient and prepared mortars. X-ray diffraction, X-ray fluorescence were used to determine the mineralogical and chemical composition of ancient and prepared ash mortars.

The physical and mechanical properties of the prepared ash-sand mortars were determined using standard cubic samples of 5x5x5 cm according to (ASTM C109. 1999). Curing is carried out at laboratory temperature under successive wetting and drying conditions to determine the compressive strength at 28 days. The analyses were carried out at the Department of Civil Engineering; Al- Balqa Applied University and the Natural Resources Authority, Amman.

A bulk representative sample of about 100 kilograms was collected from various outcrops from El-Lajjun deposits.

The sample was crushed using a jaw crusher to obtain bituminous limestone aggregates of 9 mm nominal size particles. The whole aggregates were mixed and combusted 925 ^{0}C by using an automatically controlled electrical muffle furnace.

The sample was allowed to cool down to the ambient temperature (30 ^{0}C) and then was grounded under dry conditions to obtain the possible minimum grain size. Small ball mills and Los Angles machine were used. The moisture content of the combusted ash samples was checked directly after cooling and was found to be around 0.2%. The fine ash (nominated as S1) was filled immediately in tight plastic bags for further trial mixes of ash-sand mortars according to (ASTM C 109, 1999).

The chemical composition of the ash samples is clearly dependent on the original composition of the parent bituminous limestone and the temperature of combustion (Abdul Hadi et al., 2007).

Glass sand and tuff were mixed with variable percentages with S1 ash sample. The ash-glass sand mixtures are designated as S1-1, while S1-T is ash-tuff mixtures.

The various ash S1-glass sand and S1-tuff were tested at variable ash content (mention these percentages) and different curing periods (mention them also); the following tests were carried out according to the indicated standards:

1. Density - (ASTM C 29, 2003).
2. Specific gravity and absorptions (ASTM C128, 2007) .
3. Grain size analysis (ASTM C136, 2006)
4. 4. Compressive strength of hydraulic cement mortars (ASTM C109, 1999).

4. Results and Discussion

4.1. Physical Properties of Ancient Mortar

The tested ancient mortar has white, cream, gray, and yellow colors. The apparent specific gravity varies between 1.62 and 2.07. Some samples have shown a very high water absorption value up to 47%. Compressive strength of the tested mortar is estimated using the point load strength index test because it is not possible to get standard testing samples dimensions. The compressive strength values ranged from 5.8 Kg/cm^2 to 37.83 Kg/cm^2. Some samples have shown complete disintegration when immersed in water to determine absorption, and hence the compressive strength is not determined for these samples. The disintegrated samples were dried and sieved. The ancient mortars are composed of sand, silt and clay fractions. The weight percent of these ingredients varies from one sample to another. Total dissolved salts (TDS) have revealed that the salt content is very high in some samples as M5 and M7 (Porosity was measured and have shown a random pattern. The results of grain size distribution and total dissolved salts for the tested mortar samples are given in table (1).

4.2. Mineralogical and Chemical Composition of Ancient Mortars

The X-ray diffraction results are given in table (3).

Table . 3.X-ray diffraction results of the mortar samples

Sample No.	Sample type	Quartz	Calcite	Gypsum	Bassanite
M1	Mortar	-	***	**	*
M2	=	*	***	**	*
M3	=	*	***	*	*
M4	=	*	***	**	*
M5	=	*	***	*	-
M6	=	*	***	*	*
M7	=	*	***	**	*
M8	=	*	***	**	*
M9	=	*	***	*	-
M10	=	*	***	-	-
M11	=	*	***	*	-
M12	=	*	***	**	-

The results have indicated that calcite as the major constituent. Gypsum, quartz and bassanite as minor constituents. Moreover, the X-ray fluorescence results have shown that CaO is the major oxide while other oxides as Al_2O_3, Fe_2O_3, K_2O, Na_2O, and MgO are minor or absent as shown in table(4).

Table . 4. X-ray fluorescence results of the tested mortar

Sample No.	Sample type	SiO_2 %	Al_2O_3 %	Fe_2O_3 %	MgO %	K_2O %	Na_2O %	CaO %	L.O.I %
M1	Mortar	3.61	0.12	0.39	0.01	1.77	0.29	50.4	43.3
M2	=	3.44	0.11	0.39	0.01	1.94	0.19	50.4	43.5
M3	=	3.32	0.12	0.37	0.01	1.97	0.15	50.0	44.0
M4	=	3.41	0.20	0.43	0.01	1.99	0.23	49.4	44.2
M5	=	6.10	0.29	0.81	0.67	4.73	0.45	43.5	43.4
M6	=	3.44	0.11	0.44	0.01	1.79	0.21	49.7	44.2
M7	=	3.37	0.12	0.40	0.01	2.16	0.61	49.8	43.4
M8	=	3.52	0.15	0.39	0.01	1.91	0.01	49.6	44.3
M9	=	6.17	0.32	1.05	0.45	4.68	0.33	43.6	43.3
M10	=	3.98	0.06	0.50	0.01	4.77	0.01	45.6	44.9
M11	=	6.21	0.37	0.75	0.49	4.81	0.20	43.1	43.9
M12	=	6.21	0.37	0.75	0.49	4.81	0.20	43.1	43.9

Some of mortar samples were divided into two portions, one was dissolved in 0.1 HCl solutions and the other portion was dissolved in distilled water.

The soluble components in 0.1 HCl solutions are given in Table (5), and indicate that CaO is the major soluble oxide.

Meanwhile, the dissolved ions for the soaked disintegrated mortar and plaster samples in distilled water are given in Table (6), and shows that Ca, SO_4 and CO_2 are the most soluble components.

Table. 5. Soluble ions and oxides in 0.1 HCl solution.

Sample No.	Type of Material	0.1 HCL soluble oxides WT. %					
		Al_2O_3	Fe_2O_3	CaO	MgO	K_2O	Na_2O
M1	Mortar	0.12	0.01	19.60	0.30	0.72	0.59
M2	=	0.11	0.01	26.60	0.31	0.84	0.59
M3	=	0.12	0.01	19.60	0.31	0.72	0.59
M4	=	0.20	0.01	18.20	0.29	0.72	0.56
M5	=	0.29	0.02	18.20	0.71	2.70	1.20
M6	=	0.11	0.01	18.20	0.25	0.84	0.56
M7	=	0.12	0.01	19.60	0.31	0.72	0.59
M8	=	0.15	Nil	18.20	0.25	0.84	0.55
M9	=	0.32	0.01	16.80	0.64	2.60	1.20
M10	=	0.06	Nil	18.20	0.44	2.60	1.20
M11	=	0.14	0.01	19.60	0.36	2.70	1.20
M12	=	0.16	0.01	16.80	0.30	06.0	0.56

Table. 6.Distilled water soluble ions of the mortar samples.

Sample No	Type of Material	Na %	K %	Ca %	Mg %	Cl^- %	SO_4- %	CO_2 %
M1	Mortar	0.30	0.87	3.60	0.24	0.71	3.55	31.08
M2	=	0.30	0.90	3.26	0.48	1.07	3.55	30.59
M3	=	0.30	0.85	4.20	0.60	1.07	4.22	28.13
M4	=	0.32	0.90	4.00	0.18	1.07	3.74	27.15
M5	=	0.80	2.42	1.30	0.36	1.42	1.63	30.10
M6	=	0.32	0.92	2.78	0.66	1.07	3.07	31.41
M7	=	0.25	0.55	2.43	0.14	1.42	5.09	26.99
M8	=	0.30	0.95	1.50	0.31	1.42	4.61	31.41
M9	=	0.84	1.90	0.48	0.48	0.75	1.44	29.95
M10	=	0.95	2.10	0.72	0.5	0.82	1.92	30.0
M11	=	0.99	2.2	0.68	.53	1.53	1.63	30.8
M12	=	0.36	1.48	3.52	0.24	0.78	3.74	30.70

4.3. Ash as a Mortar and Plaster in Remedial work

The chemical composition of S1 ash sample is given in Table (7). The sample is compared with the Ordinary Portland Cement (OPC).

Table. 7. Chemical composition of S1 ash sample and standard OPC.*

Oxide Wt. %	SiO_2	Al_2O_3	Fe_2O_3	CaO	MgO	P_2O_5	Na_2O	TiO_2
S1 ash (950 °C)	25.30	2.35	137	45.21	1.63	5.47	0.85	0.14
OPC	23	4	2	64	2	-	-	-

*Analysis was done using XRF technique.

The physical properties of the ash sample S1 are given in Table (8). The chemical composition (high CaO and relatively high SiO2 content) and physical characteristics of S1 ash sample enables the use of ash as a self-cementing material.

Table. 8.Physical properties S1 ash.

Ash type	Specific gravity ASTM D 854-05	Moisture content %	Bulk density g/cm^3
S1	2.48	0.9	1.13

Ash, sand size crushed tuff and glass sand, are used in various ash-mortar mixtures.

The physical properties for the used raw materials are given in table (9).

Table. 9. properties of tuff and glass sand .

Material	Specific gravity	Absorption %	Passing #200 sieve %
Tuff fractionfraction	2.6	4.0	50
Glass sand	2.56	1.8	4

According to ASTM standards, the S1 ash sample has a lower pozzolanic content than both classes F and C ash and a very high CaO content relative to the ASTM classification. This indicates that the El-Lajjun ash can be used efficiently in some proper aspects other than that indicated for both fly ashes of type F or type C in the international standards. The production of various construction materials that can fulfill the international standards in which OPC can be substituted with proper percentages of the self-cementation ash was discussed by (Leonard and Baily, 1982). Although the El-Lajjun ash is not complying with the classification proposed by (Ferguson and Levorson, 1999), however, the S1 samples have a unique chemical composition that is characterized by its very high CaO (Abdul Hadi et. al., 2007). Sampling and testing procedures were carried out following (ASTM C109, 1999) for testing compressive strength of hydraulic cement sand mortar.

4.4. Engineering Characteristics of the Ash

All standard testing for strength determination of ash as a self-cementing material has shown a high stability. No minor features of disintegration or disturbance of the prepared samples during the curing stage in water at normal ambient temperature (28 C^0) were observed. On the contrary of normal soil behavior, it could sustain under saturation conditions. On the other hand, ash behaves as cementitious material that has the possibility to gain strength under normal curing time and conditions as the other different types of cements. This is confirmed through the compressive strength results of standard 5x5x5 cm cubic samples. The compressive strength results at 7, 28, and 56 days for the S1, S1 and S3 samples are given in table (10).

Table. 10. Compressive strength results of S1, S1 and S3 ash samples.

Mix designation	Glass sand (g)	Ash (g)	Water (g)	Density g/cm^3	7 days strength kg/cm^2	28 days strength kg/cm^2	56 days strength kg/cm^2
S1-1	1375	500	560	1.87	20.4	55.2	68.3
S1-1	1375	500	560	1.88	18.6	53.9	64.4
S1-1	1375	500	560	1.86	19.2	56.8	65.9

The average strength builds up at 7, 28 and days for the S1 ash sample has shown an increasing trend with increasing the curing period. The strength buildup in S1 ash mixtures is due to the chemical reactions that take place under the dominant ambient temperature. The addition of water under surface normal conditions would lead to the following hydration reactions:

$CaO+H_2O \rightarrow Ca(OH)_2$ (Portlandite) (1)

$SiO_2+Ca(OH)_2+H_2O \rightarrow CaSiO_2.2H_2O$ Calcium Silicate Hydrate (CSH) (2)

$SiO_2+Al_2O_3+Ca(OH)_2+H_2O \rightarrow CaSiO_2.Al_2O_3.H_2O$ Calcium Aluminates Hydrate (CAS) (3)

The compressive strength results of ash glass sand mortars have shown that the compressive strength at 7 days is low when compared with the 28 days results, this is related to the longer curing time which gave the opportunity to the ash alkalis to react with the silica to form extra cementitious matrix.

The strength increment from 28 days to 56 days is considered minor, this is due to the continuous decreasing in the free CaO content in the mix and hence the parallel decrease in the pH of the mixture which is considered an important factor that controls the rate and intensity of the ash-alkalis-silica reaction.

The compressive strength results for mortars made of S1 ash mixed with different ratios of ground tuff are summarized in table (11). The results show an ascending trend for S1 ash-tuff when mixing ratio is (1:1). The compressive strength results of S1-tuff mortars have shown higher strength than S1- glass sand mixtures. This is an expected result due to relatively high concentrations of the pozzolanic part (Al_2O_3, Fe_2O_3 and SiO_2 in the tuff sample which reacts with the alkaline part of the used ash. Such a reaction produces a self-cementing material that gains strength gradually with increasing curing time.

Table. 11.Compressive strength of S1 ash-Tuff mortars.

Mix designation	Tuff sand (g)	Ash type	Ash Wt(g)	Density g/cm^3	7 days strength kg/cm^2	28 days strength kg/cm^2	56 days strength kg/cm^2
S1-T-200	500	S1	1000	1.85	19	57	63
S1-T-200	500	S1	1000	1.86	20.5	58	62.5
S1-T-200	500	S1	1000	1.85	18	59.3	61
S1-T-100	500	S1	500	1.87	21.2	60.5	69.4
S1-T-100	500	S1	500	1.86	22	59.2	72.1
S1-T-100	500	S1	500	1.85	24.1	63	71

4.5. *Comparison between Ash as a Mortar and Plaster*

The ancient masonry and plaster mortars used in Al-Shawbak castle are very weak, sometimes friable even under dry conditions. This is revealed from the low compressive strength results using the Point Load Strength Index method Table (1). The tested samples showed high absorption values due to their high porosity. The high porosity may be a result of dissolution of gypsum and or bassinite through long term chemical weathering.

The ancient mortar is composed mainly of calcium oxide with minor gypsum and quartz. Bassanite crystals have appeared in some samples in small amounts as revealed by X-ray diffraction analysis. Poor bonding in the tested mortar and plaster samples was reflected from disintegration when soaked in water. The total dissolved salts (TDS) for the disintegrated samples have indicated that the TDS value is ranging from 112 mg/L as in M1 sample to very high value of 12250 mg/L in the M6 sample.

The mineralogical and chemical composition of the tested ancient plaster and masonry have indicated that calcined mortars was used (direct combustion of carbonaceous rocks in the vicinity of the castle). Gypsum was added to calcium oxide and mixed with water to produce the mortars.

The low strength of these mortars indicates that these mortars were not used as a bonding agent between the built stone blocks. The masonry mortar was used to level the top of the irregular surfaces of hard limestone and silicified limestone blocks.

Weathering and erosion of the mortar due to wet and dry climates made the built blocks unstable under dead loads specially when external disturbances resulted by strong winds or vibrations caused by the earthquakes.

The bituminous limestone ash mortar is similar in color and composition to the tested ancient mortar and plasters samples, but it has higher compressive strength and resistively to disintegration under saturation conditions. Therefore, the ash mortars could be used to rehabilitate parts of the archeological features at AL-Shoubak castle.

El-Lajjun bituminous limestone ash has revealed a self cementitious behavior for the various prepared samples. The free lime content of fly ash contributes to self-hardening (Yudbir and Hunjo, 1991). The ash sample S1 is essentially composed of CaO. The alkali content which is presented by CaO, and the pozzolanic content is presented by (SiO_2 +Al_2O_3+ Fe_2O_3), and the variable content of SO_3 was found in both the ash sample and OPC raw material. The strength buildup in all the ash samples is related to the setting reactions of lime (CaO) with the pozzolanic constituents to produce calcium silicate hydrate (CSH) and calcium aluminates hydrate (CAH). High pH solution due to CaO hydration is highly reactive with amorphous Al-Si rich phases at normal room temperature.

The hydration products of the S1 as identified by the XRD technique are portlandite, ettringite, calcium silicate hydrate and calcium aluminum hydrate. The reactions are not spontaneous and are time dependent. Curing period of 28 days and more has influenced the compressive strength results. High compressive strength values were obtained with intact samples indicating no disintegration features under fully saturated conditions. All hydrated samples have shown a similar behavior to the hydrated OPC products but with lower compressive strength.

The compressive strength of the S1 mortar is 20.4, 55.2 and 68.3 kg/cm^2 at 7, 28 and 56 days respectively. Ash concrete mixes must be properly cured due to slow strength development, and hence moisture must be retained in the concrete for longer period of time (ACI, 1996).

Portlandite Ca $(OH)_2$ plays an important role in the setting reaction. Portlandite reacts with silicates and aluminum rich phases to form insoluble compounds which contribute to the strength formation (pozzolanic reactions). Excess portlandite reacts with atmospheric CO_2 to precipitate calcium carbonate that helps in strengthening the product after aging (Khoury and Nassir, 1982; and Khoury, 1993).

5. Conclusions

The study shows the suitability of bituminous limestone ash as self cementitious material in rehabilitation works of all archeological monuments in Jordan.

Utilization of ash in remedial works has advantageous characters as color, higher compressive strength and resistance to disintegration compared with old used masonry and plaster mortars in historical places.

References

[1] Abdul Hadi, Nafeth., Khoury, H., and Kharabsheh, M (2008): Utilization of Bituminous Limestone Ash from EL-LAJJUN Area for Engineering Applications. Acta Geotechnica 3:139-151.

[2] ACI 211. 4R. (2003). "Guide for Selecting Properties for High-Strength Concrete with Portland cement and Fly Ash," ACI Manual of Concrete Practice, Part 1. American Concrete Institute, Detroit, Michigan.

[3] Amrat, A. F., 1992 Seismic hazard in Jordan . Jordan Seismological Observatory “Earthquakes in Jordan and adjacent areas”, Amman, Jordan. Bull. 24, 8-18.

[4] ASTM C109. (1999) Standard Test Method for Compressive Strength of Hydraulic Cement Mortars (Using2-in. or (50-mm) Cube Specimens), ASTM International.

[5] ASTM C29/C29M-97 (2003). Standard Test Method for Bulk Density ("Unit Weight") and Voids in aggregates, ASTM International.

[6] ASTM C136. (2006). Standard Test Method for Sieve Analysis of Fine and Coarse Aggregates. ASTM International.

[7] ASTM C 128. (2007). Standard Test Method for Density, Relative Density (Specific Gravity), and Absorption of Fine Aggregate ASTM International.

[8] Brown, R. M., (1988) « Report of the 1986 Excavations: Late Islamic Shobak », in ADAJ*, 32, . 225 - 245.*

[9] Ferguson G., and Levorson, S. M., (1999). Soil and Pavement Base Stabilization with Self-Cementing Coal Fly Ash. American Coal Ash Association International. Alexandria, Virginia.

[10] Leonards, G. A. and Bailey, B., (1982). Pulverized Coal Ash as Structural Fill, J. of Geotech. Engineering Div. ASCE, 108, 517–531.

[11] Khoury, H., and Nasser, S., (1982). A Discussion of on the Origin of Daba-Siwaqa Marble, Dirasat, 9:55-66.

[12] Khoury, H., (1993). Mineralogy and Isotopic Composition of the Metamorphic Rocks in the Bituminous Limestone of the Maqarin Area, Jordan, Dirasat vol. 20 B, number 2.

[13] Parker, S. Thomas, (1985). Romans and Saracens. A history of Arabian frontier. New York.

[14] Yudbir, K., and Honjo, Y., (1991). Applications of Geotechnical Engineering to Environmental Control. Ninth Asian Regional Conf., Bangkok, 2, 431–469.

[15] www.atlastours.net

JJEES

Volume 4, (Special Publication, Number 2), Jan. 2012
ISSN 1995-6681
Pages 7- 14

Jordan Journal of Earth and Environmental Sciences

The Effect of Chemical and Thermal Treatments on the Buffering Capacity of Phillipsite Tuff

Bassam El-Eswed[a,*] , Rushdi I. Yousef[b]

[a] *Zarka University College, Al-Balqa Applied University, P.O. Box 313, Zarka, Jordan. Telephone: 0799952202*

[b] *Associate professor, Chemistry Department, Faculty of Science, Preparatory Year Program,*

King Faisal University, P.O. Box. 380, Al-Ahsaa 31982. Saudi Arabia.

Abstract

Phillipsite tuff samples from Jebal Aritayn (Jordan) was treated chemically by acid, base, and salt and thermally at 200 and 400 **°C**. Both treated and untreated phillipsite samples were titrated with HCl and NaOH. The potentiometric titration curves showed that Jordanian phillipsite tuff exists in the base form (pH 8.5) and thus has a remarkable buffering capacity toward H^+. The effect of chemical and thermal treatments on the buffering capacity of zeolite was studied by employing a simple model. The model enables estimating the pK_a values and the acid sites densities for zeolite samples. Depending on the pK_a values of buffering regions and relative to what was reported in literature, it was concluded that the aluminosilicate sites ($>SOH_2^+$ and $>SOH$, $>S$ = Al or Si) as well as the associated silicates, carbonates and bicarbonates of Al, Mg, Ca, and Fe are responsible for the buffering behavior of phillipsite tuff samples. It was also clear that the buffering capacity of phillipsite tuff was reduced by treatment with salt (NaCl), acid (HCl), and base (NaOH). On the other hand, the buffering capacity of phillipsite tuff was enhanced by thermal treatment at 400 °C.

Keywords: Phillipsite Tuff; Chemical Treatment; Thermal Treatment; Buffering Capacity; Acidity and Basicity.

Abbreviations

ZW: Jordanian phillipsite tuff washed with distilled water.

ZS: Jordanian phillipsite tuff treated with NaCl.

ZA: Jordanian phillipsite tuff treated with HCl.

ZB: Jordanian phillipsite tuff treated with NaOH.

ZT200: Jordanian phillipsite tuff heated to 200 °C.

ZT400: Jordanian phillipsite tuff heated to 400 °C.

x and y: The amounts (mol/g) of zeolite sites in the deprotonated and protonated forms, respectively.

t: The amount of H^+ (mol/L) added.

$K`$*:* Acid dissociation constant.

$[\mathrm{Site}]_t$: Site density (mol/g) of buffering region belongs to K`.

SSR: The sum of square residual.

1. Introduction

Acidification of Earth's terrestrial and oceanic biospheres is now receiving growing attention. This acidification is due to two anthropogenic sources. The first is land acidification, which is caused by nitric and sulfuric acid. The second is ocean acidification, which is due to storage of CO_2 released by human activities (Turley and Scholes, 2009; Bouwman et al, 2002; Unlu *et al.*, 1999).

As a response to the problem of acidification, scientists have to develop their knowledge about the acid-base properties of natural minerals. One of the most important natural minerals is zeolites group, which has a continuous conjugated network of SiO_4 and AlO_4 tetrahedra. Adjacent tetrahedra are linked at their corners via a common oxygen atom, which result in an inorganic macromolecule with structurally distinct three-dimensional framework (Weitkamp, 2000). Zeolites acidity arises from the substitution of Si^{4+} by Al^{3+}. This substitution creates a negative charge that requires a proton (or another positive ion: Na^+, K^+, Mg^{2+}, Ca^{2+}, etc.) to be balanced (Chu and Chang, 1985; Stoyanov *et al.*, 2008).

The acid-base properties of zeolites are also very important in determining their catalytic activity (Weitkamp, 2000) and their adsorption behavior toward pollutants (Yousef and El-Eswed, 2009). The satisfactory application of surface complexation models to describe the adsorption of metal ions onto clays and minerals is limited by the availability of information about the surface acid sites density of these materials (Goldberg, 1991, 1995). The acidity of synthetic zeolites has been extensively studied because of its importance in catalysis applications. Numerous techniques have been devoted to the investigation of the nature, strength, and distribution of the acid sites in synthetic zeolites. The methods frequently employed have induced ^1H MAS NMR (Pfeifer *et al*, 1985), IR analysis of the O-H vibrations and the

---

[*] Corresponding author. Email: bassameswed@bau.edu.jo, bassameleswed@yahoo.com..

deformation features of probes (Ward, 1976), temperature-programmed desorption of adsorbed basic molecules (Karge and Dondur, 1990; Karge *et al*, 1991), titration of acid sites in aprotic solvents (Tanabe, 1970) and microcalorimetric measurements of differential heats of adsorption of basic molecules on acid sites (Chen *et al*, 1992; Jozefowicz *et al*, 1994). Base like pyridine, ammonia, and *n*-butylamine are commonly used in the characterization of the acidity of catalyst. In the determination of the zeolites acidity it is considered that the basic molecules enter the zeolite channels to react with acid sites and the number of acid sites is calculated from the amount of base required to saturate the surface (Ghosh and Curthoys, 1983). To the best of our knowledge, there is no reported study on the acid–base properties (pK_a and acid sites density) of natural zeolites depending on potentiometric titration with H^+ and OH^-. A mere observation was made by Wingenfelder *et al* (2005), who concluded from titration of natural zeolite (clinoptilolite) with HNO_3 that zeolite has a buffering capacity.

In the present work, the Jordanian phillipsite tuff was chemically treated with salt (ZS), acid (ZA), and base (ZB) and thermally treated at 200˚C (ZT200) and at 400 ˚C (ZT400). Both treated (ZS, ZA, ZB, and ZT) and untreated (ZW) zeolites were titrated with HCl and NaOH solutions. A simple model was derived for estimating the acid sites densities ($[\text{sites}]_t$) of zeolite samples and their acid dissociation constants (p$K`_a$). Relative to p$K`_a$ values reported in literature, the obtained p$K`_a$ values of zeolite samples (ZW, ZS, ZA, ZB, ZT200 and ZT400) were assigned and thus the effect of treatment on the buffering capacity was evaluated.

2. Materials and Methods

2.1. Pretreatment of Phillipsite Tuff and Characterization (Yousef and El-Eswed, 2009)

The preparation and characterization of Jordanian phillipsite tuff were reported elsewhere (Yousef and El-Eswed, 2009). Briefly, the phillipsite tuff (from north–east Jordan deposit in Jabal Aritayn area) was crushed using Jaw crusher, homogenized, and sieved to different particle size portions. A sample of the particle size 500–1000 µm was washed twice with distilled water and dried in an oven (Thermo Lab Industries, HO 900D) at 110-120°C. The XRD pattern of the dried phillipsite tuff showed the characteristic peaks of phillipsite. The chemical composition of this tuff obtained from XRF analysis was SiO2 42.01, Al2O3 14.10, Fe2O3 11.34, MnO2 0.33, MgO 10.33, CaO 8.42, TiO2 2.15, K2O 0.93, Na2O 1.92, P2O5 0.43, L.O.I. 8.04 (wt %).

2.2. Phillipsite Tuff Treatment

Three chemically treated samples, i.e. ZS, ZA, and ZB, were prepared by treating the zeolite, pretreated in section 2.1, with a salt (NaCl), an acid (HCl), or a base (NaOH), respectively. The treatment performed by impregnating 2.00 g of zeolite in 1 L of 2 M NaCl (purity 99 %), 0.1 M HCl (purity 33 %), and 0.1 M NaOH (purity 98-99 %). After 1 hour, the solution was decanted and the zeolite was reimprignated in the same solution for another 1 hour. Then the treated zeolite was filtered off, washed with distilled water, and dried overnight in the oven at 105 ˚C. The same procedure was followed to prepare a reference sample (ZW) but in distilled water instead of salt, acid, or base. Furthermore, a thermally treated sample (ZT200 and ZT400) were prepared by heating the zeolite, pretreated in section 2.1, at 200 and 400 °C in a Muffle furnace (Lenton Furnaces, Lenton Thermal Design L.T.D). The salt (NaCl), acid (HCl), and base (NaOH) solutions as well as the heating temperature employed in thermal treatments were chosen to be mild to avoid changes in zeolite framework.

2.3. Potentiometric Titration

The pH titration curves were obtained by means of a pH-meter (Metrohm 744). Two suspensions were prepared from 0.10 g sample of zeolite (ZW, ZS, ZA, ZB, ZT200, and ZT400) and 100.0 mL of distilled water. With continueous stirring, the first suspension was titrated with 0.01 M HCl whereas the second with 0.01 M NaOH at room temperature. As a reference, 100.0 mL distilled water sample (without zeolite) was titrated in a similar manner.

3. Results and Discussion

3.1. Potentiometric Titration

Natural phillipsite tuff samples that were prepared by impregnating the phillipsite tuff in 2 M NaCl salt (ZS), 0.1 M HCl acid (ZA), and 0.1 M NaOH base (ZB) as well as by heating at 200 and 400 °C (ZT200 and ZT400) beside a reference sample (ZW) were studied in the present work. The acidity/basicity of the product was investigated in relation to their potentiometric titration curves with 0.01 M HCl and 0.01 M NaOH as shown in Figure 1. The pH titration curve for distilled water is also given for the purpose of comparison.

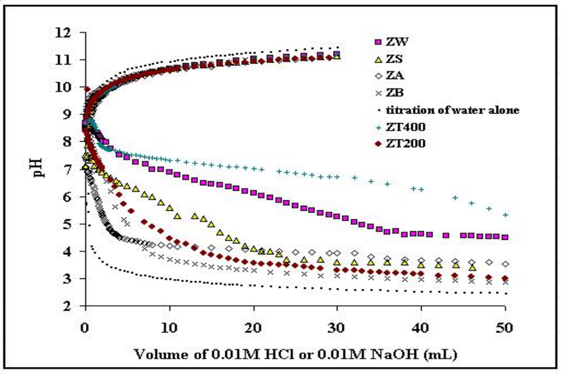

Fig 1. The pH titration curves for water, ZW, ZS, ZA, ZB, ZT200 and ZT400 samples.

The titration curves of water in the presence of zeolite samples have significantly higher pH values when titrated with HCl and very slightly lower pH values when titrated with NaOH relative to the pH titration curve of solid-free water (Figure 1). This indicates that zeolite sites are mainly in the form of salts or conjugate bases so that these sites have higher ability to react with H^+ than with OH^- titrant. This is further supported by the observation that the initial pH at $V_{HCl/NaOH} = 0$ (before titration with acid or base) of zeolite suspensions are higher than 7 (ZW 8.48, ZS 7.5, ZA 7.05, ZB 9.04, ZT200 8.42 and _ZT400 8.85). Accordingly, the titration curves with HCl rather than NaOH titrant will be investigated in the present article.

3.2. Modeling for Estimating the Acid Sites Density ([sites]$_t$) and Acid Dissociation Constant (pK`$_a$).

Comparison of pH titration curves of zeolite samples (Figure 1) with those of water alone indicates the high buffering capacity of zeolite samples.

Thus, it is of importance to investigate this buffering capacity and to propose the phillipsite tuff components that are responsible for this capacity.

A simple model was derived for estimating the acid sites densities ([sites]$_t$) of zeolite samples and their acid dissociation constants (p$K`_a$). The model assumes that zeolite acid/base sites initially present in either the deprotonated form (Z^-) or the protonated form (HZ) in the amounts *x* and *y*, respectively.

$$\underset{x}{Z^-} + H^+ \rightleftharpoons \underset{y}{HZ}$$

The reaction can be described by an equilibrium mass law with equilibrium constant *K*.

$$K = \frac{[HZ]}{[Z^-][H^+]} \qquad 1$$

When an amount (*t*) of H^+ is added, part of Z^- reacts with H^+ to produce HZ.

$$\underset{x-t}{Z^-} + H^+ \rightarrow \underset{y+t}{HZ}$$

Thus, after each addition of H^+ during titration, equation 1 can be rewritten as:

$$K = \frac{(y+t)}{(x-t)[H^+]} \qquad 2$$

The sum of [Z^-] and [HZ], or *x* and *y*, can be expressed as total sites density [Sites]$_t$ accompanied with the equilibrium constant *K*.

$$[Z^-] + [HZ] = [Sites]_t \qquad 3$$
$$x + y = [Sites]_t$$

The substitution of equation 3 in equation 2 followed by rearrangement of parameters gives equation 4.

$$[H^+] = \frac{1}{K}\left[\frac{[Sites]_t - x + t}{x - t}\right] \qquad 4$$

Where *K`(=1/K)* is the acid dissociation constant of HZ (conjugate acid of $Z^-$). The value of [$H^+$] at each amount added (*t*) of $H^+$ is known from the pH titration of each zeolite sample. The value of the acid dissociation constant of conjugate acid HZ ($K`$=1/*K*), acid sites density ([Sites]$_t$), and the initial amount of sites in the deprotonated form (*x*) can be evaluated by nonlinear regression of equation 4 using the following constrains:

$$[Sites]_t - x \geq 0 \qquad 5$$
$$x - t > 0$$

Beside the plateau region, the pH titration curves of zeolite samples (ZW, ZS, ZA, ZB, ZT200 and ZT400) were divided into different buffering capacity regions, as shown in Figure 2. Three regions for ZW, three for ZS, two for ZA, four for ZB, three for ZT200 and three for ZT400. Thus, the p$K`_a$ ($K`$=1/*K*), [Sites]$_t$, and *x* parameters were evaluated for each buffering region using the nonlinear regression of equation 4. The results are given in Table 1 showing an excellent sum of square residuals (10^{-18}-10^{-8}). The fitting curves for each region are shown in Figure 2. The final plateau regions, (V_{HCl} > 35 mL, Figure 1) were not considered although they show buffering capacity when compared with the titration curve of solid-free water (Figure 1) because species resulted during the course of titration are very complex to be considered.

Table 1. The fitting parameters of pH titration curves for zeolite samples ZW, ZS, ZA, ZB, and ZT using equation 4.

Sample	**Buffering region**	**p$K`_a$**[a]	***X* mol/g**	**[Sites]$_t$ mol/g**	**SSR**[b]	**Number of points**[c]	**Assignment**[d]
ZW	1st	8.3	6.0×10^{-4}	9.9×10^{-4}	2.3×10^{-16}	20	$>SO^-$, $CaH_3SiO_4^+$, $MgH_3SiO_4^+$, MgH_2SiO_4
	2nd	7.6	1.2×10^{-3}	2.5×10^{-3}	5.0×10^{-15}	11	$CaCO_3$, $MgCO_3$, $Al_2(OH)_2CO_3^{2+}$
	3rd	5.6	1.8×10^{-3}	1.8×10^{-3}	7.8×10^{-12}	21	$>SOH$, $CaHCO_3$, $MgHCO_3$
ZS	1st	6.8	6.1×10^{-4}	7.1×10^{-4}	1.8×10^{-15}	12	$CaCO_3$, $MgCO_3$, $Al_2(OH)_2CO_3^{2+}$
	2nd	5.5	1.2×10^{-3}	1.2×10^{-3}	2.0×10^{-11}	11	$>SOH$, $CaHCO_3$, $MgHCO_3$
	3rd	1.8	6.3×10^{-2}	6.3×10^{-2}	1.0×10^{-8}	10	-
ZA	1st	5.9	2.7×10^{-4}	2.7×10^{-4}	1.8×10^{-11}	26	$>SOH$, $CaHCO_3$, $MgHCO_3$
	2nd	3.0	1.1×10^{-2}	1.2×10^{-2}	3.4×10^{-10}	26	-
ZB	1st	8.3	1.2×10^{-4}	1.2×10^{-4}	5.1×10^{-17}	10	$>SO^-$, $CaH_3SiO_4^+$, $MgH_3SiO_4^+$, MgH_2SiO_4
	2nd	7.5	1.5×10^{-4}	2.5×10^{-4}	2.2×10^{-16}	10	$CaCO_3$, $MgCO_3$, $Al_2(OH)_2CO_3^{2+}$
	3rd	5.4	4.0×10^{-4}	4.0×10^{-4}	1.9×10^{-12}	5	$>SOH$, $CaHCO_3$, $MgHCO_3$
	4th	2.4	1.0×10^{-2}	1.0×10^{-2}	7.1×10^{-10}	13	-
ZT400	1st	8.0	9.0×10^{-4}	1.0×10^{-3}	1.5×10^{-18}	11	$>SO^-$, $CaH_3SiO_4^+$, $MgH_3SiO_4^+$, MgH_2SiO_4
	2nd	7.5	1.7×10^{-3}	2.4×10^{-3}	3.1×10^{-16}	27	$CaCO_3$, $MgCO_3$, $Al_2(OH)_2CO_3^{2+}$
	3rd	5.8	1.7×10^{-2}	1.7×10^{-2}	5.5×10^{-15}	22	$>SOH$, $CaHCO_3$, $MgHCO_3$
ZT200	1st	8.1	1.8×10^{-4}	2.8×10^{-4}	5.8×10^{-16}	15	$>SO^-$, $CaH_3SiO_4^+$, $MgH_3SiO_4^+$, MgH_2SiO_4
	2nd	5.1	7.8×10^{-4}	8.1×10^{-4}	4.0×10^{-12}	8	$>SOH$, $CaHCO_3$, $MgHCO_3$
	3rd	2.6	9.1×10^{-3}	9.2×10^{-3}	1.2×10^{-8}	33	-

[a] p$K`_a$ of conjugate acid. [b] Sum of square residuals in the value of [H^+] calculated. [c] Number of experimental points used in nonlinear regression.

[d] Assignment to species reacted in titration with 0.1 M HCl.

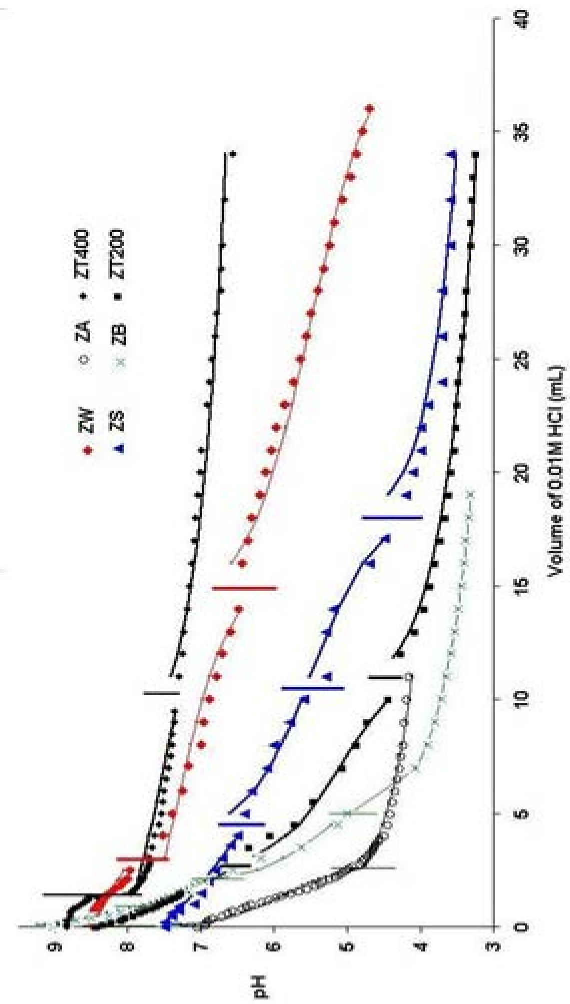

Fig 2. The results of fitting buffering regions of zeolite samples ZW, ZS, ZA, ZB, ZT200 and ZT400.

3.3. Buffering Capacity

Jordanian phillipsite tuff consists of about 50 % of zeolite and 50 % of non-zeolite content (Al-Rashdan, 2000). The zeolite content is in the form of aluminusilicate ($>SOH_2^+$, $>SOH$ and $>SO^-$, where $>S$ is Al or Si):

$$>SOH_2^+ \overset{K_{a1}}{\leftrightarrow} >SOH + H^+ \qquad >SOH \overset{K_{a2}}{\leftrightarrow} >SO^- + H^+ \ ,$$

whereas the non-zeolite contents are assumed to be in the form of metal silicates which accounts for olivine, pyroxene and feldspars content of phillipsite tuff. Metal carbonates are also possible because of the calcite content of phillipsite tuff. Metal bicarbonates results during titration of carbonates.

The XRF results of Jordanian phillipsite tuff indicate the presence of significant amounts of Si, Al, Fe, Mg, and Ca relative to Na, K, P, and Mn (see Experimental Part). Brønsted acidity in zeolite is attributed to aluminum substitution. The Si and Al are present in the aluminosilicate zeolite framework, which has a buffering effect (Chu and Chang, 1985; Stoyanov *et al.*, 2008). Aluminum may present in extra-framework (Sokol *et al.*, 2000). The Al, Fe, Mg, and Ca elements may occur in the silicate, carbonate, or bicarbonate forms which also have buffering effects. Accordingly, the phillipsite tuff species that contribute to the buffering capacity are the aluminosilicate framework as well as the Al, Fe, Mg, and Ca silicates, carbonates, and bicarbonates.

The assignment of specific acid/base sites for each buffering region in the zeolite samples (ZW, ZS, ZA, ZB, ZT200, and ZT400) can be attempted by comparing the obtained $pK`_a$ values of acid sites of zeolite samples (Table 1) with those reported in literature for both the zeolitic and non-zeolitic components present in phillipsite tuff.

3.3.1. Buffering Capacity of Untreated Zeolite (ZW)

To our knowledge, there is no reported $pK`_a$ values for zeolite aluminosilicate framework. The situation is different in clays where there are many reports on potentiometric titration of clays. Such reports lead to estimates, shown in Table 2, for $>SOH/>SOH_2^+$ and $>SO^-/>SOH$ ($>S$: Al or Si); average pK_{a1} 5.1 and pK_{a2} 8.4 (equations 6 and 7, Table 2). Furthermore, the reported values using nonelectrostatic interaction approach on clay, which is similar to our approach are pK_{a1} 4.9 and pK_{a2} 8.4 (Lu and Smith, 1996). This leads to the suggestion that the buffering regions of zeolite sample (ZW) at $pK`_a$ 5.6 and $pK`_a$ 8.3 (Table 1) are due to aluminosilicate sites.

For pure phillipsite mineral, the Si/Al mol ratio is 1.7 (Baerlocher *et al*, 2001). The Brønsted acid sites density estimated for phillipsite depending on this Si/Al ratio is 2.70×10^{-3} mol/g (Baerlocher *et al*, 2001). The phillipsite content of Jordanian phillipsite tuff is about 50 % (Al Rashdan, 2000), thus the Brønsted acid site density of aluminosilicate in phillipsite tuff is expected to be about 1.35×10^{-3} mol/g. This value is close to the site density in sample ZW at $pK`_a = 8.3$ ($9.9 \times 10^{-4}$ mol/g, Table 1). The site density for ZW sample at $pK`_a = 8.3$ and at $pK`_a = 5.6$ should be equal if they are due only to aluminosilicates. Thus, the extra amount of site density at $pK`_a = 5.6$ (1.8×10^{-3} mol/g, Table 1) relative to that at $pK`_a = 8.3$ (9.9×10^{-4} mol/g, Table 1) is due to non-zeolitic sites of Ca-Mg silicates which have pKa values in this regions (Table 2, equations 12, 15, 16).

Table 2. The pK_a values and the corresponding equations of compounds of Si, Al, Ca, Mg, and Fe present in clays.[a]

Species	Equation (Equation no.)	pK_a	ref
$>SOH/>SOH_2^+$ ($>S$: Al or Si)	$>SOH_2^+ \leftrightarrow >SOH + H^+$ (6)	4.5	b
		6.0, 5.2	c
		4.9, 5.2	d
		average 5.1	
$>SO^-/>SOH$ ($>S$: Al or Si)	$>SOH \leftrightarrow >SO^- + H^+$ (7)	7.9	b
		8.6, 8.1	c
		8.4, 7.6	d
		average 8.4	
$Al^{3+}/H_3SiO_4^-$, CO_3^{2-}, HCO_3^-	$Al^{3+} + H_4SiO_4 \leftrightarrow AlH_3SiO_4^{2+} + H^+$ (8)	2.5	e
	$2Al^{3+} + HCO_3^- \leftrightarrow Al_2(OH)_2CO_3^{2+} + 3H^+$ (9)	7.3	e
	$3Al^{3+} + HCO_3^- \leftrightarrow Al_3(OH)_4HCO_3 + 4H^+$(10)	9.4	e
$Ca^{2+}/ H_2SiO_4^{2-}$, $H_3SiO_4^-$ CO_3^{2-}, HCO_3^-	$Ca^{2+} + H_3SiO_4^- \leftrightarrow CaH_2SiO_4 + H^+$ (11)	9.8	e
	$Ca^{2+} + H_4SiO_4 \leftrightarrow CaH_3SiO_4^+ + H^+$ (12)	9.1	e
	$Ca^{2+} + HCO_3^- \leftrightarrow CaCO_3 + H^+$ (13)	7.1	e
	$Ca^{2+} + H_2CO_3 \leftrightarrow CaHCO_3^+ + H^+$ (14)	5.2	e
$Mg^{2+}/ H_2SiO_4^{2-}$, $H_3SiO_4^-$ CO_3^{2-}, HCO_3^-	$Mg^{2+} + H_3SiO_4^- \leftrightarrow MgH_2SiO_4 + H^+$ (15)	8.6	e
	$Mg^{2+} + H_4SiO_4 \leftrightarrow MgH_3SiO_4^+ + H^+$ (16)	8.8	e
	$Mg^{2+} + HCO_3^- \leftrightarrow MgCO_3 + H^+$ (17)	7.4	e
	$Mg^{2+} + H_2CO_3 \leftrightarrow MgHCO_3^+ + H^+$ (18)	5.3	e
$Fe^{3+}/ H_2SiO_4^{2-}$, $H_3SiO_4^-$ CO_3^{2-}, HCO_3^-	$Fe^{3+} + H_4SiO_4 \leftrightarrow FeH_3SiO_4^{2+} + H^+$ (19)	0.6	e
	$Fe^{3+} + H_2O + CO_3^{2-} \leftrightarrow Fe(OH)CO_3 + H^+$(20)	3.8	e
	$Fe^{3+} + 2HCO_3^- \leftrightarrow Fe(CO_3)_2^- + 2H^+$ (21)	11.3	e
	$Fe(OH)_3$ (21)	5.1	e

From Table 2, the bicarbonates of Ca and Mg, which have p$K`_a$ values 5.2 (equation 14) and 5.3 (equation 18) may contribute to the buffering region of ZW sample at pK_a 5.6 (Table 1) in addition to aluminosilicate sites.

The carbonates of Al, Ca, and Mg have pK_a values 7.3, 7.1, and 7.4, respectively (equations 9, 13, and 17). Thus, the buffering regions of ZW sample at p$K`_a$ 7.6 (Table 1) can be assigned to $Al_2(OH)_2CO_3^{2+}$, $CaCO_3$, and $MgCO_3$.

3.3.2. Buffering Capacity of Treated Zeolites (ZA, ZB, ZS, ZT200 and ZT400)

The buffering regions of treated zeolitic samples ZS, ZA, ZB, ZT200 and ZT400 were assigned according to those of ZW sample. The pK'_a values 5.9 (ZA), 5.4 (ZB), 5.5 (ZS), 5.1(ZT200) and 5.8 (ZT400) are assigned to aluminosilicate and calcium and magnesium bicarbonates and aluminum and iron hydroxides; 7.5 (ZB and ZT400) and 6.8 (ZS) are assigned to calcium, magnesium, and aluminum carbonates; 8.3 (ZB) , 8.1 (ZT200) and 8.0 (ZT400) are assigned to aluminosilicate (Table 1).

The buffering regions with pK_a values less than 4 (1.8, 2.4, 2.6 and 3.0, Table 1) are difficult to be assigned because several species resulted during the course of titration may contribute to these regions.

3.4. Effects of Treatment on the Buffering Capacity of Zeolite

On the light of the assignment of treated samples (ZS, ZA, ZB, ZT200 and ZT400**),** the effect of acid, base, salt, and thermal treatment upon buffering capacity of zeolite can be evaluated.

Acid-treatment of phillipsite tuff using 0.1 M HCl leads to the (i) vanishing of buffering region at p$K`_a$ 8.3 (in ZW sample, assigned to $>SO^-$) due to the destruction of phillipsite structure, (ii) vanishing of buffering region at p$K`_a$ 7.6 (in ZW, assigned to carbonates) due to the neutralization of carbonates of Ca, Mg, and Al, (iii) decrease of site density $[Sites]_t$ at p$K`_a$ 5.6 (ZW, assigned to $>SOH$ and bicarbonates of Ca/Mg) due to destruction of phillipsite structure and neutralization of bicarbonates species.

Base-treatment of phillipsite tuff using 0.1 M NaOH leads to (i) a decrease in the site density of the buffering region at $pK`_a$ 8.3 (ZW, assigned to $>SO^-$) (ii) a decrease of the site density of the buffering region at 7.5 and 5.4. These two observations can be attributed to the ability of sodium ions to substitute Ca and Mg ions in their aluminosilicates and silicates leading to dissolution of these species.

Salt-treatment of phillipsite tuff using 2 M NaCl leads to (i) disappearance of the buffering region at $pK`_a$ 8.3 (in ZW sample, assigned to $>SO^-$), (ii) decrease of site densities of buffering region at 6.8 (assigned to carbonates) and 5.5 (assigned to $>SOH$ and bicarbonates). This loss of part of the buffering capacity can also be attributed to the ability of sodium ions to substitute Ca and Mg ions in their aluminosilicates, silicates, carbonate, and bicarbonates leading to their dissolution.

Heating phillipsite tuff at 400°C did not affect the sites at p$K`_a$ 8.0 (assigned to $>SO^-$) and 7.5 (assigned to carbonates), however the sites at p$K`_a$ 5.8 (assigned to $>SOH$ and bicarbonates) increased significantly. On the other hand, heating phillipsite tuff at 200°C leads to decrease of the sites at 8.1 (assigned to $>SO^-$) and 5.1(assigned to $>SOH$ and bicarbonates). The carbonates and bicarbonate are reported to be not affected by thermal treatment up to 600 °C (Gunasekaran and Anbalagan, 2007). The effect heating on the XRD pattern of natural phillipsite was reported by Rykl and Pechar (1991). Heating at 200 ºC and 500 ºC resulted in transforming phillipsite into wairakite and metawairakite, respectively. Wairakite is considered as feldspathoid and has an ion exchange ability which contributes to acid site density. Other XRD studies (Komarneni, 1985; Liguori *et al.*, 2006; Cappelletti ***et al.*** 2011) indicated that heating phillipsite loaded with cesium, strontium, and chromium at 600-800 ºC leads to collapse of the phillipsite structure and formation of metal-feldspar phase.

Thus, the buffering capacity of phillipsite tuff enhances through thermal treatment to 400 °C and reduces by HCl, NaOH, and NaCl-treatments and thermal treatment at 200 °C. According to the sum of total sites ($[\text{Sites}]_t$) at $pK`_a$ 5.4-5.9, which includes both aluminosilicate and bicarbonate species, the buffering capacity of zeolite samples decreases in the order: ZT400 > ZW > ZS > ZT200> ZB > ZA.

4. Conclusions

The potentiometric titration curves showed that natural zeolite exists in the salt or base form and thus has a remarkable buffering capacity when titrated with HCl. Both chemical and thermal treatments affect such capacity. Chemical treatment of zeolite with NaCl, HCl, and NaOH and thermal treatment at 200˚C decrease the buffering capacity of zeolite whereas heating the zeolite at 400˚C enhances its buffering capacity. Natural zeolite which is available in low cost and huge quantities can be used to solve the problem of acidification of soils and aquatic systems.

References

[1] Al Rashdan Z. (2000). Investigation of natural zeolitic tuffs on their ability for sewage cleaning. Ph.D. thesis, Oldenburg University, Germany.

[2] Baerlocher C., Meier W. M., Olson D. H. (2001) Atlas of zeolite framework types, 5th edition, Elsevier, Amsterdam.

[3] Bouwman A. F., Van Vuuren D. P., Derwnet R. G., Posch M. (2002). A global acidification and eutrophication of terrestrial ecosystyms. Water, Air and Soil Pollution, 141, 349-382.

[4] Cappelletti P., Rapisardo G., de Gennaro B., Colella A., Langella A., Graziano S., Bish D., de Gennaro A. (2011). J. Nuclear Materials. 414, 451-457.

[5] Chen D.T., Sharma S.B., Filimonov I., Dumesic J.A. (1992). Microcalorimetric studies of zeolite acidity. Catalysis Letters. 12(1-3), 201-211.

[6] Chu C. T-W., Chang C. D. (1985). Isomorphous substitution in zeolite frameworks: 1. Acidity of surface hydroxyls in [B]-, [Fe]-, [Ga]- and [Al]-ZSM-5. Journal of Physical Chemistry, 89, 1569-1571.

[7] Goldberg S. (1991). Sensitivity of surface complexation modeling to the surface site density parameter. Journal of Colloid and Interface Science, 145, 1-9.

[8] Goldberg S. (1995). Adsorption models incorporated into chemical equilibrium models. Soil Science Society of America, American Society of Agronomy, 677 S. Segoe Rd., Madison, W1 53711, USA. Chemical equilibrium and reaction models, SSSA special publication 42.

[9] Ghosh A..K., Curthoys G. (1983). Journal of Chemical Society, Faraday Transactions. 1, 79, 2569-2572.

[10] Gunasekaran S., Anbalagan G. (2007). Thermal decomposition of natural dolomite. Bulletin of Material Science, 30, 339-344.

[11] Karge H.G., Dondur V.(1990). Investigation of the distribution of acidity in zeolites by temperature-programmed desorption of probe molecules. I. Dealuminated mordenites. Journal of Physical Chemistry. 94(2), 765-772.

[12] Karge H.G., Dondur V., Weitkamp J..(1991). Investigation of the distribution of acidity strength in zeolites by temperature-programmed desorption of probe molecules. 2. Dealuminated Y-type zeolites. Journal of Physical Chemistry. 95(1), 283-288.

[13] Komarneni S. (1985). Phillipsite in Cs decontamination and immobilization. Clays and Clay Minerals., 33, 145-151.

[14] Jara A. A., Goldeberg S., Mora M. L. (2005). Studies on the surface charge of amorphous aluminosilicate using surface complexation models. Journal of Colloid and Interface Science., 292, 160-170.

[15] Jozefowicz L.C., Karge H.G., Coker E.N. (1994). Microcalorimetric Investigation of H-ZSM-5 Zeolites Using an Ultrahigh-Vacuum System for Gas Adsorption. Journal of Physical Chemistry. 98 (33), 8053-8060.

[16] Li W., Sun Z., Forsling W., Du Q., Tang H. (1999). A comparative study of surface acid-base characteristics of natural illites of different origins. Journal of Colloid and Interface. Science, 219, 48-61.

[17] Liguori B., Cassese A., Collella C. (2006). Safe immobilization of Cr(III) in heat- treated zeolite tuff compacts. J. Hazardous Materials B137, 1206-1210.

[18] Lu W., Smith E. H. (1996). Modeling potentiometric titration behaviour of glauconite. Geochimica. Cosmochimica Acta., 60, 3363-3373.

[19] Maher P. K., Hunter F. D., Scherzer. (1971). Crystal Structures of unstable faujasites. Advances in Chemistry Series (1971), 101(Molecular Sieve Zeolites-I), 266-278.

[20] Pfeifer H.; Freuede D.; Hunger M.. (1985). Nuclear magnetic resonance studies on the acidity of zeolites and related catalysts. Zeolites, 5, 274-286.

[21] Rykl D., Pechar F. (1991). Thermal decomposition of natural phillipsite. Zeolites., 11, 680-683.

[22] Sokol A. A., Richard C., Juan A. C., Garces M., Kuperman (2000). A. Computational investigation into the origin of Lewis acidity in zeolites. Advanced Materials, 12, 1801-1805.

[23] Stoyanov S. R., Gusarov S., Kuznicki S.M., Kovalenko A. (2008). Theoretical modeling of zeolite nanoparticle surface acidity for heavy oil upgrading. Journal of Physical Chemistry C., 112, 6794-6810.

[24] Tanabe K.. (1970) Solid Acids and Bases, Kodansha, Tokyo and Academic press, New York, chapter 2, pp. 5-10.

[25] Tournassat C., Ferrage E., Poinsigon C., Charlet L. (2004). The titration of clay minerals II: Structure-based model and implications for clay reactivity. Journal of Colloid and Interface Science. 273, 234-246.

[26] Turley C., Scholes M. (2009). The acidification of Planet Erath. In: Richardso, K. (Ed.), Synthesis report, climate change, global risks, challenges and decisions. Copenhagen, 10-12 March.

[27] Unlu K., Ilbeyi A., Soyupak S., Yurteri C. (1999). A geochemical equilibrium modeling approach to assessing soil acidification impacts due to depositions of industrial air emissions. Water, Air and Soil Pollution, 113, 395-409.

[28] Ward J.W. (1976) In Zeolite Chemistry and Catalysis, ed. J.A.Rabo, ACS Monogr. 171, Am. Chem. Soc., Washington, D.C., p. 171.

[29] Weitkamp J.(2000). Zeolites and catalysis, Solid sate ionics., 131, 175-188.

[30] Wingenfelder U., Hansen G., Furrer G., Schulin R. (2005). Removal of heavy metals from mine waters by natural zeolites. Environmental Science and Technology, 39, 4606-4613.

[31] Yousef R. I. and El-Eswed B. (2009). The effect of pH on the adsorption of phenol and chlorophenols onto natural zeolite. Colloids and Surfaces A: physicochemical and Engineering Aspects. 334, 92-99.

JJEES

Jordan Journal of Earth and Environmental Sciences

Volume 4, (Special Publication, Number 2), Jan. 2012
ISSN 1995-6681
Pages 15- 22

Preparation of Natural Standard Reference Material (SRM) for El-lajjun Oil Shale/Jordan

Mousa Magharbeh[a], Manar Fayyad[a], Mufeed Batarseh[b,]*

[a] *Department of Chemistry, University of Jordan, Amman - Jordan*

[b] *Department of Chemistry and* Prince Faisal Center for Dead Sea Enviromental and Energy Reserach,
Mutah University, PO Box 7, 61710 Karak–Jordan.

Abstract

The standard reference materials (SRMs) represent a key tool for the quality control of chemical analyses and the demand on these materials is constantly increasing worldwide. A standard reference material of oil shale (SJL-1) collected from El-lajjun area in Jordan was prepared and certified to be used for quality control of analyses and calibration particularly for the oil shale characterization and testing laboratories. This work was a part of the Arab collaborative projects initiated by Arab Atomic Energy Agency (AAEA) during the period from 2007 to 2009.

The paper describes the certification procedure and the inter-laboratory comparison study results, which was carried out through participation of twelve national and international laboratories applying eleven different analytical techniques used to determine the analytes concentration. Details of the production, homogeneity and stability of SJL-1 standard reference material were reviewed as well as the results of certification. The Certificate of Analysis for SJL-1 provides assigned certified values for almnuium oxide, phosphorus pentoxide, calcium oxide, titanium dioxide, magnesium oxide, potassium oxide, ferric oxide, sodium oxide, manganese oxide, sulfur, uranium, vanadium, chromium, zinc, nickel, copper, and strontium. Reference values are provided for Loss on Ignition (LOI), silicon oxide, cadmium, molybdenum, cobalt, lead, barium and arsenic. Finally, range values are assigned for other thirty-seven constituents of oil shale.

Keyword: SJL-1; Standard Reference Materials; Oil Shale; El-Lajjun; Jordan.

1. Introduction

The lack of quality control of chemical analyses carried out particularly in industrial testing laboratories may lead to inaccurate data and wrong assessment of the product quality. The oil shale mining is a promising industry in Jordan. However, in the Middle East region few studies were concerned with preparation of natural Certified Reference Materials (CRMs) that can be used for quality control and calibration (Al-Masri, et al. 2006).

Recently, the Arab Atomic Energy Agency (AAEA) sponsored a project entitled "Standard Reference Materials (SRMs)" aiming for encouraging cooperation between researchers in Arab World for preparation of CRMs to be used as reference materials for quality assurance in laboratories testing, methods validation and instruments calibration. The overall project efforts lead for the following: Egyptian team prepared two materials: Olive leaves and black sand as SRMs, Syrian team prepared sewage sludge and Jordan team prepared Oil Shale and Phosphate. Additionally, an in-house reference soil sample containing high level of naturally occurring radioactivity was prepared by Syrian Atomic Energy Agency (Al-Masri, et al. (2006).

The National Institute of Standards and Technology (NIST), United States Geological Survey (USGS) and the institute of Geochemistry SB RAS (IGI) prepared and purchased several number of standard reference materials (SRMs) for oil shale worldwide. Most of these SRMs are used for validating and calibrating analytical methods with certified oxide, metals and organic components, while others oil shale constituents reported as averages or ranges only. However, limited numbers of SRMs were prepared for quantification of trace level of organic compounds such as polycyclic aromatic (PAHs) (Heidelberg, 1988). There are thirty-six organic SRMs have been prepared in natural matrix and forty-four solutions for instruments calibration. Future goals include certifying more organic constituents such as polychlorinated Biphenyls (PCB), dioxins, and emerging contaminants such as brominated flame retardant (Wise, 2002).

The numbers of SRMs prepared worldwide for shale and accordingly assigned for some certified values are limited. The Green River Shale (SGR-1) has been certified for nine oxides and twenty six elements, while others constituents such as total carbon, ash and moisture content were neither certified nor measured (Gladney et al, 1988). Devonian Ohio Shale (SDO-1) was certified for ten oxides

---

[*] Corresponding author. e-mail: Batarseh@mutah.edu.jo.

and twenty five elements, while total carbon, organic carbon and moisture content were reported as measured values only, ash was not measured (Kane et al. 1990**)**. Cody Shale (SCO-1) has been certified for ten oxides and twenty seven elements, but organic carbon and total carbon were reported as measured values, ash and moisture were not measured (Gladney et al, 1988). Sukhoy Log Shale (SLg-1) was certified for ten oxides and twenty six elements, while, organic carbon and total carbon reported as measured values, only (Petrov et al. 2004). Finally, Khomolkho Shale (SCHS-1) certified for eleven oxides, thirty nine elements and LOI but again organic carbon and total carbon reported as measured values (Petrov et al. 2004).

The present work describes the preparation, analysis and certification of oil shale standard reference materials called (SJL-1), which can be valuable on the national and international levels for laboratory testing, analytical method validation, quality assurance, and instruments calibration. It can be used also on industrial level for economical studies related to oil shale exploitation and performing interlaboratory comparison studies. The SJL-1 material constituents including carbon content, ash, moisture, macro- and microelements, minerals and metal oxides concentrations were measured according to standard certification procedure using different analytical techniques at national and international accredited laboratories.

2. Methods and Materials

2.1. Sample Collection and Pre-treatment

An oil shale test material was collected from the El-lajjun deposits, located 120 km south of Amman city, Jordan, Figure 1. The sampling was carried out at a new mining area that was established recently by Jordanian Natural Resources Authority (NRA). About 100 kg of oil shale rocks material was collected and pooled together. The sample had a composition adequately representative of oil shale and containing measurable quantities of major and minor constituents similar to the candidate standard reference material (SRM).

The sample preparation was including crushing using a Jaw crusher and removal of the coarse material (> 2 mm). Then sample was ground using an Agate Ball Mill to pass 200 mesh (75µm). The fine material was homogenized in a polyethylene-lined mixing drum. Finally, the sample was left to settle down and packed in sealed polyethylene bottles each of 100 g. About 200 sample bottles were produced as a candidate SRM of oil shale and ready for analysis. A sophisticated protocol for testing the homogeneity and stability was developed as described in section 2.2.

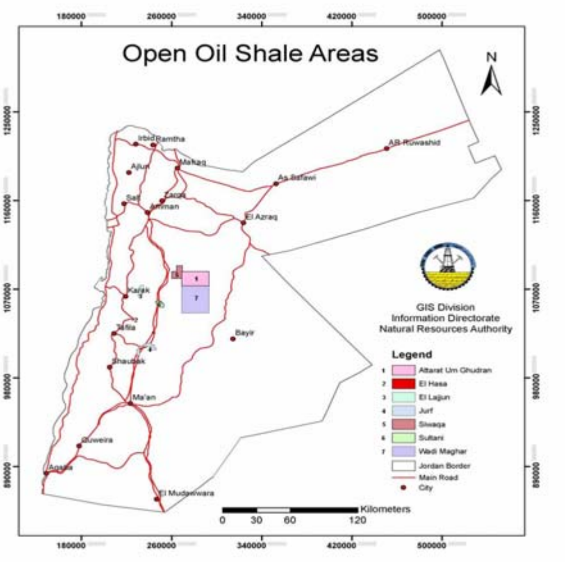

Fig 1.Map of oil shale deposits in Jordan and sampling site location, (Alali, 2003)

2.2. Homogeneity testing

The prepared sample material should be homogenous and has same distribution of analytes within the individual sample bottle and among all prepared sample bottles (units). Homogeneity was tested according to the British Standard Methods for sampling and chemical products number BS5309 part 1 (Walker and Brookman, 1998). The number of sub-samples to be tested for homogeneity were chosen according to the following formula ($3x\ \sqrt[3]{n}$ = number of tested units), n is number of prepared units. Each unit contains 100 g of the homogenous oil shale sample material. The homogeneity of the sample was tested using two-factor analysis of variance (ANOVA) without replication by comparing calculated F value (F_{calc}) with critical F value (F_{crit}) at 95% confidence level.

Three methods were used for homogeneity testing namely: sieve analysis, total (cross) alpha/beta activity, and Gamma spectrometry. The particle size distribution performed for 10 sub-samples by passing each sample through an automatic sieve machine shaker with four different sieves (<45, 53-45, 53-63, and 63-75µm), each particle size portion was weighed and percentage was calculated. These results were double checked using laser grain size analyzer for selected samples, there was a significant conformity between sieve analysis and laser grain size analyzer results. Total (cross) alpha/beta activity measurements were carried out for 10 sub-samples using low background alpha/beta counting system model Tennelec LB 4100 (Canberra Proportional counter, USA). The sample from each unit (6-10) mg/cm^2 was placed in 5-cm stainless steel discs and counted for alpha/beta activity. Gamma spectrometry activity and their daughters measurements were performed for 10 sub-samples using a special counting container. The gamma emitting daughter activity (Bk/kg) was monitored for 1 hour using gamma spectrometry at high resolution (1.85KeV at 1.33 MeV).

2.3. Chemical and Mineralogical Characterizations

The oil shale sample (SJL-1) chemical composition was analyzed using the following analytical techniques namely: X-ray fluorescence(XRF), inductively coupled plasma mass spectrometry (ICP-MS), Inductively coupled plasma atomic emission spectroscopy (ICP-OES), neutron activation (NA), atomic absorption spectrometer (AAS), Gamma spectrometry, total organic carbon analyzer (TOC), Kjeldahli, and Fischer assay was used for determination of oil content and organic carbon. The mineralogical content was investigated mainly using X-ray diffraction (XRD) which indicated that the oil shale mainly composed of calcite and quartz.

2.4. Determination of the Water Content

Water content was determined by calculating the weight difference of an oil shale sample (1.5-3.0 g) before and after drying using two methods, an oven at 105ºC for 24 hours and an Infrared (IR) apparatus model UHra-X210 (Gronert, Germany).

2.5. Determination of Total Organic Carbon (TOC)

About 5g of the homogenized oil shale sample was treated with excess HCl (12.5 %, v/v), until the disappearance of bubbles. The treated samples were filtered on a pre-weighed filter paper and washed with double deionized water to remove the excess amount of HCl. Then the filter paper was placed in an aluminum tray and dried in an oven for 24 hours at 108ºC. After complete dryness, samples were reweighed, ground and five replicates of 5 to 10 mg aliquot of each sample was analyzed for their TOC content using DC-90 Total Organic Carbon Analyzer (Dohrmann, USA).The calibration curve was prepared using a mixture of oxalic acid with alumina ($H_2C_2O_4/Al_2O_3$) in a ratio of (1:9) that ranged from 28 to 87µg carbon.

2.6. Elemental Analysis (ELEM)

Elemental analysis of hydrogen, nitrogen, carbon and sulfur in oil shale material was carried out according to the standard operating procedure of EURO EA Elemental Analyzer (HEKAtech GmbH, Germany). A 12 mg of oil shale sample was mixed with (V_2O_5) as catalysts for measuring sulfur using sulphanilamide and BBOT (2-4 mg) as reference standards.

2.7. XRF Analysis

The homogenous oil shale sample was analyzed for oxides content using Energy Dispersive XRF Spectrometer (EDXRF). The sample placed into a polyethylene cup together with SGR-1 reference standard material. Additionally, the quantitative oxides analysis using Wavelength Dispersive X-Ray Fluorescence Spectrometer (WDXRF) was performed through preparing XRF disk by mixing 0.3g of oil shale sample with (2.7g + 3*x* LOI) of $Li_2B_4O_7$ and 0.3g of absorbing X-ray reagent (La_2O_3), the mixing ratio of sample to ($Li_2B_4O_7$ and La_2O_3) was 1:10. The oxides concentrations were determined as percentages.

2.8. Sample Preparation for Elements Analysis

The elements were determined by ICP-MS, ICP-OES, NA and AAS after digestion using two methods, an open acid digestion in a mixture of ($HF-HNO_3-HClO_4$) and a microwave digestion in a mixture of (HNO_3, H_2O_2, and HF). The detailed digestion procedures are described in the following sections.

2.8.1. Open Acid Digestion

A 0.2 g of oil shale sample was placed into a polytetraflouroethylene (PTFE) bottle. A mixture of ($HF-HNO_3-HClO_4$) was added in the ratio (v/v) of 7ml HF (47%), 7ml HNO_3 (69%) and 2ml $HClO_4$ (70%) and allowed to heat at 120ºC for 3 hour using heating blocks. Then switched to 160ºC for 24 hours and evaporated to dryness, to the residue a 10 ml of 1M $HNO_3$was added and resulting solution was transferred to 20ml polyethylene volumetric flask and complete to mark with deionized water. Finally, the solution filtered through a 0.45 µm syringe filter and the sample was ready for measurement. All glassware were cleaned, dried and rinse with 5% HNO_3 before use.

2.8.2. Microwave Digestion

A 0.2 g of oil shale sample was digested in a cleaned PFA Teflon vessels with a mixture of 8ml HNO_3 (69%), 2ml H_2O_2 (30%), and 4ml HF(47%) using a microwave digestion system model star*-system (MHS-product, Germany). The vessels left opened for 12 hours to get rid of gasses, and then vessels were capped and placed inside the rotor bodies, sealed, tightened and digested in the microwave digestion system. Then the solution poured into PFA beaker and heated at 110ºC until dryness to get rid of HF. Then 20ml of 10% HNO_3 was added to each sample and transferred into 20ml polyethylene volumetric flask. Each digestion series included a sample reference and sample blank which was cleaned Teflon vessel containing the same type and amount of the reagents only.

2.9. Quality Control

The results of the analytical methods (ICP/OES, ICP/MS, ICP-OES, XRF, NA, AAS and Elemental analysis) were validated by analyzing the following certified reference materials: SGR-1, BBOT, Sulfanilamide, OREAS24P, OREAS45P and Basalt Rock SRM-688, following the same analytical procedures used for the oil shale samples analyses. The accuracy of the method was evaluated by comparing the mean measured values with the certified values.

3. Results and Discussion

3.1. Homogeneity test results

The between-bottle homogeneity of the oil shale samples was verified using three types of analysis namely: sieving analysis, Gamma spectrometry, and total alpha/beta spectrometry. Ten sub-samples were selected randomly from the total number of prepared samples according to the British Standard methods for sampling and chemical products number BS5309 part 1 (Walker and Brookman, 1998). The homogeneity of the samples was tested using two-factor analysis of variance (ANOVA) without replication by comparing calculated F value (F_{calc}) with critical F value (F_{crit}) at 95% confidence level. Additionally, single factor analysis of variance (ANOVA) was applied to verify between-bottle and within-bottle homogeneity (between groups and within group homogeneity).

3.1.1. Sieving analysis

The particle size distribution analysis of the oil shale samples showed that 82% of the total particles size were less than 45µm, 4% ranged between 45-53µm, 6% in the range of 53-63µm and 4% in the range of 63-75 µm, Table 1. The statistical results of ten sub-samples using Two-factor analysis of variance (ANOVA) without replication showed that the sample was homogenous, where calculated F value (F_{calc}=0.693) was less than critical F value (F_{crit}=2.250) at 95% confidence level, Table 1.

The analysis of variance (ANOVA) had been used often worldwide to check whether the variance among sample batches is significant at 95% confidence level (Biagini, et al. 1995; Walker and Brookman, 1998; Van der Veen et al. 2001; Zischka et al. 2002).

Table 1. Sieving analysis for 10 sub-samples of SJL-1.

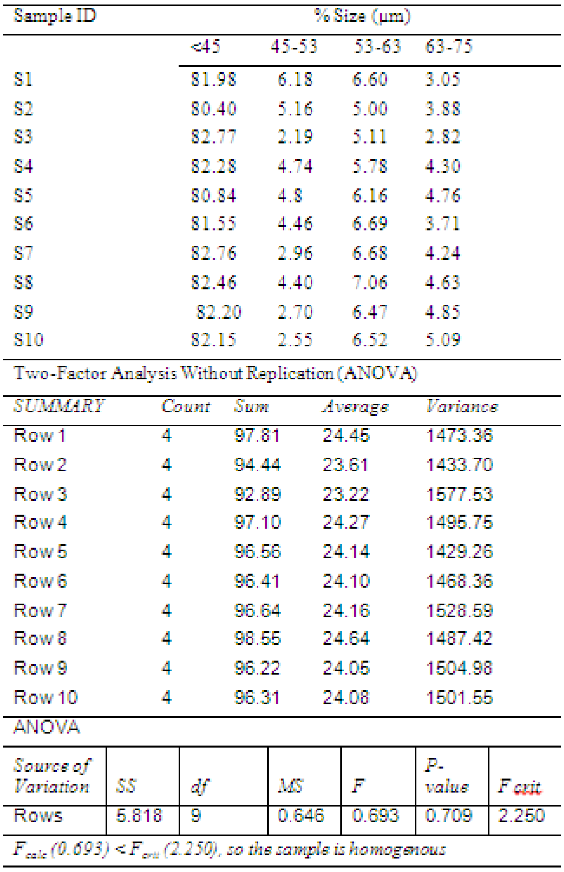

Sample ID	% Size (µm)			
	<45	45-53	53-63	63-75
S1	81.98	6.18	6.60	3.05
S2	80.40	5.16	5.00	3.88
S3	82.77	2.19	5.11	2.82
S4	82.28	4.74	5.78	4.30
S5	80.84	4.8	6.16	4.76
S6	81.55	4.46	6.69	3.71
S7	82.76	2.96	6.68	4.24
S8	82.46	4.40	7.06	4.63
S9	82.20	2.70	6.47	4.85
S10	82.15	2.55	6.52	5.09

Two-Factor Analysis Without Replication (ANOVA)

SUMMARY	*Count*	*Sum*	*Average*	*Variance*
Row 1	4	97.81	24.45	1473.36
Row 2	4	94.44	23.61	1433.70
Row 3	4	92.89	23.22	1577.53
Row 4	4	97.10	24.27	1495.75
Row 5	4	96.56	24.14	1429.26
Row 6	4	96.41	24.10	1468.36
Row 7	4	96.64	24.16	1528.59
Row 8	4	98.55	24.64	1487.42
Row 9	4	96.22	24.05	1504.98
Row 10	4	96.31	24.08	1501.55

ANOVA

Source of Variation	*SS*	*df*	*MS*	*F*	*P-value*	*F crit*
Rows	5.818	9	0.646	0.693	0.709	2.250

F_{calc} (0.693) < F_{crit} (2.250), so the sample is homogenous

3.1.2. Gamma Spectrometry

The single factor analysis of variance (ANOVA) was applied to calculate the F value according to equation (1). Also, P–value of ANOVA analysis which presents the probability of exceeding the observed value was used for the same purpose as F value. Both tests verified the sample homogeneity between groups and within group equally.

$$F = \left(\frac{MSbs}{MSws}\right) \qquad (1)$$

Where:

MSbs: is the normalized variance between samples.

MSws: is the normalized variance within the sample.

The gamma spectrometric analysis performed on ten randomly selected oil shale sub-samples showed Uranium (^{238}U) average radio activity of 366.89 (Bq/kg). The data were analyzed statically using single factor analysis of variance (ANOVA) and showed that the oil shale sample was homogenous, where F_{calc} (0.893) was less than F_{crit} (2.393), Table 2. Additionally, P-value confirmed the sample homogeneity. Therefore, the candidate SRM oil shale material was verified for its homogeneity between groups and within group, Table 2.

Table 2. Gamma activity (Bq/kg) for ^{238}U in ten sub-samples of SJL-1.

Sample ID	**Trial 1**	**Trial 2**	**Trial 3**
S1	333.88	326.79	373.23
S2	395.08	363.64	406.58
S3	330.03	335.51	385.87
S4	356.16	355.70	378.28
S5	317.87	365.19	341.10
S6	346.05	322.94	392.81
S7	385.01	335.79	359.24
S8	386.09	390.67	370.78
S9	365.26	339.03	370.46
S10	358.37	318.65	420.93

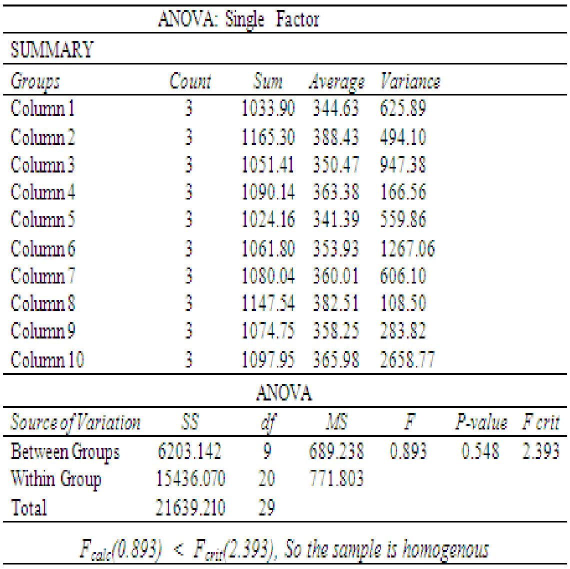

ANOVA: Single Factor

SUMMARY

Groups	*Count*	*Sum*	*Average*	*Variance*
Column 1	3	1033.90	344.63	625.89
Column 2	3	1165.30	388.43	494.10
Column 3	3	1051.41	350.47	947.38
Column 4	3	1090.14	363.38	166.56
Column 5	3	1024.16	341.39	559.86
Column 6	3	1061.80	353.93	1267.06
Column 7	3	1080.04	360.01	606.10
Column 8	3	1147.54	382.51	108.50
Column 9	3	1074.75	358.25	283.82
Column 10	3	1097.95	365.98	2658.77

ANOVA

Source of Variation	*SS*	*df*	*MS*	*F*	*P-value*	*F crit*
Between Groups	6203.142	9	689.238	0.893	0.548	2.393
Within Group	15436.070	20	771.803			
Total	21639.210	29				

F_{calc}(0.893) < F_{crit}(2.393), So the sample is homogenous

3.1.3. Total Alpha/Beta Activity

The total alpha/beta activity spectrometric analysis performed on ten randomly selected oil shale sub-samples indicated a total average activity of 2.2 (Bq/kg). Their single factor analysis of variance (ANOVA) showed that the oil shale sample was homogenous, where F_{calc} (1.349) was less than F_{crit} (2.393), additionally P-values confirmed this results, Table 3. Therefore, the candidate SRM oil shale material was verified for its homogeneity between groups and within group.

The analysis of soil and oil shale samples using either gamma spectrometry or total alpha beta activity is affected often by different factors such as sample geometry, stability, homogeneity, and the complexity of the obtained spectrums. Therefore, it was necessary to use the same homogeneity testing method protocol for the spiked reference materials and the candidate SRM (Biagini et al. 1995).

Table 3. Total alpha/beta activity (Bq/kg) for 10 sub-samples of SJL-1.

Sample ID	Trial 1	Trial 2	Trial 3
S1	2.36	2.10	2.34
S2	2.26	2.18	2.26
S3	2.69	2.09	2.28
S4	2.34	2.10	2.23
S5	2.56	2.36	2.40
S6	1.74	2.03	2.29
S7	2.12	2.24	2.03
S8	2.38	2.09	2.28
S9	2.36	2.14	2.02
S10	2.02	2.31	2.17

Single Factor Analysis (ANOVA)

SUMMARY

Groups	*Count*	*Sum*	*Average*	*Variance*
Column 1	3	6.80	2.267	0.021
Column 2	3	6.70	2.233	0.002
Column 3	3	7.06	2.353	0.094
Column 4	3	6.67	2.223	0.014
Column 5	3	7.32	2.440	0.011
Column 6	3	6.06	2.020	0.076
Column 7	3	6.39	2.130	0.011
Column 8	3	6.75	2.250	0.022
Column 9	3	6.52	2.173	0.030
Column 10	3	6.50	2.167	0.020

ANOVA

Source of Variation	*ss*	*df*	*MS*	*F*	*P-value*	*F crit*
Between Groups	0.367	9	0.041	1.349	0.274	2.393
Within Group	0.604	20	0.030			
Total	0.971	29				

F_{calc}(1.349) < F_{crit} (2.393), So the sample is homogenous

3.2. Results of Interlaboratory Study

Twelve laboratories from Jordan, Canada, Germany and Saudi Arabia participated in the preliminary interlaboratories study. The different analytical methods used by the participating laboratories for the different analytes were summarized in Table 4. Calibration was performed by a calibration graph or standard addition methods. Each participating laboratory received two sample bottles containing 100 g of candidate oil shale SRM and was asked to conduct a minimum of five independent replicates on the available analytical methods (Quevauviller, 2001; Zischka, 2002).

The results collected from the participation laboratories were analyzed statistically after outlying the extreme values applying Q-test. The satisfying result for each laboratory was evaluated using z scores method ($|z| \leq 2$). Based on statistical analyses which are described in the following sections, the oil shale candidate SRM constitutes were classified into three groups: 16 certified 8 averages and 37 either range or information. Two examples of interlaboratory study results for Fe_2O_3 and Zn are presented with lab codes and methods, Figure 2-a and 2-b.

Table 4. Summary of analytical methods used for certification of SJL-1 analytes.

Analyte	Method
Al_2O_3, TiO_2, MgO, Fe_2O_3	WDXRF, EDXRF, ICP/MS, ICP/OES, AAS
P_2O_5, K_2O	WDXRF, EDXRF, ICP/MS, ICP/OES
Na_2O, CaO	WDXRF, EDXRF, ICP/MS, ICP/OES, AAS, NA
MnO	WDXRF, ICP/MS, ICP/OES
SiO_2	WDXRF, XRF
S	ELEM, EDXRF, ICP/MS, ICP/OES
C, H, C_{org}	ELEM
N	ELEM, Kjeldahl
U	ICP/MS, EDXRF, NA, Gamma
Zn, Cr	WDXRF, EDXRF, ICP/MS, ICP/OES, AAS, NA
Ni	WDXRF, ICP/MS, ICP/OES, AAS, NA
V	WDXRF, EDXRF, ICP/MS, AAS
Sr	WDXRF, EDXRF, ICP/MS, ICP/OES-MIC
Cu	WDXRF, EDXRF, ICP/MS, ICP/OES-MIC, AAS
Mo	ICP/MS, ICP/OES, AAS, NA
Ba, Co	ICP/MS, ICP/OES, NA
Cd	EDXRF, ICP/MS, ICP/OES
As, Rb	EDXRF, ICP/MS, ICP/OES, NA
Li	ICP/MS
Sb, Ce, Ta, Th,	ICP/MS, NA
Se, Hf, La, Ag, W, Sc,	EDXRF, NA
Y	EDXRF, ICP/MS
Zr	WDXRF, EDXRF, ICP/MS
Ru	WDXRF, EDXRF
LOI, Ash	Gravimetery
H_2O	Gravimetery, IR

a) Fe_2O_3T z scores

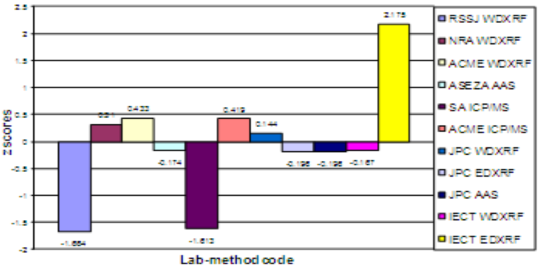

b) Zn z scores

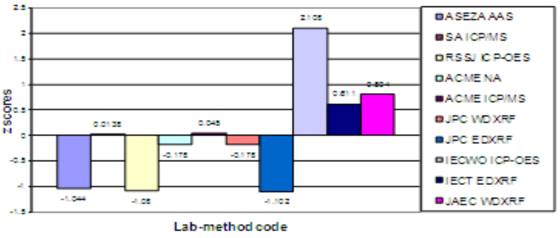

Fig 2. Z scores from interlaboratory study results a) Fe_2O_3 b) Zn including lab codes and methods.

3.3. Certification Measurements

Certified values of the analytes in candidate SRMs were determined using different statistical approaches that frequently used for preparation and certification of SRMs **(**Abbey, et al., 1979; Kane, et al. 1990; Quevauviller, 2001; Zischka, 2002; Al-Masri**)**. Q-test was applied to check whether a certain suspected data joined belongs to the set of data or not, then average value should lie within ± 2S (standard deviation) to be accepted. The criteria used in the present work for determining the certified concentrations was developed according to the following procedure:

1. Estimation of the following parameters at 95% confidence level: arithmetic mean, standard deviation, median, coefficient of skewness, coefficient of kurtosis and relative standard deviation (RSD).
2. If RSD, skewness and kurtosis coefficients deviate from the normal distribution significantly at 95% confidence level. Then extreme values are rejected one at a time until the coefficients (skewness and kurtosis) and (RSD) indicate a normal distribution.
3. If RSD<15% stop rejection as attainable conformity between individual data and overall means is achieved, then go to step 6.
4. Use (two – sided T-test) to determine whether additional rejection is needed. If ($T > T_c$) reject until no T-test rejection is needed, If ($T < T_c$) proceed to step 6.
5. Check new RSD after each rejection and compare it as in step 3.
6. After getting acceptable RSD as in step 3, use ANOVA single factor analysis to check for the analyte results obtained from different methods. If ($F_{calc} < F_{crit}$) at 95% confidence level and P-value are insignificant. Then agreement between at least three independent methods of analysis was verified according to the requirement for certificating a constituent concentration (Biagini et al. 1995; Walker and Brookmeen, 1998; Vander Veen et al. 2001).

After performing the last rejection according to the previous criteria, the oil shale candidate SRM analyte concentrations were classified into three groups: certified, average and range.

1. Certified value is reported, if:
    - At least five laboratory averages remain after last rejection.
    - At least three different methods of analysis used after last rejection without significant difference by using ANOVA single factor analysis as in step 6 ($F_{calc} < F_{crit}$) at 95% confidence level.
    - RSD < 15% after last rejection.
2. Average value is reported if at least five laboratory averages remain after last rejection, but either or both of the other conditions for certification are fail.
3. Range value is only reported for the surviving laboratory average if there are fewer than five laboratory averages remain after the last rejection.

3.4 Certificate

The results of the certificated values of SJL-1 were calculated using equation (2) according to the same procedure used often for certification worldwide (Griepink and Muntau, 1987; Al-Masri, et al., 2004; Kane and Potts, 2007), and they were presented as means at ± 95% confidence level.

$$\bar{x} \pm T, (\pm S, P\%, n) \qquad (2)$$

Where

$\bar{x}$: The mean of the measurements.

$p\%$: Confidence level.

T : The scattering of the individual results, which is given in the following equation:

$$T = \frac{t*S}{\sqrt{n}}$$

Where

t : The student factor for the ten replicates at 95% certified level.

S: Standard deviation.

n = Number of individual results.

The final concentration of analytes in the oil shale sample (SJL-1) expressed as certified and average values with their uncertainty are shown in Table 4. However, range values were mentioned only without the statistical uncertainty.

Table 5. Certificate for El-Lajjun Oil Shale (SJL-1).

	Certified values	
Oxide	**wt%**	**± uncertainty**
Al_2O_3	2.513	0.130
P_2O_5	2.899	0.092
CaO	25.512	1.434
TiO_2	0.134	0.014
MgO	0.686	0.060
K_2O	0.360	0.020
Fe_2O_3 total	0.967	0.088
Na_2O	0.178	0.015
MnO	0.0037	0.0005
Element	**ppm**	**± uncertainty**
S	3.638	0.450
Element	**ppm**	**± uncertainty**
U	27.26	3.68
V	265.28	10.89
Cr	396.40	28.28
Zn	755.42	61.95
Ni	193.61	19.66
Cu	97.09	6.98
Sr	800.52	65.08
	Average values	
Constituent	**wt%**	**± uncertainty**
LOI	37.01	1.02
SiO_2	26.163	٠,٨3
Element	**ppm**	**± uncertainty**
Cd	69.33	24.65
Mo	197.06	50.61
Co	2.62	0.70
Pb	22.26	12.40
Ba	56.33	13.78
As	14.40	6.78
	Range values	
Element	**ppm**	
H	2.235	
N	0.435	
C_{total}	21.591	
C_{org}	16.153	
Rb	11.314	
Sb	2.900	
La	10.430	
Ce	12.330	

Ag	3.550
Li	8.362
W	0.785
Th	1.429
Sc	3.265
Se	41.835
Y	22.733
Hf	0.716
Ru	48.000
Zr	26.177
Ta	0.300
Rh	<1- 65
Cl	<1- 814
Nb	2.370
Be	<1
Sm	1.170
Nd	8.670
Bi	0.100
Yb	1.200
Tb	0.500
Cs	1.000
Ir	5.000
Sn	0.870-100
Au	0.00087-5
Br	4.730
Eu	0.300
Constituents	**Wt%**
Gas loss	4.720
Total oil	13.790
Calorific value	8508.7 J/g

4. Availability

The SJL-1 standard reference material is avialble from Prince Faisal Center for Dead Sea Enviromental and Energy Reserach at Mutah University, Karak, Jordan. Email: Batarseh@mutah.edu.jo, Fax: 00962 32397169. A full report and certificate of analysis is deliveried upon the request of the refrence material, containing detailed information on the preparation of the material, homoginity, technical and statistical evalution results and anlytical methods used and individaul results for each analyte.

The final product of the certified standard reference material packed as 100 g in polyethylene bottles and supplied with a certificate of analysis. This oil shale material (SJL-1) can be used as standard reference material (SRM) for quality assurance, laboratory methods validation and instruments calibration for the analysis of the oil shale ores on national and international research and industrial studies.

Acknowledgements

The authors would like to acknowledge the University of Jordan for the financial support of this work. The authors are also extending their thankful to all national and international contributing laboratories for their invaluable help and support for conducting the different analyses of the oil shale sample SJL-1.

Dedication

The authors are dedicating this work for the spirit of deceased Prof. Najwa Zaharan, who was served as vice president of Egyptian Atomic Energy Agency and the coordinator of this project within the Arab collaborative projects initiated by Arab Atomic Energy Agency (AAEA), 2007-2009.

References

[1] Alali, J., 2006. International Conference on Oils Shale: “Recent Trends in Oil Shale”, Jordan Oil Shale, Availability, Distribution, and Investment Opportunity. 7-9 November 2006, Amman, Jordan.

[2] Abbey, S., Meeds, R., Belanger., 1979. Reference samples of rocks, the search for best values, Geostandards Newslett, 3: 121- 133.

[3] Al-Masri, M. Aba, A. Al-Hamwi, A. and Shakhashiro, A., 2004. Preparation of in house reference soil sample containing high levels of naturally occuring radioactive materials from the oil industry, Appl Radiat Isotopes, 61:1397-1402 .

[4] Biagini, R. Dersch, R. De Felice, P. Jerome, S.M. Perkin, E. Pona, C. De Sanoit, J. Woods, M.J., 1995. Homogenity testing of spiked reference materials, Sci.Total Environ, 173/174: 267-274.

[5] Gladney, E.S. and Roelandts, I., 1988. Compilation of elemental concentration data for USGS BHVO-1, MAG-1, QLO-1, RGM-1, SCo-1, SDC-1, SGR-1 and STM-1, Geostandards Newslett, 12: 253-362.

[6] Heidelberg, S.B., 1988. Standard reference materials for the determination of polycyclic aromatic hydrocarbons, Fres. J Anal. Chem, 332(6): 573-582.

[7] Kane, J.S, Arbogast, B. and Leventhal, J., 1990. Characterization of Devonian Ohio shale SDO-1 as a USGS geochemical reference sample, Geostandards Newslett, 14:169–196.

[8] Petrov, L.L, Korotaeva, I.Ya, Kornakov, V.V. Yu.H, Persikova, Malykh, L.A, Prokopchuk, S.I. and Susloparova, V.E., 1999. Development of multi element reference samples of the composition of rocks in the black-shale formation with certification of some noble metals, Platinum of Russia, Collection Transact, 4: 263–280.

[9] Petrov, L., Kornakov, Y., Korotaeva, I, Anchutina, E., Persikova, L., Susloparova, V., Fedorova, I., Shibanov, V., 2004. Multi-Element Reference Samples of Black Shale. Geostandards and Geoanalytical Research 28(1), 89–102.

[10] Quevauviller, Ph., 2001. Certified refrence materials for the quality control of inorganic analyses of manufacturing products (glass, polymers, paint coatings). Trends in Analytical Chemistry 20(8), 446-456.

[11] Smirnova, E. V, Fedorova, I. N, Sandimirova, G. P, Petrov, L. L ,Balbekina, N. G. and Lozhkin, V. I., 2003. Determination of rare earth elements in black shales by inductively coupled plasma mass spectrometry, Spectrochim. Acta B, 58 (2): 329-340.

[12] Schmid, S and Andersson, J.T., 1997. Critical Examination of the Quantification of Aromatic Compounds in Three Standard Reference Materials, Anal. Chem, 69(17): 3476-3481.

[13] Vander Veen, A.M.H., Linsinger, T., Pauwels, J., 2001. Uncertainty calculations in the certification of reference materials (2-Homogeneity study), Accred. Qual. Assur, 6: 26.

[14] Walker, R.F., Brookman, B., 1998, Guidelines for the in-house production of reference LGC/VAN/1998/040.

[15] Wise, S.A., 2002. Standard Reference Material (SRM) for the determination of polycyclic aromatic compounds—twenty years of progress, Polycycl. Aromat. Comp, 22(3): 197-230.

[16] Zischka, M., Schramel, P., Muntau, H., Rehnert, A., Gomez, M., Stojanik, B., Wannemaker, G., Dams, R., Quevauviller, P., and Maier, E., 2002. A new certified reference material for the quality control of palladium, platinum and rhodium in road dust, BCR-723. Trends in Analytical Chemistry 21(12), 851-868.

JJEES

Volume 4 (Special Publication, Number 2), Jan. 2012
ISSN 1995-6681
Pages 23- 27

Jordan Journal of Earth and Environmental Sciences

Production of Natural β-Carotene from *Dunaliella* Living in the Dead Sea

Sadeq Emeish*

Al-Balqa' Applied University Faculty of Engineering TechnologyDepartment of Chemical Engineering

,P.O.Box (15008), 11134 Marka, Amman-Jordan.Fax: 00962-64790350

Abstract

The main aim of this work was to investigate the possibility of Beta Carotene production using micro algae *Dunaliella salina* existing in the Dead Sea. The research being carried out covers a number of interdependent steps and, is focusing_on laboratory scale cultures. Under stress conditions such as high light intensity or nutrient starvation, cells of the unicellular alga *Dunaliella salina* overproduce β-carotene, which is accumulated in the plastids in newly formed triacylglycerol droplets. *Dunaliella* was isolated from the Dead Sea and cultivated using a certain media until the cell count was 500,000 cell/mL. The cultivation step was monitored and video captured using a digital microscope with USB camera, then it was centrifuged and extracted using different kinds of organic solvents. The amount of dry weight was 3 g/L of which 3-6% was β-carotene. Freeze drying step was performed to obtain β-carotene as powder. The analysis of the powder was carried out by the research and development department at one of the pharmaceutical companies. It was evident that a pilot plant investigation should be the next step on the way of commercialization of such a profitable process.

Keywords:*Dunaliella*; Cultivation; Harvesting; Centrifugation; β-Carotene;β-Carotene Extraction; Freeze drying; Dead Sea.

1. Introduction

The green unicellular flagellate *Dunaliella* salina is the richest natural source of the carotenoid β-carotene. The halophilic species of *Dunaliella* also accumulate very high concentrations of glycerol. *Dunaliella salina* was first proposed as a commercial source of β-carotene and latter as a source of glycerol. β-carotene from *Dunaliella* is now being produced on a commercial scale in Australia, the USA and Israel. *Dunaliella* is a unicellular, bi-flagellate, naked green alga which is morphologically similar to chlamydomonas with the main difference being the absence of a cell wall in *Dunaliella* [1]. In *Dunaliella* salina and *Dunaliella* parva the chloroplast accumulate large quantities of β-carotene (as droplets) so that the cells appear orange-red rather than green. Teodoresco described tow species: *D.salina* and *D. viridis* .*D.salina* has somewhat larger cells and under suitable conditions it synthesizes massive amounts of carotenoid pigments, coloring the cells brightly red while *D.viridis* never produces such red cells [1, 6].

To investigate the apparently strict interdependence of carotenoid overproduction and the formation of sequestering structures, we exploited the unicellular alga *Dunaliella Salina* as a laboratory system inducible for enhanced carotenoid formation [7]. When exposed to stress conditions such as high light intensity or nutrient starvation, two stereoisomers of β-carotene, all-*trans* and 9-*cis* β-carotene, accumulated, reaching up to 14% of the cell's dry weight, with the pigment being deposited into plastid. We now know that not all *Dunaliella* species produce massive amounts of carotene and those that can do so only under suitable conditions [1].

1.1. Historical overview:

Hundred years have passed since the description of the genus *Dunaliella*, the unicellular green alga which is responsible for most of the primary production in hypersaline environments worldwide. First sighted in 1838 in saltern evaporation ponds in south France by Michel Flix, *Dunaliella*, was named after its discoverer by Teodoresco in 1905. In the century that has elapsed since its formal description of the genus *Dunaliella* has become a convenient model organism for the study of salt adaptation in alga. The establishment of the concept of organic compatible solutes to provide osmotic balance was largely based on the study of *Dunaliella* species. Moreover, the massive accumulation of β-carotene by some strains under suitable growth conditions has led to interesting biotechnological applications [8, 9].

---

* Corresponding author. Email:s_emeish@yahoo.com

.

1.2. Dunaliella in the Dead Sea:

Systematic quantitative studies on the biology of the Dead Sea have been performed only since 1980. It is now well established that the Dead Sea biota are domained by the unicellular green alga *Dunaliella.* The pigment responsible for the brightly red coloration displayed by *D. salina* was recognized already very early as a carotenoid. The carotenoids are of fundamental importance to life. Not all their functions are fully understood, but it is evident that carotenoids are intimately involved in the protection of organic molecules from oxidative destruction and in light-induced energy production via photosynthesis [10].

In the alga, this β-carotene seems to act a sun screen to protect the chlorophyll and the cell DNA from high irradiance which characterizes the normal habitat of *D. salina*. β-carotene is a valuable chemical, in high demand as a natural food coloring agent, as a pro vitamin A as additive to cosmetics and as a health food [10]. The purified β-carotene compositions may be administrated for a variety of therapeutic or prophylactic uses to humans or in veterinary applications, the compositions may used as a vitamin preparation, alone in conjunction with other vitamins to supplement dietary intake of vitamin A and in thus to treat or prevent conditions associated with vitamin A insufficiency. The compositions of invention can also be used in prevention or treatment of a variety of diseases pathological conditions associated with free radicals and lipid auto-oxidation. In other uses the high purity natural β-carotene is administrated therapeutically or prophylactically for a variety of cancers particularly epithelial cell cancers [10]. Preparations have shown significant protection against various tumors in animals. Accordingly, the beta carotene preparation is indicated for use in therapeutic methods for a variety of cancers including in humans. β-carotene preparations have shown to be useful in treating, inhibiting or otherwise preventing tumors in humans. β-carotene is generally regarded as the most commercially important and widely used carotenoid. It is used as a food coloring agent, an antioxidant and an important and safe pro-vitamin A source.

2. Methodology

2.1. Cultivation

The development of culture conditions is very important step in terms of favoring growth of the chosen strain and, at the same time, discouraging growth of contaminants. It has already been concluded that carotenoid production has to be carried out under a different set of conditions from those favoring the increase in biomass. Therefore the optimization of both sets of conditions is necessary, see Figure (1), the cultivation was monitored and video captured by a digital microscope with USB camera, Figure (2). *Dunaliella* also has a very wide pH tolerance ranging from pH 1 t o pH 11. In fact *D.*salina is one of the most environmentally tolerant eukaryotic organisms known and can cope with a salinty range from seawater 3% NaCl to NaCl saturation 31% NaCl, and a temperature range from < 0ºC to >38ºC [2, 3, 4, 5, 7].

When the sunlight, fertilizer, and water temperature are excellent photosynthesis is often limited by the concentration of carbon-dioxide. Extra carbon-dioxide could be added to aquaculture waters and this could increase production, but it is necessary to keep the carbon-dioxide from escaping to the atmosphere.

Fig 1. Dunaliella Culture.

Fig 2. Digital microscope with USB camera.

The following table illustrates the optimized cultivation media for the Dunaliella species:

Table 1. Modified Johnson media

To 5 L of distilled water add :	
NaCl	24% per unit volume
$MgCl_2.6H_2O$	7.65 g
$MgSO_4.7H_2O$	2.6 g
KCl	1.02 g
$CaCl_2.2H2O$	1.02 g
KNO_3	5.1 g
$NaHCO_3$	0.2 g
KH_2PO_4	0.2 g
Fe-solution	51 mL
Na_2EDTA	945 mg
$FeCl_3.6H2O$	1220 mg
Trace element solution	51 mL
H_3BO_3	305 mg
$(NH_4)6Mo_7O_{24}.4H_2O$	190 mg
$CuSO_4.5H_2O$	30 mg
$CoCl_2.6H_2O$	25.5 mg
$ZnCl_2$	20.5 mg
$MnCl_2.4H_2O$	20.5 mg
Adjust pH to 7.5 with HCl	

2.2. Cell Counting

When the algal culture reaches the desired density (about 0.25 - 0.5 g dry weight/L), the algae were harvested from the tank by pumping out the water slurry containing the dispersed algae. Transfer 1 mL of each cell type to different test tubes, and fix the Tetrahymena by adding 1 mL of formaldehyde. First count the algae. Position the hemocytometer on the microscope stage and adjust the objective so you are foucsed on the grid lines. Count the number of cells in the 4 A squares plus the central C square and average them by dividing by 5. Each value, multiplied by 10 gives you the cells per mL.

2.3. Using a Counter Chamber

A device used for determining the number of cells per unit volume of suspension is called a counting chamber. The most widely used of chamber is called a hemocytometer, since it was originally designed for performing blood cell counts.

2.4. Harvesting

Harvesting the crop is one of the most critical steps. Swimming species are usually harvested by partially draining a tank then sieving it. Sessile crops are usually removed manually. Large plankton can be filtered from the water. Harvesting techniques vary depending on the nature of cultivation media and the degree of management employed [8]. Different methods were tested including flocculation, centrifugation and flotation, and it was found that centrifugation is the best one, but it will be very costly for large scale application. The dry weight content was 3g/L of which 3-6% was β-Carotene.

Fig 3 Extraction of Beta Carotene.

2.5. Concentration

The slurry is then concentrated in algal content, typically by evaporation, centrifugation, flocculation, ultra filtration, flotation, etc. Results have shown that the flocculation using alum followed by centrifugation will be efficient and less energy consuming rather than direct centrifugation [8]. Following the concentration step of the slurry the salt was largely removed by the addition of fresh hot water and ultra filtration. This also breaks the algal cells, liberating the beta-carotene.

2.6. Centrifugation

The concentrate was then centrifuged in a suitable continuous flow centrifuge, such as cream separator, to yield an upper cream phase of carotene and lipid, which is continuously removed [9]. The block flow diagram of the process is shown in Figure (4).

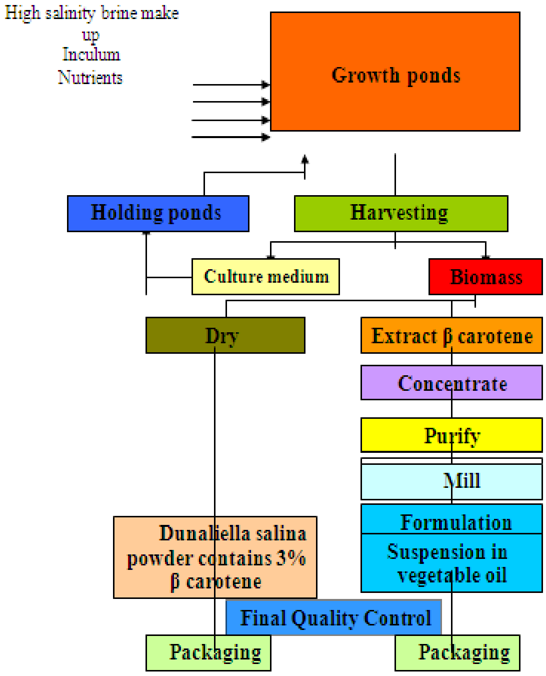

Fig 4. Block flow diagram.

2.7. Extraction

Another critically important aspect of *Dunaliella* β carotene production is the extraction of β carotene, see Figure (3). The process used for extraction depends, in part, on the harvesting procedure used and on market requirements. Extraction using conventional organic solvents is efficient, but may not be acceptable to customers seeking a natural product [6, 9]. More acceptable alternative extraction methods use hot vegetable oil or jojoba oil.

2.8. Freez Drying

In chemical synthesis, products are often freez dried to make them more stable, or easier to dissolve in water for subsequent use. In bio separation, freeze drying can also be used as a late-stage purification procedure, because it can effectively remove solvents. Furthermore, it is capable of removing molecules with low molecular weights that are too small to be filterd out by a filtration concentration membrane. Freeze drying has a long process time, because the addition of too much heat to the material can cause melting or structural deformations [6, 8]. Therefore, freeze drying is often reserved for materials that are heat sensitive, such as proteins, enzymes, microorganisms, and blood plasma. The low operating temperature of the process leads to minimal damage of these heat sensitive products. The freeze drying process was carried out under -50°C and 1.63 hecta pascal using the freeze dryer of type Heto Power Dry PL 3000. The obtained powder was analyzed by the research & development department at one of the Pharmaceutical companies.

3. Results

3.1. Cultivation

Dunaliella cells were found in samples collected from the Dead Sea. The cells were observed under digital microscope with USB camera, so that *Dunaliella* cells were cultivated in an inorganic media (Johnson media). Ordinary air was supplied at room temperature 25±2°C under high illumination.

3.2. Cell Counting

The number of *Dunaliella* cells was found to be about 500,000 cell/mL using Hemocytometer slide under microscope. Cell filtration was performed for five samples and a sequential curve was plotted with a slope near to 0.0407 (approximately horizontal line resulted) and an intercept of 2.1129 indicating a cell density of 2.1129 g dry weight per litter, Figure (5). The number 2.1129 indicates that harvesting can be started. A 1 m^3 cultivation media is found to contain approximately 114.1 g β-carotene. The fluctuation in the dry weight can be attributed to the manual filtration of the samples.

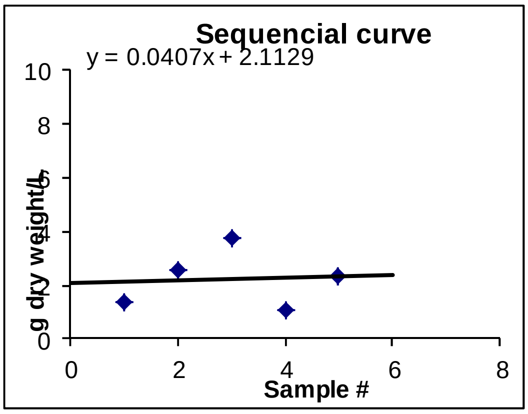

Fig 5. Sequential curve of filtered samples.

3.3. Extraction

After cells were harvested by centrifugation with 4000 rpm, β-carotene was extracted from *Dunaliella* cells using 2 solvents, 96% n-hexane and hot vegetable oil /jojoba oil separately, see Figure (6). Jojoba oil was chosen as extraction solvent due to:

- Jojoba Oil is used medicinally. It contains vitamins E and B complexes. It also has the minerals silicon, chromium, copper and zinc. It has a very high percentage of iodine. The iodine concentration gives the Jojoba oil a great power to heal.
- Jojoba is liquid wax highly penetrating and closely resembles human serum.
- Inflammatory, anti-oxidant, prolong shelf life.
- Jojoba Oil is highly rich in Vitamin C, as well as processing sulfur, copper, and cobalt and has traces of tin, and a volatile oil.

Fig 6. β-carotene extracted with jojoba oil

3.4. Freeze Drying

A centrifuged suspended in distilled water samples were dried using a freeze dryer device at a temperature of -85 °C and 0.32 hpa pressure, the run time was four hours to obtain powder. 1g *Dunaliella* powder was obtained, Figure (7).

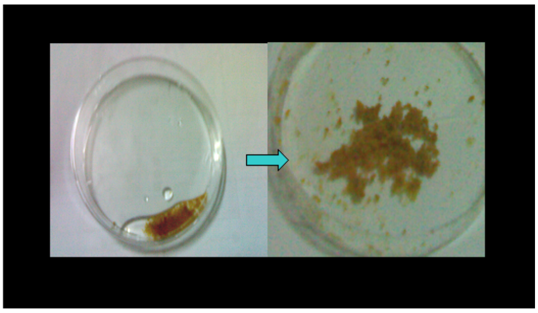

Fig 7. Freeze dried Dunaliella powder.

Scanning spectrum of the extracted pigments is shown in Figure (8).The highest peak was appeared at 440 nm wave length and indicated an optical density value of 2.7. The shorter wave length peak is related to other carotenoids .

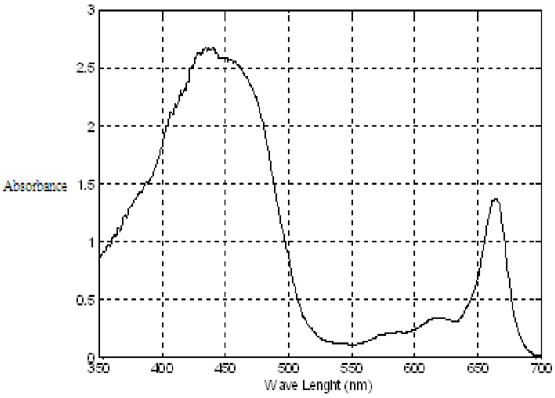

Fig 8. Absorption Spectra of β-carotene extracted with hexane .

4. Discussion of Results

Although β-carotene can be synthesized or extracted from other natural sources, *Dunaliella* is still the richest and best natural source of this cartenoid. The most suitable media for the isolated *Dunaliella* species at lab scale cultivation was found to be modified Johnson media, which gave the highest growth and β-carotene production. Pigment analysis using spectrophotometer indicates the presence of β-carotene, in addition to other related pigments. As can be seen from Figure (5), the dry weight per litter cultivation media was 2.1 gram of which 5.8% was β-carotene. Then in 1m^3 cultivation media 114.1 g highly pure β-carotene exists. To obtain 1 kg of highly purified β-carotene 8.8 m^3 cultivation media is needed, its selling price is about 3000 US$/kg.

The best method for concentrating the algal material without smashing its clusters was found to be gathering it in aseparatory funnel and permit it to sediment by gravity force. The best extraction solvents were hexane, ether, jojoba oil or light vegetable oil for dietary uses. It was noted that sun-dried or heat dried samples of *Dunaliella* were rapidly degraded in terms of keeping β-carotene not oxidized, so freeze drying process employed and showed high efficiency in drying samples without oxidizing any part of β-carotene [8].

Furthermore, the use of β-carotene as a food or food additive and a nutritional supplement means that a high quality product is required. This means that great care must be taken in the extraction and formulation steps.

5. Conclusions

The following points can be concluded as the main results of this study:

1. Natural Beta Carotene can be produced from *Dunaliella* microalgae existing in the living Dead Sea.
2. Tanks are adequate for the cultivation of microalgae *Dunaliella*.
3. Harvesting by centrifugation and solvent extraction are necessary steps for the production of natural β-carotene.
4. Adjusting the ratio of 9-cis to all-trans is of vital importance as natural β-carotene is a precursor of vitamin A.
5. Freeze drying step is necessary to obtain β-carotene as powder without affecting its sensitive structure.

References

[1] Gonzalez, M.J., Moreno,J., Monzano, J.C., Florencio, F.J., Guerrero, M.G., Production of *Dunaliella salina* biomass rich *in 9-cis- beta-carotene* and lutein in a closed tubular photo bioreactor, Journal of Biotechnology, 115 (2005) 1, 81-90.

[2] Ben-Amotz, A., The biotechnology of cultivating Dunaliella for production of β-carotene rich algae, Bio resource Technology, 38 (1991) 2-3, 233-235.

[3] Hejazi, M.A., Wiiffels, R.H., Effect of light intensity on β-carotene production and extraction by Dunaliella salina in two phase bioreactors, Biomolecular Engineering, 20 (2003) 4-6, 171-175.

[4] Borowistzka, L.J., Development of western biotechnology's algal β-carotene plant, Bio resource Technology, 38 (1991) 2-3, 251-252.

[5] Ben-Amotz, A., New mode of Dunaliella biotechnology two-phase growth for β-carotene production, Journal of Applied Phycology, 7 (2003) 1, 65-68.

[6] Raja, R., Hemaiswarya, S., Rengasamy, R., Exploitation of Dunaliella for β-Carotene Production,Applied Microbiology and Biotechnology, 74 (2003) 3, 517-523.

[7] Ali Hosseini Tafreshi and Mansour Shariati, Pilot Culture of Three Strains of Dunaliella salina for β-Carotene Production in Open Ponds in the Central Region of Iran, World Journal of Microbiology and Biotechnology, 22 (2006) 9, 1003-1006.

[8] Chidambara Murthy, K.N., Production of β-Carotene from Cultured Dunaliella Sp. And evaluation of Biological Activities, PhD Thesis, University of Mysore, India, December-2005.

[9] Chidambara Murthy, K.N., Rajesha ,J., Vanitha,A., Sowmya, P.R., Mathadera Swamy, M., Ravishankar, G.A., In-VivoAntioxidant Activity of Cartenoids From Dunaliella salina-A green Microalgae, Life Sciences 76 (2005)12, 1381-1390.

[10] Avron,M., Ben-Amotz,A., Dunaliella Physiology, Biochemistry and Biotechnology, CRC Press,1992.

JJEES

Volume 4 (Special Publication, Number 2), Jan. 2012
ISSN 1995-6681
Pages 29- 34

Jordan Journal of Earth and Environmental Sciences

The Leachability Propensity of El-Lajjun Jordanian Oil Shale Ash

Adnan Al-Harahsheh[a,b,*], Awni Al-Otoom[c], Mohammad Al-Harahsheh[d], Mamdouh Allawzi[c], Rida Al-Adamat[b], a Mohammed Al-Farajat [b] , Omar Al-Ayed[e]

[a]Department of Chemical Engineering, Mutah University, Karak Jordan

[b]Institute of Earth & Environmental Sciences, Al al-Bayt University, Al-Mafraq, Jordan

[c] Department of Chemical Engineering, Jordan University of Science and Technology, Irbid, Jordan

[d]Department of Mining Engineering, Al-Hussein Bin Talal University, Ma'an, Jordan

[e]Department of Chemical Engineering, Al-Balqa Applied University, Amman Jordan

Abstract

This work reports the leachability of heavy metals and major anions from Jordanian spent oil shale after combustion. Oil shale samples were combusted at temperatures of 550°C, 650°C, 750°C and 850°C. Characterization of the produced solid ash was performed based on XRD analyses. Leaching tests on the ash samples were conducted for different periods of time. Experimental results indicate that the level of heavy metals such as Cd, Pb, Zn, Cu, Cr in the leachate is below the maximum levels set by the Environmental Protection Authority (EPA). For instance, the maximum level of Cd measured in the leachate solution was 0.14 ppm, which is below the EPA limit. Results also indicate that even though the level of heavy metals in all samples was below the EPA limits, yet the level of heavy metals increases as the temperature of the ashing process increases. The effect of ashing temperature on ash cation exchange capacity (CEC) and the pH of ash solution were studied and found to increase with increasing ashing temperature.

Keywords: Oil Shale; Ash; Leachability; Heavy Metals.Introduction

1. Introduction

Jordan has limited energy resources such as crude oil or natural gas compared to its neighboring countries. However, oil shale is an important and unutilized energy source in the country. More than 50 billion tons of oil shale deposits are discovered in different areas especially in the middle and southern parts of the country (Dabbas, 1997). The soaring prices of oil have led many investors to consider oil- alternative energy resources. The oil equivalent of oil shale around the world is estimated to be around 30 times the reserve of the crude oil (Russell, 1990). Commercialization of Jordanian oil shale in the form of utilizable oil is being studied. The high percentage of ash in the Jordanian oil shale (50-60%) makes the future of utilization of oil shale as a source of liquid fuel uncertain (Jaber *et al.*, 1999). One method is widely used in utilizing oil shale is the retorting process. This process involves extraction of bituminous oil at elevated temperatures in non-oxidizing conditions.

There are growing concerns over the fate of spent shale after retorting process. One of these concerns is mainly the leachability propensity of trace elements of the spent oil shale into underground water.

The chemical nature of the minerals in the spent shale can change considerably during both the retorting and the combustion stages. These chemical changes will affect both the physical and chemical stability of the spent shale and are important when determining disposal strategies for the waste solid (Bell *et al.*, 1986).

Disposal of mining wastes, spent shale (semicoke) and combustion ashes needs additional land use. According to the study of the European Academies Science Advisory Council (Francu *et al.*, 2007)**,** after processing, the waste material occupies a greater volume than the material extracted, and therefore cannot be wholly disposed underground. The primary threat to water quality is generally considered to be the leachate from spent, i.e. retorted, oil shale. Typically oil shale retorting result in the generation of slightly over one tone of spent shale per barrel of shale oil (EASAC, 2007) .

In order to study the migratory behavior of trace elements in oil shale at retorting, tests were performed in laboratory with oil shale of the Huadian deposit of China at different temperature from 360 to 560^{o}C (Bai *et al.*,

---

[*] Corresponding author. e-mail: adnan@mutah.edu.jo.

2008)). Results indicate that trace elements are richer in oil shale than earth crust. Also, for most of the elements, their release from oil shale can be promoted by higher heating rate.

The physical and thermal properties of spent shale affect the design and characteristics of embankments used for storing the material prior to ultimate disposal. Leaching tests are used to determine if spent shale must be treated as a hazardous material for disposal. The Institute of Gas Technology and the Illinois Institute of Technology conducted tests to determine some physical and thermal properties and leaching characteristics of spent shale samples from six states in the Eastern United States (Michael and Surendra, 1991). The samples were processed in the continuous, laboratory scale, pressurized fluidized bed hydro-retorting (PFH) reactor at 4.2 MPa (600 psig) and a temperature of 482°C. The physical and thermal properties determined included particle size distribution, permeability, compressibility, compatibility, consolidation, shear stress, cohesion and thermal conductivity. The samples of spent shale were also agglomerated with air at a temperature of 1093°C to determine the effects on leachability. The results showed that the physical and thermal properties of the six spent PFH shales differ considerably. The results also showed that none of the spent shale samples exhibited any significant metals leachability under the acidic test conditions. In general, thermal agglomeration further reduced the levels of metals leached from the spent shales.

Recently the leachability of retorted Jordanian oil shale at a temperature of 500ºC was studied (Ibrahim and Jaber, 2007). They found no detectable release of heavy metals from the ash to percolating water. However, to the authors' best knowledge there was no single study which investigated the release of heavy metals from Jordanian oil shale ash after combustion.

The main objective of this work is to study the leachability propensity of spent oil shale after ashing process at different temperatures. The release of trace elements such as cadmium, lead, zinc and copper from oil shale ash was investigated.

2. Methods

2.1. Samples Locations

Samples were collected from El-Lajjun oil shale area, which is located in the central part of Jordan as shown in Figure (1), with an estimated area of 33.6 km^2. The oil shale deposits in El-Lajjun area are shallow, near the surface and can be utilized by open cut mining method (Ibrahim and Jaber, 2007).

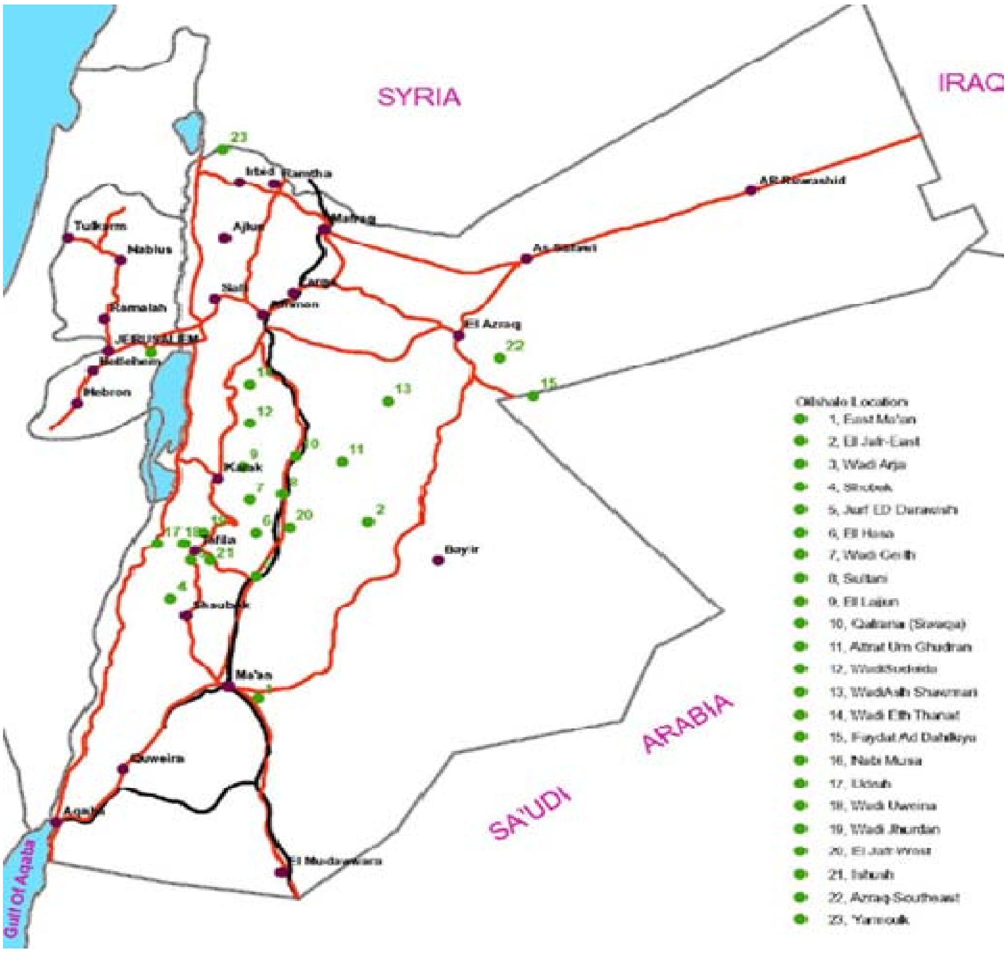

Fig 1.Oil shale Location map (Ellajun No 9) (NRA, 2011)

2.2. Experimental Work

2.2.1. Materials

A representative fresh oil shale samples were obtained from the outcrop of El-Lajjun deposit. These samples were collected from several positions of the outcrop. They were mixed together and crushed and milled. A representative sample (about 5 kg) was then taken by cone and quartering method which was then sieved to several particle size fractions. A size fraction of 125-250µm was used in this study. Typical characteristics of El-lajjun oil shale samples are presented in Table (1).

Detailed analysis of the oil shale samples used in this study has been obtained in a previous study (Al-Otoom *et al.*, 2005) .The content of some heavy and trace elements of prepared oil shale ash at 850 °C was measured according to standard procedure and the obtained data are illustrated in Table 2.

Table (1) Proximate analysis (air dried) for the El-Lajjun oil shale deposit used in this study according to ASTM D 5142 (Al-Ottom *et al*, 2005).

Property	**Proportions (wt%)**
Moisture	1.1
Volatile Matter	44.0
Ash	54.5
Fixed Carbon	0.4

Table 2. Chemical composition of El-lajjun oil shale Ash in terms of heavy metals.

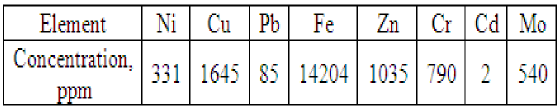

Element	Ni	Cu	Pb	Fe	Zn	Cr	Cd	Mo
Concentration, ppm	331	1645	85	14204	1035	790	2	540

2.2.2. Ashing Process

Oil shale samples were placed in a ceramic crucible, which were then heated in a carbolite furnace to different temperatures of 550°C, 650°C, 750°C and 850°C. A heating rate of 10°C/min was used for this purpose. Samples were kept isothermally at the required temperature for 30 minutes and then cooled to room temperature.

2.2.3. Leaching Process

Dried spent oil shale samples collected by ashing (approximately 10 g) were placed in a volumetric flask (200 ml) and filled with distilled water to the 200 ml mark. Samples were soaked for different time intervals with regular shaking. After each leaching time, the mixture was then filtered out using 0.5 micron filter paper and liquid solutions were then analyzed using ICP. Distilled water was used as the blank.

3. Results and Discussion

3.1. Effect of Temperature and Time on Heavy Metals Leachability.

The level of trace elements such as cadmium, lead, copper, zinc as obtained by ICP (Optima 2000, from Perking) was compared to the maximum levels as set by the EPA. As shown in the Figures (2-6) below, all the above mentioned trace elements were below the maximum level as per the EPA for drinking water within the whole temperature range used. It can be observed that the level of heavy metals in all samples was below the EPA limits. The level of cadmium, as shown in Figure 2, increases with increasing the combustion (ashing) temperature while this level remains almost constant irrespective of the leaching time. On the other hand, the level of lead did not show any significant change with increasing the combustion temperature, while increasing with increasing the leaching time (Figure 3).

Shawabkeh et al. (2004) has shown a propensity of the same oil shale ash to be adsorbing both copper and zinc. Similar observation was obtained in this study; this propensity was found to increase if ash was treated with nitric acid. This result explains the disappearance of zinc and copper from samples of the leachate at all ashing temperatures (Figure 4 and Figure 5)

With regards to chromium leachability from ash (Figure 6), it seems that the highest release of Cr is from oil shale combusted at 650ºC, regardless of soaking time. The release on Cr from oil shale combusted is minimal compared to that ashed at higher temperature. Shawbkeh (2006) observed that Cr adsorption is highest at lower pH. At ashing temperature 550ºC, the pH of the slurry is the lowest as can be seen later (Figure 8). At temperature 650ºC, where the pH is higher, there is no decomposition of carbonates to their oxides (Al-Harahsheh *et al.*, 2011). At temperature 750ºC and higher all carbonates should have been decomposed to oxides like CaO which contribute to formation of more hydroxide groups. At the same time, at high pH values, Cr presents in trivalent state and therefore, with the present of high OH^- concentration there is little chance for Cr to be released from oil shale ash.

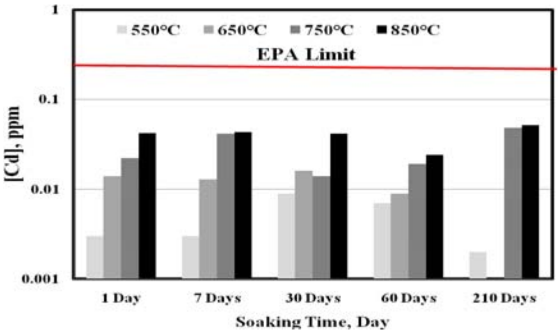

Fig 2. Concentration of cadmium (in ppm) in the leachate at different temperatures as determined by ICP.

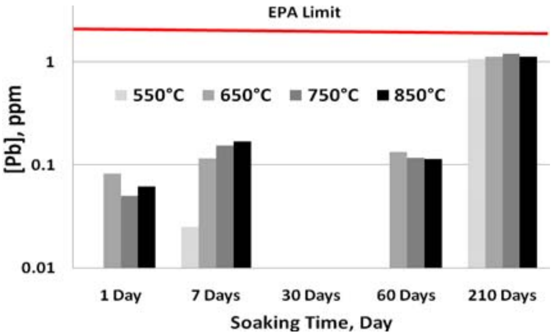

Fig 3. Concentration of lead (in ppm) in the leachate at different temperatures as determined by ICP.

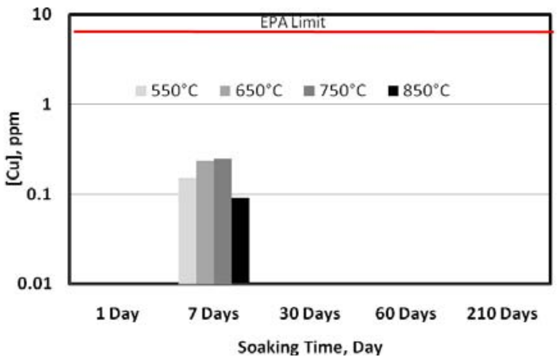

Fig 4. Concentration of zinc (ppm) in the leachate at different temperatures as determined by ICP.

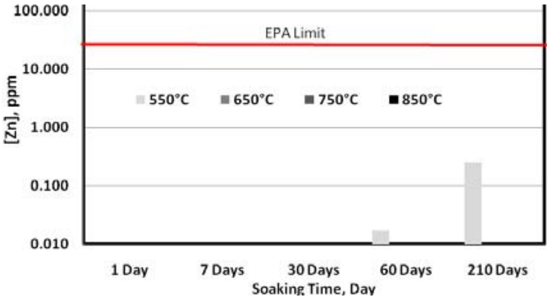

Fig 5. Concentration of copper (ppm) in the leachate at different temperatures as determined by ICP.

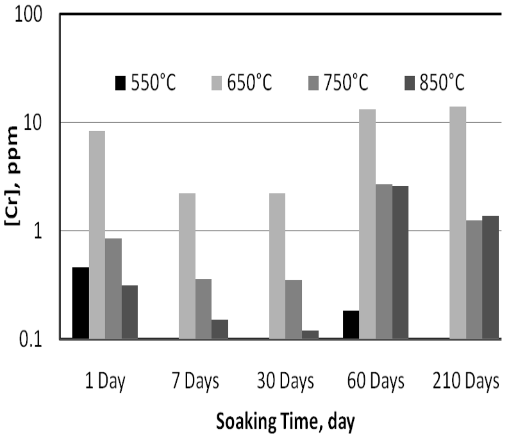

Fig 6. Concentration of chromium (ppm) in the leachate at different temperatures as determined ICP.

3.2. Effect of Ashing Temperature on Ash Cation Exchange Capacity (CEC)

It was found that the cation exchange capacity of oil shale ash increases with the increase of ashing temperature. This could be explained based on the increase of surface area due to release of carbon dioxide and combustion of organic matter present in oil shale. Additionally, due to removal of these compounds the content of Ca and clay matter present in the ash increases which consequently increases the electronegativity of the ash therefore the CEC increases.

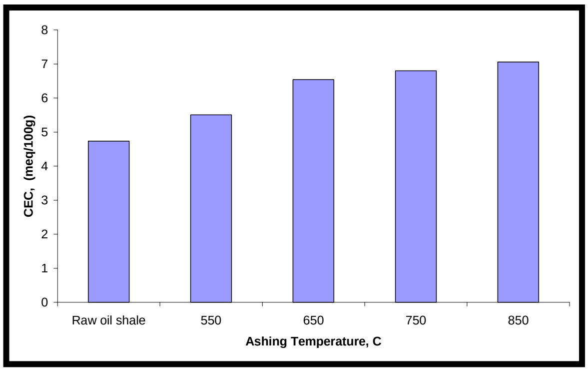

Fig 7. Variation of CEC of oil shale ash as a function of ashing temperature.

3.3. Effect of Ashing Temperature on Ph Value

Figure (8) shows the effect of ashing temperature on the pH of ash mixture with water. It was found that the pH of solution mixture increased considerably when ashing temperature increase from 550 to 650ºC then remains almost constant with further increase of ashing temperature demonstrating high level of alkalinity of the ash (pH ≈ 12). This could be explained by the fact that above the temperature of 600°C calcium carbonate present in oil shale starts to decompose to CaO and CO_2. The solubility of CaO is much higher than that of $CaCO_3$. The presence of CaO in water leads to formation of $Ca(OH)_2$. Soaking time was found to marginally affect the pH value of the mixture.

The decomposition temperature of $CaCO_3$ was confirmed by Thermogravemetric Analysis (TGA) of raw samples as shown in Figure (9). Oil shale TG and DTG curves show several stages in the mass loss profile. Some clay minerals may lose their interlayer water from 200°C up to 550°C depending on their crystal structure. Kaolinite, for example loses its bound water at about 430°C (Al-Otoom *et al.*, 2009). The main mass loss occurring in the temperature range of about 320 to 550°C is due to pyrolysis of bitumen and kerogen present in oil shale. The last region of mass loss (~17%) from oil shale sample occurs in the temperature range from about 630 to 780°C due to the decomposition of carbonates (Aboulkas *et al.*, 2008).

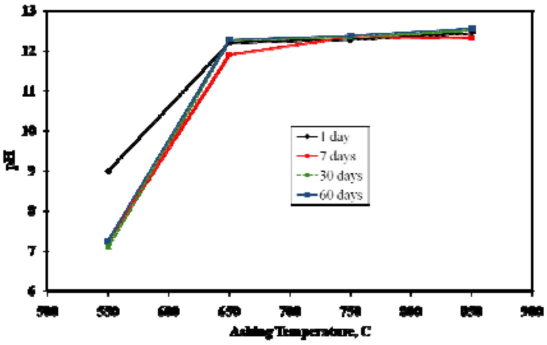

Figure (8). Effect of ashing temperature on the pH of solution mixture

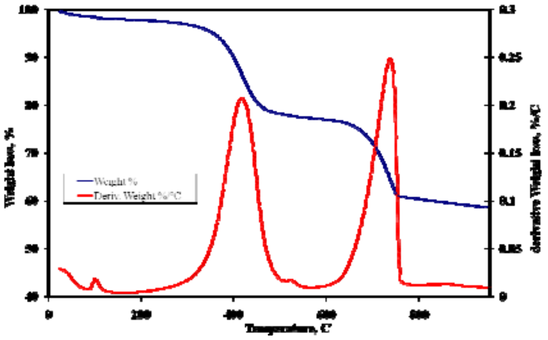

Fig 9. TGA and DTG of oil shale sample at a heating rate of 10C/min.

The high content of calcite in Jordanian oil shale, which varies between 30 to 70% of its mass ((Hamarneh *et al.*, 2006), and the subsequent high content of calcium oxide after combustion at temperatures higher than 650ºC is considered as advantageous. This is because of the formation of high pH when oil shale ash comes into contact even with acidic mine drainage (AMD). It is well known that AMD is normally neutralized by the addition of lime to increase the pH and reduce the release of heavy metals by AMD, which would reach the ground water (Johnson and Hallberg, 2005; Dutta *et al.*, 2009).

3.4. Characterization of Solid Products

Ashing of oil shale at 850ºC leads to complete combustion of organic matter. Decomposition of carbonates present in the sample in large quantity and volatilization of both organic and inorganic sulphur as can be seen from the XRD pattern of oil shale ash (Figure 10) Anhydrite ($CaSO_4$) was formed as a result of reaction between SO_3 (product of organics and CaO (product of calcite decomposition).

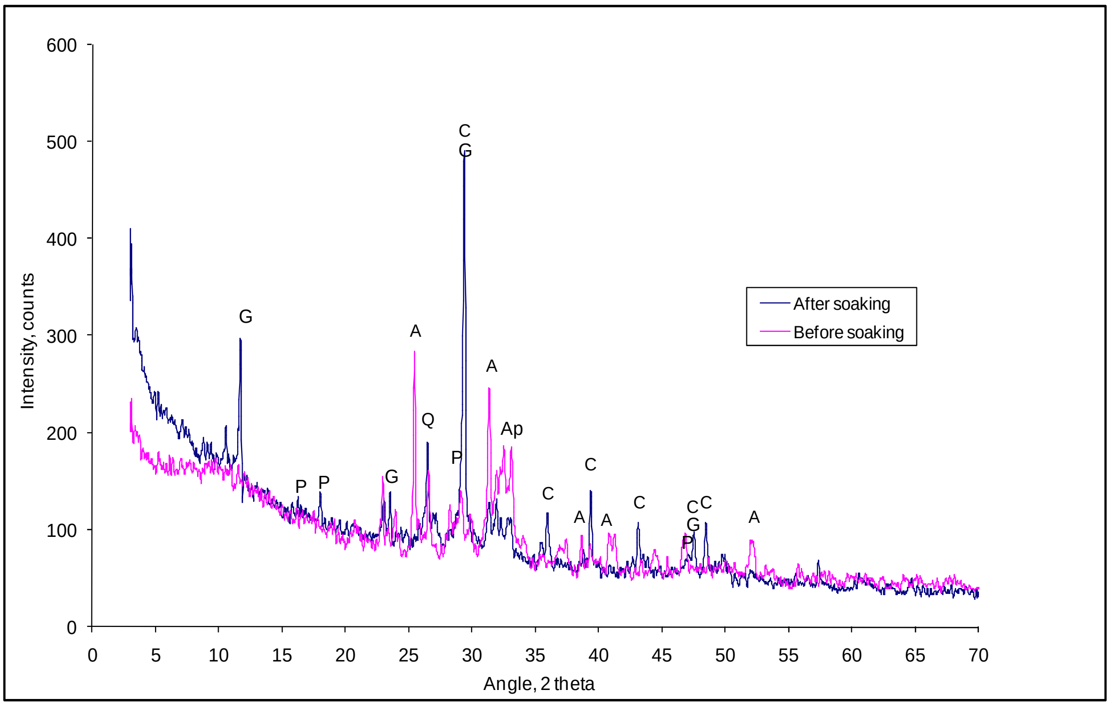

Fig 10. XRD patterns of oil shale ash (850ºC) before and after soaking in water for 7 months (G-Gypsum, A-Anhydrite, Ap- Apatite, C-calcite, Q-Quartz, P-portlandite).

The analysis of XRD pattern of oil shale ash after soaking shows that almost all anhydrite was transformed to gypsum (Figure 10). More importantly, it was observed that CaO (the product of calcite decomposition) was also transformed into calcium carbonate again. There is no evidence of the calcite in the ashed sample before soaking, however after soaking very intense calcite peaks appear in the XRD pattern (Figure10). This phenomenon can be explained as follows:

The quicklime formed as a result of ashing hydrolyzes in water according to the following reaction:

$$CaO + H_2O \rightarrow Ca(OH)_2$$

The presence of CO_2 available in surrounding environment (the soaking vessel was not tightly closed, dissolves in the slurry solution. As a results this dissolved CO_2 reacts with portlandite ($Ca(OH)_2$) according to the following reaction:

$$Ca(OH)_2 + CO_2 \rightarrow CaCO_3 + H_2O$$

The mechanism of carbonate formation from quicklime was described earlier by Bruno et al (2009) and Cizer et al (2008).

At ashing temperatures of 550, 650 and 750ºC, the anhydrite XRD peaks are less intense and they also disappear after soaking in distilled water. Furthermore, the peaks of gypsum appear after soaking with much lower intensity compared to that ashed at 850ºC.

3.5. Release Anions From Spent Shale.

The release of (Cl^-) and (SO_4^{-2}) was measured by ion chromatography after 7 months soaking of ash in distilled water. Table 3 shows the level of these anions in leachate for ashes combusted at different temperatures. The release of (SO_4^{-2}) from ash combusted at a temperature of 550ºC is considerably higher than that at temperatures 650, 750 and 850ºC. It can be seen from the TGA curves that the dissociation of calcite starts at temperature above 620°C. Upon the formation calcium oxide sulphate ions will be captured to form anhydrite as it is evident from XRD patterns shown in Figure 10 which was transformed to gypsum after soaking. However, at an ashing temperature of 550°C there was no CaO to react with sulphur oxides. Therefore, it was easy for (SO_4^{-2}) to be released.

4. Conclusion

Experimental data indicate that none of the spent shale samples exhibited any significant metal release and have indicated low concentrations of trace elements when compared to the EPA limits for drinking water. This could be explained by the low level of these elements in El-lajjun oil shale and more importantly due to the high level of alkalinity of the ash produced. High ashing temperatures have led to decomposition of calcite present in large quantity and the formation of anhydrite and amorphous CaO. Anhydrite was transformed in gypsum after soaking in water, whereas, CaO was partially transformed into portlandite leading to high level of alkalinity. Additionally, CEC was found to increase with the increase of ashing temperature due to the increase of surface area of ash as a result of carbon dioxide release and combustion of organic matter present in oil shale. The removal of these compounds also increases the content of Ca and clay matter present in the ash which consequently increases the electronegativity of the ash therefore the CEC increases.

Acknowledgment

The authors greatly acknowledge Al-alBayt University for its financial support to this work and the technical staff of Water, Environment & Arid Zones Research Center / Al al-Bayte University for carrying out the analyses.

References

[1] Aboulkas, A., K. El harfi and A. El bouadili (2008). "Kinetic and mechanism of Tarfaya (Morocco) oil shale and LDPE mixture Pyrolysis." Journal of Materials Processing Technology **206**: 16-24.

[2] Al-Harahsheh, M., O. Al-Ayed, J. Robinson, S. Kingman, A. Al-Harahsheh, K. Tarawneh, A. Saeid and R. Barranco (2011). "Effect of demineralization and heating rate on the pyrolysis kinetics of Jordanian oil shales." Fuel Processing Technology **92**(9): 1805-1811.

[3] Al-Otoom, A., M. Allawzi, A. M. Al-Harahsheh, M. Al-Harahsheh, R. Al-Ghbari, R. Al-Ghazo and H. Al-Saifi (2009). "A parametric study on the factors affecting the froth floatation of Jordanian tar sand utilizing a fluidized bed floatator." Energy **34**(9): 1310.

[4] Al-Otoom, A. Y., R. A. Shawabkeh, A. M. Al-Harahsheh and A. T. Shawaqfeh (2005). "The chemistry of minerals obtained from the combustion of Jordanian oil shale." Energy **30**(5): 611.

[5] Bai, J., Q. Wang, S. Li, C. Li and X. Guan (2008). "Research on release of trace elements at retorting of Huadian oil shale",, 2008, 25(1), 17-26." Oil Shale **25**(1): 17-26.

[6] Bell, P. R. F., A. A. Krol and P. F. Greenfield (1986). "Factors controlling the leaching of major and minor constituents from processed rundle oil shale." Water Research **20**(6): 741.

[7] Bruno, V., J. Hower, C , D. Flores and A. Guedes (2009). Laminar calcite Aggregate formation in the fly ash fraction. World of coal ash conference, Lexington, KY, USA.

[8] Cizer, O., K. Van Balen, J. Elsen and D. Van Gemert (2008). Carbonation reaction kinetics of lime binders measured using XRD. Proc. ACEME08, 2nd International Conference on Accelerated Carbonation for Environmental and Materials Engineering, Rome, Italy.

[9] Dabbas, M. A. (1997). Oil shale: hopes and ambitions (in Arabic). Second Jordanian Conference for Mechanical Engineering, JIMEC '97., Amman-Jordan, JAE.

[10] Dutta, B. K., S. Khanra and D. Mallick (2009). "Leaching of elements from coal fly ash: Assessment of its potential for use in filling abandoned coal mines." Fuel **88**(7): 1314.

[11] EASAC. (2007). "A study on the EU oil shale industry viewed in the light of the Estonian experience. A report submitted to the Committee on Industry Research and Energy of the European Parliament by European Academies Science Advisory Council (EASAC)." Retrieved 20/03/2010, 2010.

[12] Francu, J., B. Harvie, B. Laenen, A. Siirde and M. Veiderma, 2007. A study on the EU oil shale industry viewed in the light of the Estonian experience. A report by EASAC to the Committee on Industry, Research and Energy of the European Parliament.

[13] Hamarneh, Y., J. Alali and S. Sawaqed, 2006. Oil shale resources development in Jordan

[14] Ibrahim, K. M. and J. O. Jaber (2007). "Geochemistry and environmental impacts of retorted oil shale from Jordan." Environmental Geology **52**: 979-984.

[15] Jaber, J. O., S. D. Probert and P. T. Williams (1999). "Evaluation of oil yield from Jordanian oil shales." Energy **24**: 761-781.

[16] Johnson, D. B. and K. B. Hallberg (2005). "Acid mine drainage remediation options: a review." Science of The Total Environment **338**(1-2): 3.

[17] Michael, C. M. and K. S. Surendra (1991). "Physical and thermal properties and leachability of Eastern oil shales hydroretorted in a pressurized fluidized bed." Fuel **70**(11): 1285-1292.

[18] NRA. (2011). "Oil shale location map." Retrieved 03/12/2011, 2011.

[19] Russell, P. L. (1990). Oil shale's of the world; their origin. Occurrence and exploitation. Oxford, Pergamon Press.

[20] Shawabkeh, R. A. (2006). "Adsorption of chromium ions from aqueous solution by using activated carbo-aluminosilicate material from oil shale." Journal of Colloid and Interface Science **299**(2): 530-536.

JJEES

Volume 4 (Special Publication, Number 2), Jan. 2011
ISSN 1995-6681
Pages 35- 45

Jordan Journal of Earth and Environmental Sciences

Review of Uranium in the Jordanian Phosphorites: Distribution, Genesis and Industry

Abdulkader M. Abed*

Present address: Researcher, Deanship of Scientific Research

Jordan University of Science and Technology, Irbid

Abstract

Phosphorites are well-known, world wide, to accommodate a substantial amount of U relative to other sedimentary rocks. This is due to a great extent to the crystal structure of apatite (carbonate flour apatite, francolite) where U substitutes Ca. Phosphorites form in shallow marine environments through the accumulation of planktonic fossils debris on the sea floor in areas characterized by upwelling currents. Once the organic-rich sediments are buried below the sea floor and the organic matter is decomposed, PO_4 is released to the interstitial solutions. These PO_4-rich solutions either precipitate phosphorites directly (authigenic) or the solutions react with pre existing sediments and transform them to phosphorites (early diagenentic). The Jordanian deposits are dominantly of the former type. Consequently, phosphorites are also well known to be associated with high percentage of organic matter which makes them a good source rock for petroleum.

In Jordan, phosphorites are wide spread from its extreme NW to the SE. Uranium contents are not the same in each locality. It is not also the same in each bed in the same locality. In Al-Kora Basin, NW Jordan, U ranges between 60-379 ppm (parts per million or g/ton) with an average of 153 ppm. In Ruseifa, just east of Amman, the range is 132-195 ppm and average of 123 ppm. Central Jordan phosphorites (Al-Abiad and Al-Hasa) have a lower U %. The range is 34-190 ppm with an average of 105 ppm. Eshidiyya Basin has a much less U concentration. The range is 7-125 ppm with an average of 70 ppm. However, a recent work on the uppermost phosphorite horizon, the A0, in Eshidiyya Basin proved the presence of a 3 m thick bed with 242 ppm U. Furthermore, certain phosphorite horizons are known to have much more than the average U in that locality; e.g. in Al-Kora Basin, the average U is 153 ppm while certain horizons have up to 379 ppm U, the uppermost bed in Ruseifa has up to 195 ppm while the average is 123 ppm, and in Eshidiyya the A0 has 242 ppm while the average of the lower horizon (A1-3) average is 70 ppm. Obviously, if the U is to be extracted from the phosphorite, the horizons with higher concentrations of U should be explored and used.

Uranium sticks to francolite in its behavior from precipitation in the marine environment, through mining and beneficiation, and the fertilizer industry. 1) There is a significant high correlation coefficient between CaO and P_2O_5 in the hundreds of samples analyzed. 2) Fines (clays) produced when washing the ore have very little U and consequently, washing water for the last 45 years has not contaminated groundwater with U in central Jordan. 3) Uranium is concentrated in the phosphoric acid then into diammonium phosphate (DAP) in the fertilizer industry and not in the phosphogypsum.

Keywords: Phosphorite; Upper Cretaceous; Uranium; Francolite; Jordan; Diammonium Phosphate; Phosphogypsum .

1. Introduction

Phosphorites are the carrier of uranium, thus the study of them is a prerequisite to the study of U. Phosphorites are widespread in Jordan and cover a relatively large area of the country from the extreme northwest to its south. Low and high grade phosphorites are supposed to have been deposited throughout the country, but subsequent uplift and erosion, from the Oligocene onwards, had removed it from various parts of the country; e.g. Ajlun dome the western parts of the western mountain range, and the extreme south (Bender, 1974; Powell, 1989, Abed, 2000). Furthermore, high grade phosphorites are also present in the subsurface of the eastern desert of Jordan; e.g. Zgaimat Al-Hasat (Abed and Amireh, 1999).

High grade phosphorites were discovered in Jordan in 1908 during the construction of the Hijaz Railway. In 1938, small scale mining from Ruseifa started and was exported by mules through Haifa. The Jordan Phosphate Mines Company (JPMC) commenced its work by 1953 in Ruseifa, 1965 in Al-Hasa, 1979 in Al-Abiad, and 1988 in Eshidiyya (Abed, 2000). Ruseifa mines were closed in 1988 despite the fact that there are several tens of millions of high grade phosphorites south of Amman-Zarqa Highway (Zarqa B area) (Abed, 1989). Central Jordan

---

* Corresponding author. e-mail: aabed@ju.edu.jo.

phosphorites (Al-Hasa and Al-Abiad) are near depletion); consequently, Eshidiyya is going to be the centre for phosphorite mining and industry. However, several hundred millions of high grade phosphorites are present in Al-Kora Basin NW Jordan (Mikbel and Abed, 1985; Abed and Al-Agha, 1989), likewise, huge, but not estimated, subsurface deposits in the SE desert continuing into Saudi Arabia are present (Abed and Amireh, 1999). In short, there seems to be no shortage of high grade phosphorites in Jordan even for the distant future.

On the other hand, uranium is well known to be several folds enriched in phosphorites compared with other sedimentary rocks such as sandstones, carbonates and shales. Average U in phosphorite is 120 ppm compared with 3.5, 0.5 and 2.2 ppm in shale, sandstone and carbonate respectively; an enrichment factor of around 30 relative to shale (Altschuler, 1980; Slansky, 1986; McArthur *et al*., 1987; Krauskopf and Bird, 1995).This is basically due to the nature of the crystal structure of francolite (carbonate flour apatite) where U is substituting for calcium, both having a close radius (Ca^{+2}= 0.99Å and U= 0.97Å (e.g. Nathan, 1984; Mcclellan and Van Kauwenberg, 1990). The enrichment of U in phosphorites may also be due to the association of the latter with abundant organic matter in the depositional environment of the phosphorites (Barnett, 1990). Uranium, in the Jordanian phosphorite, was studied by Coopens et al., (1977), Khalid and Abed (1982), Abed and Khalid (1985) and Sadaqah *et al*., 2005 amongst others).

The aim of this paper is to discuss a) the distribution of U in the various localities and the phosphorite horizons within each locality; b) the genesis of phosphorite formations in Jordan; and c) the behavior of U throughout the processes of mining, upgrading and fertilizers industry.

2. GEOLOGICAL SETTING

The phosphorites of Jordan form part of the Cretaceous-Eocene phosphorite episode which deposited one of the most extensive deposits in the world in the Eastern Mediterranean (Saudi Arabia, Iraq, Syria, Jordan and Palestine) and North Africa (Egypt, Tunisia, Algeria, Morocco, Mauritania, Senegal, …), and parts of the Caribbean and NE S. America. It is second to the Miocene North American episode (Sheldon 1981; Riggs, *et al*., 1985; Notholt *et al*. 1989; Abed, 1994; Follmi 1996).

The phosphorites of Jordan are present within Al-Hisa Phosphorite Formation (AHP). Fig. 1 shows the location of high grade phosphorites in Jordan. The age of the AHP is most probably early Maastrichtian, Uppermost Cretaceous (Quennell, 1951; Hamam, 1977; Cappetta et al., 1996). In general, the AHP consists of phosphorites, bedded chert, limestones, oyster buildups, organic-rich marl (oil shale) and other rock types (Powell, 1989; Abed, 2000). However, the lithology and thickness of the AHP are variable from one locality to the other. The total thickness of the AHP is around 10 m in NW Jordan, 30 m in Ruseifa, 40-60 m in central Jordan, 10-17 m in Eshidiyya and 5-6 m in Zgaimat Al-Hasat in the SE desert ((Powell, 1989; Abed, 2000).

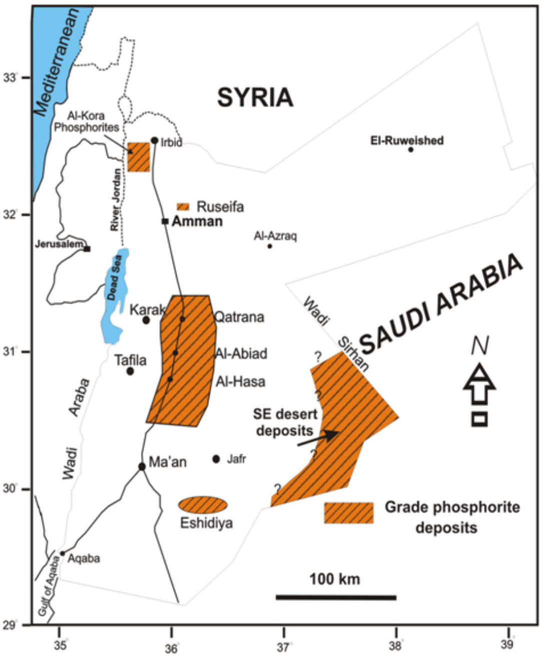

Fig. 1 Location map of the grade phosphorite deposits in Jordan.

The AHP consists of three formal members, from older to younger Sulatani, Bahiyya and Qatrana. The three members are well displayed throughout central Jordan where the terminology was first used by El-Hiyari (1985) (Table 1). In central Jordan, the Sultani Member consists of alternating limestones, bedded chert and minor phosphorites. The Bahiyya Member consists of oyster banks or buildups up 30 m in thickness that are made of oyster fragment in clinoforms dipping general to the SE (Abed and Sadaqah, 1998). The Qatrana Member is the host of the high grade phosphorites. The grade phosphorites are friable with little calcareous cement. They are present as lenses (small basins) with a diameter ranging up to few kilometers and a thickness up 13 m.

Table 1. Nomenclature of the Upper Cretaceous rock units in Jordan (Al-Hiyari, 1985)

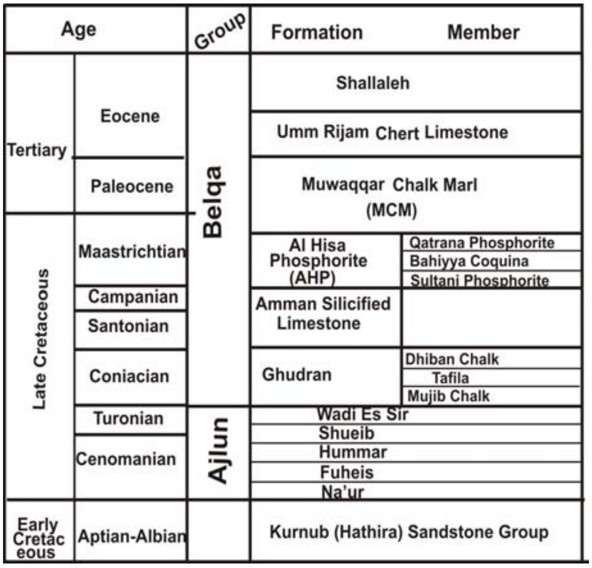

Age		Group	Formation	Member
Tertiary	Eocene	Belqa	Shallaleh	
			Umm Rijam Chert Limestone	
	Paleocene		Muwaqqar Chalk Marl (MCM)	
Late Cretaceous	Maastrichtian		Al Hisa Phosphorite (AHP)	Qatrana Phosphorite
				Bahiyya Coquina
				Sultani Phosphorite
	Campanian		Amman Silicified Limestone	
	Santonian			
	Coniacian		Ghudran	Dhiban Chalk
				Tafila
				Mujib Chalk
	Turonian	Ajlun	Wadi Es Sir	
	Cenomanian		Shueib	
			Hummar	
			Fuheis	
			Na'ur	
Early Cretaceous	Aptian-Albian		Kurnub (Hathira) Sandstone Group	

In Eshidiyya Basin, the three formal members are present only in the northern parts of the basin. The Bahiyya coquina thins gradually towards the SE until it disappears completely. The Sultani Member or the lower member is hosting the main (high) grade phosphorite deposits. It is divided by the miners into three producing phosphate horizons from top to bottom; A1, A2 and A3, separated by non phosphorite strata like; chert, porcelanite, and minor beds of marl, limestone and dolomite. (Sofremines, 1987; Abed *et al*., 2007). The A3, at the base, is rich in quartz sand, while A2 is a friable, high grade phosphorite. The A1 is a low grade indurated by calcite cement (Fig. 2). The Qatrana Member or the upper member is designated A0 and consists of up to 3 m of friable high grade phosphorite in the north thinning to the SE to few centimeters only.

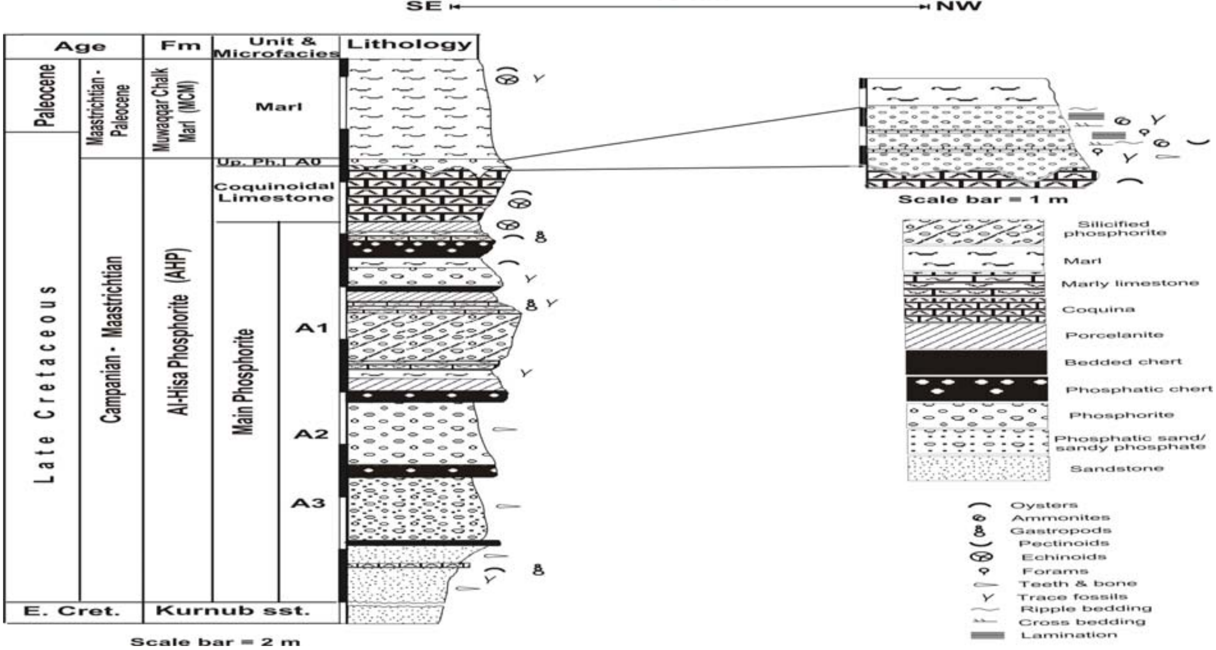

Fig. 2 A columnar section describing the lithology of Eshidiyya phosphorites. A detailed section , right, shows the lithology of the A0 deposits in northern Eshidiyya.

Fig. 3 is a columnar section in central Jordan. The SE desert deposits were discovered by Abed and Amireh (1999). They are deep seated in the subsurface, but crop out as windows at the cores of anticlines such as that of Zgaimat Al-Hasat. Total thickness is 5-6 m consisting of friable phosphorites with same quartz sand increasing to the SE (Fig. 4). The age, most probably Turonian, seems older than other phosphorites of Jordan (Khalifa and Abed, 2011).

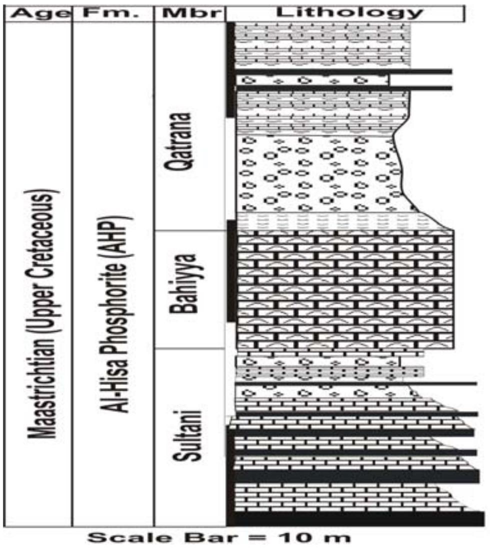

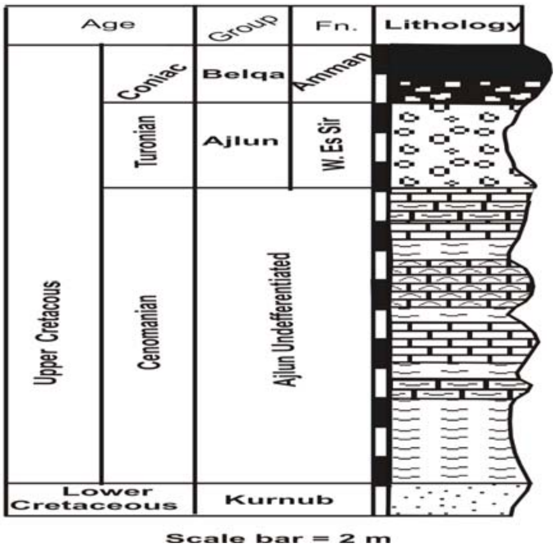

Fig. 3 (left) Generalized lithological section in central Jordan.

Fig. 4 (right) Detailed columnar section of the Ajlun Group and the phosphorites of the SE desert at Zgaimat Al-Hasat (Khalifa and Abed, 2011). For legend, see Fig. 2.

The Ruseifa mines were closed in 1988, however, the deposits consists of four phosphorite horizons designated from bottom A1, A2, A3, and A4, separated by limestone, trace fossils and some chert (Fig. 5). Al-Kora deposits, NW Jordan, were discovered by Mikbel and Abed (1985) with several million tons of grade phosphorites. The deposits are up to 10 m thick, the lower part consists of alternating chert and phosphorite caped by about 3 m thick high grade, friable phosphorite horizon rich in organic matter (Abed and Al-Agha, 1989). Fig. 6 shows the lithology near the village of Tobna. These deposits have not been mined yet.

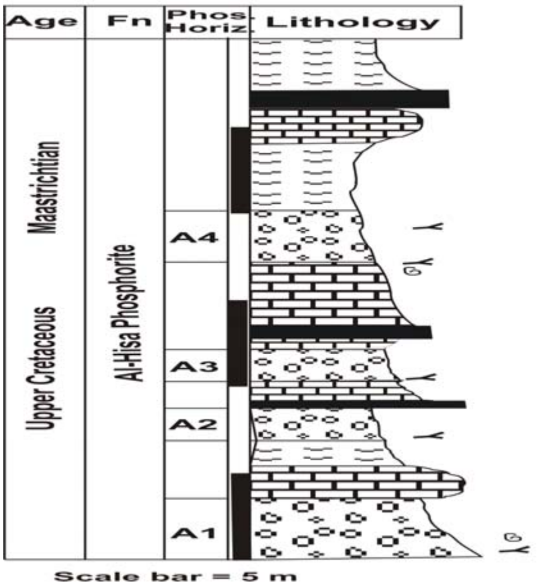

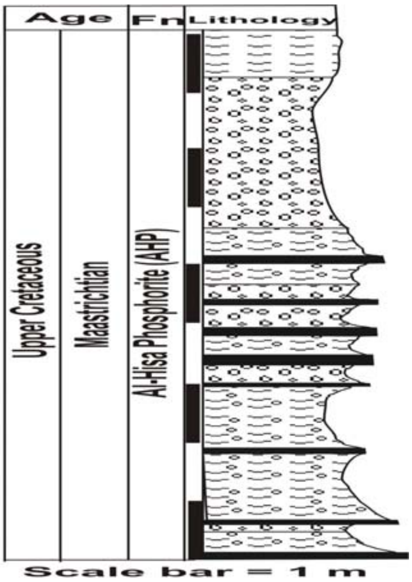

Fig. 5 (left) columnar section describing the phosphorites at Ruseifa Basin.

Fig. 6 (right) Columnar section describing the phosphorites at Tobna, Al-Kora Basin, NW Jordan. For legend, see Fig. 2 .

3. Results and Discussion

3.1. Petrography and Mineralogy

The phosphorites of Jordan are granular in nature with subordinate pristine (primary or not reworked) especially in NW Jordan deposits. Grain types are phosphate intraclasts, peloids, coprolites and skeletal fragments (bone and teeth). The former two types are due mainly to reworking of originally precipitated phosphate material, or may partially be due to the nature of deposition between the pore spaces of pre existing sediments (Riggs, 1979, 1980; Burnett, 1990; Abed and Fakhouri, 1996; Abed et al., 2007 amongst many others).

Phosphate particles or grains, in marine phosphorites, consist of the mineral carbonate flour apatite (francolite), a variety of the mineral apatite. The phosphorites of Jordan have the following chemical formula of francolite $[Ca_{9.86}\ Mg_{.005}\ Na_{.14}]\ [PO_{4\ 4.93}\ CO_{3\ 1.07}\ F_{2.06}]$ (Abed and Fakhouri, 1996). The crystal structure of francolite is rather open, thus enhancing substitution (e.g. McClellan and Van Kauwenberg, 1990). Uranium is one of many elements that substitutes for Ca. Consequently, U is present within the crystal structure of francolite and behaves more similar to Ca than to P, simply because the ionic radii are very close to each other. To shed more light on this relationship, U ppm is correlated with each of CaO%, P_2O_5%, U/ P_2O_5 and U/CaO in 184 samples from the Jordanian phosphorites (Fig. 7). It is clear that a better correlation is present between U and Ca than between U and P, meaning that U is not only present within the structure of francolite but it occupies same positions of Ca in that structure.

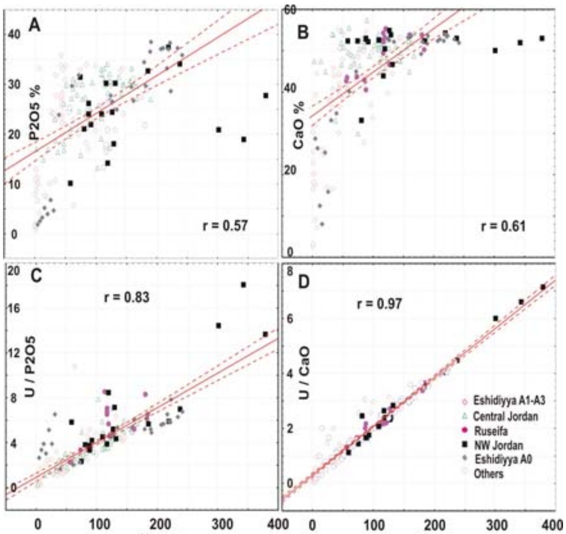

Fig. 7 Correlation between U and A) P_2O_5%, B) CaO%, C) U/P_2O_5 ratio, and D) U/CaO ratio. Solid line is the best fit while dotted lines are for the 95% confidence. Number of samples is 184.

The yellowish-greenish U minerals found on the surface of joints and fractures are due to leaching by groundwater of the original U; i.e. secondary in origin. Consequently, this type occurrence is very limited in abundance, and thus, of minor importance and of no economic value for U exploration.

3.2. Distribution of Uranium

In this title, the distribution of U in the various localities in Jordan is discussed based on data acquired by the author, his coworkers and students since 1980.

3.2.1. Eshidiyya Deposits

Phosphorites are present in two members, the lower member (A1, A2 and A3 horizons) who accommodates the main phosphorite reserves, and the upper member (A0 horizon) with limited reserves (Fig. 2). Tables 2 and 3 display the contents of U in both upper and lower members respectively.

The U average of 60 samples analyzed from the lower member is 51 ppm with a range 1 -175 ppm. If the samples with less than 11 % P_2O_5 % are removed, because they are not typical phosphorites, then the average U will be 70 ppm. The higher U concentrations up to 175 ppm can be found in the calcareous, high grade A2 horizon. The A3 has the lowest U content, partially, because of the high dilution with silica sand which can be present up to 50 % in certain samples. The A1 is slightly higher than the A3 (Khaled and Abed, 1982). Upgrading the lower member will certainly enhance the contents of U in these phosphorites.

Table 2.Uranium, P_2O_5 and CaO contents and other ratios in the lower phosphorite member in Eshidiyya Basin (Khaled and Abed, 1982; Abed and Khaled, 1985).

	U ppm	P_2O_5%	CaO%	U/ P_2O_5	CaO/ P_2O_5	U/ CaO		Uppm	P_2O_5 %	CaO%	U/ P_2O_5	CaO/ P_2O_5	U/ CaO
1	45	23.96	41.23	1.88	1.72	1.09	31	63	5.83	39.53	10.81	6.78	1.59
2	96	21.93	37	3.14	1.69	2.59	32	5	9.88	32.05	0.51	3.24	0.16
3	143	33.13	53.12	4.23	1.60	2.69	33	5	10.27	39.35	0.49	3.83	0.13
4	146	23.98	53.3	4.43	2.22	2.74	34	5	6.55	9.17	0.76	1.40	0.55
5	44	27.22	40.4	1.62	1.48	1.09	35	50	30.88	48.04	1.62	1.56	1.04
6	44	23.16	40.78	1.75	1.76	1.08	36	35	31.74	45.96	1.10	1.45	0.76
7	45	25.68	39.04	1.75	1.52	1.15	37	50	22	38.47	2.27	1.75	1.30
8	45	22.18	36.49	2.02	1.65	1.23	38	75	32.84	49.08	2.28	1.49	1.53
9	44	27.63	44.1	1.39	1.60	1.00	39	85	33.96	49.94	2.50	1.47	1.70
10	141	32.63	48.8	4.32	1.50	2.89	40	100	33.76	49.93	2.96	1.48	2.00
11	111	25.33	44.3	4.38	1.75	2.51	41	88	26.6	43.65	3.31	1.64	2.02
12	72	19.99	42.91	3.6	2.15	1.68	42	85	18.27	27.87	4.65	1.53	3.05
13	45	26.14	42.06	1.72	1.61	1.07	43	100	20.7	33.79	4.83	1.63	2.96
14	44	33.82	30.25	1.30	0.89	1.45	44	46	28.25	50.63	1.63	1.79	0.91
15	18	7.45	24.94	2.42	3.35	0.72	45	45	20.05	44.57	2.24	2.22	1.01
16	7	4.1	7.26	1.71	1.77	0.96	46	63	22.92	40.46	2.75	1.77	1.56
17	16	7.7	25.96	2.08	3.37	0.62	47	8	33.13	44.52	0.24	1.34	0.18
18	29	24.15	37.82	1.20	1.57	0.77	48	75	29.91	48.33	2.51	1.62	1.55
19	43	35.91	55.09	1.20	1.53	0.78	49	125	29.7	39.63	4.21	1.33	3.15
20	30	24.21	38.22	1.24	1.58	0.78	50	1	0.83	2.82	1.20	3.40	0.35
21	35	27.78	43.86	1.26	1.58	0.80	51	2	10.89	18.19	0.18	1.67	0.11
22	51	33.66	54.18	1.52	1.61	0.94	52	1	1.5	3.14	0.67	2.09	0.32
23	69	30.34	47.19	2.27	1.56	1.46	53	5	11.38	17.59	0.44	1.55	0.28
24	34	10.68	16.8	3.18	1.57	2.02	54	2	8.8	18.11	0.23	2.06	0.11
25	125	26.71	55.35	4.68	2.07	2.26	55	25	10.1	16.93	2.48	1.68	1.48
26	89	17.07	54.58	5.21	3.20	1.63	65	3	13	20.36	0.23	1.57	0.15
27	175	27.32	52.24	6.41	1.91	3.35	57	1	11.07	16.56	0.09	1.50	0.06
28	34	23	40.84	1.48	1.78	0.83	58	1	7.78	30.47	0.13	3.92	0.03
29	46	33.01	50.55	1.39	1.53	0.91	59	1	2	22.79	0.50	11.40	0.04
30	34	23.94	36.28	1.42	1.52	0.94	60	1	1.66	25.56	0.60	15.40	0.04
Av	51	20.83	36.71	2.24	1.76	1.39	Av. of >11% P2O5 = 70 ppm						

On the other hand, the upper phosphorite member (A0) is much more enriched in U. Table 3 shows the analysis of 28 samples of the A0 with an average U of 133 ppm and a range of 5-242 ppm. If the samples of less than 10% P2O5 % are removed, then the average U becomes 172 ppm and the range 40-242 ppm, The data clearly indicates that U is more than twice that of the lower member (Abed and Sadaqah, 2011 in press). The A0 consists of two phosphorite beds up to 3 m thick. The phosphorite beds are calcareous with slight calcite cement, ammonites and trace fossils. The A0 overlies the coquina member (middle member) with subaerial unconformity. Abed and Sadaqah (2011 in press) concluded that the U enrichment is, at least partially, due to slight leaching of the carbonates and phosphorites at the unconformity. That is why the lower bed of the A0 has more U compared with the upper bed away from the unconformity.

Table 3.Uranium, P_2O_5 and CaO contents and other ratios in the upper phosphorite member (A0) in Eshidiyya Basin (Abed and Sadaqah, 2011 in press).

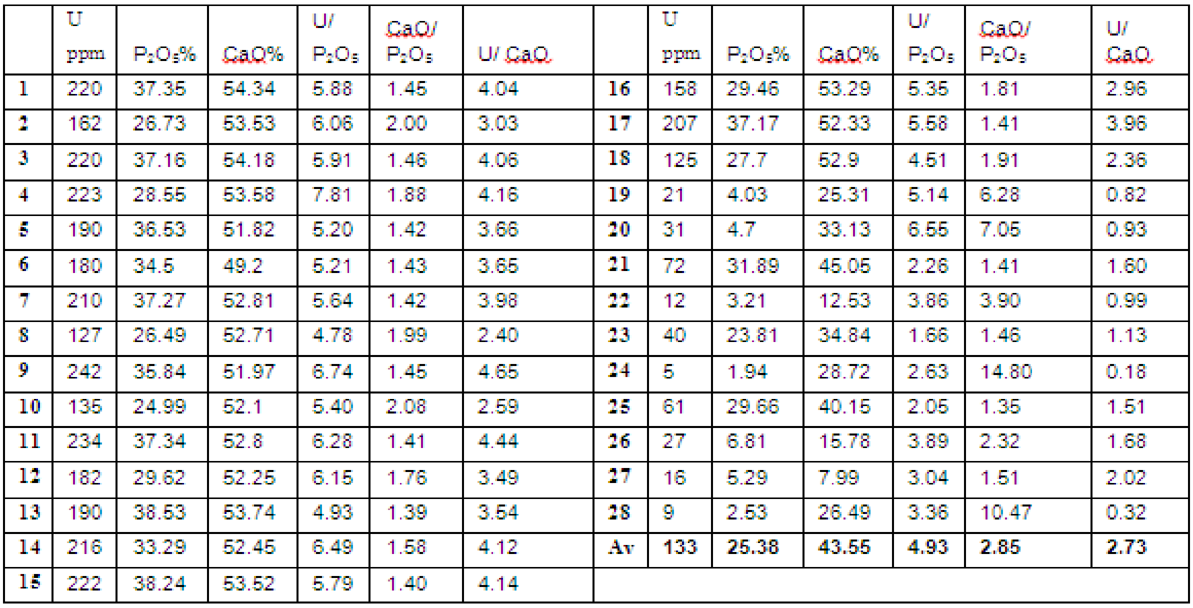

	U ppm	P_2O_5%	CaO%	U/ P_2O_5	CaO/ P_2O_5	U/ CaO		U ppm	P_2O_5%	CaO%	U/ P_2O_5	CaO/ P_2O_5	U/ CaO
1	220	37.35	54.34	5.88	1.45	4.04	16	158	29.46	53.29	5.35	1.81	2.96
2	162	26.73	53.53	6.06	2.00	3.03	17	207	37.17	52.33	5.58	1.41	3.96
3	220	37.16	54.18	5.91	1.46	4.06	18	125	27.7	52.9	4.51	1.91	2.36
4	223	28.55	53.58	7.81	1.88	4.16	19	21	4.03	25.31	5.14	6.28	0.82
5	190	36.53	51.82	5.20	1.42	3.66	20	31	4.7	33.13	6.55	7.05	0.93
6	180	34.5	49.2	5.21	1.43	3.65	21	72	31.89	45.05	2.26	1.41	1.60
7	210	37.27	52.81	5.64	1.42	3.98	22	12	3.21	12.53	3.86	3.90	0.99
8	127	26.49	52.71	4.78	1.99	2.40	23	40	23.81	34.84	1.66	1.46	1.13
9	242	35.84	51.97	6.74	1.45	4.65	24	5	1.94	28.72	2.63	14.80	0.18
10	135	24.99	52.1	5.40	2.08	2.59	25	61	29.66	40.15	2.05	1.35	1.51
11	234	37.34	52.8	6.28	1.41	4.44	26	27	6.81	15.78	3.89	2.32	1.68
12	182	29.62	52.25	6.15	1.76	3.49	27	16	5.29	7.99	3.04	1.51	2.02
13	190	38.53	53.74	4.93	1.39	3.54	28	9	2.53	26.49	3.36	10.47	0.32
14	216	33.29	52.45	6.49	1.58	4.12	Av	**133**	**25.38**	**43.55**	**4.93**	**2.85**	**2.73**
15	222	38.24	53.52	5.79	1.40	4.14							

3.2.2. Central Jordan Deposits

Central Jordan phosphorites are represented by Al-Hasa and Al-Abiad deposits and their surroundings. The deposits are calcareous, granular, and slightly cemented by calcite and are present in single isolated lenses. Several hundred million tons or high grade phosphorites were mined since 1965, and consequently these deposits are near depletion. Table 4 shows the chemical results of 34 samples with an average of 105 ppm and a range 60-168 ppm (Abed and Khaled, 1985; Sadaqah et al., 2005; Abed et al., 2008). However, there are no much deposits for future U industry.

Table 4.Uranium, P_2O_5 and CaO contents and other ratios in central Jordan phosphorites, Al-Abiad and Al-Hasa (Abed and Khaled, 1985; Abed *et al*., 2008).

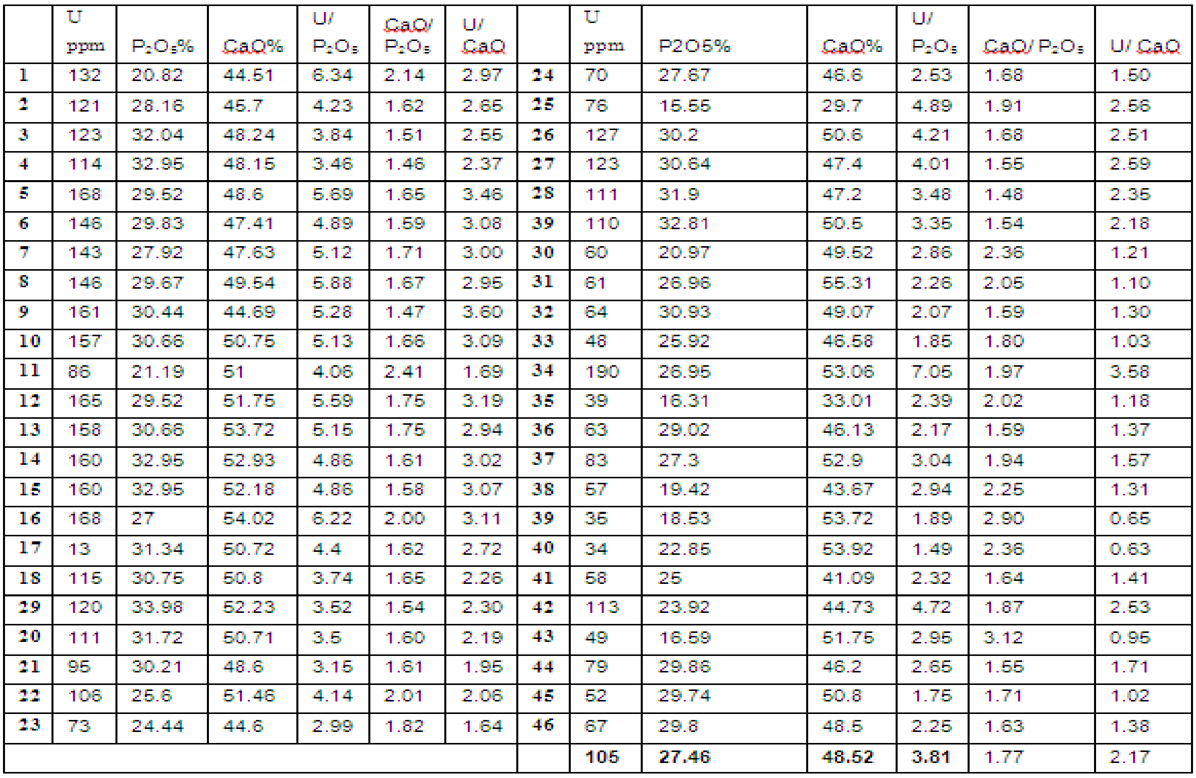

	U ppm	P_2O_5%	CaO%	U/ P_2O_5	CaO/ P_2O_5	U/ CaO		U ppm	P2O5%	CaO%	U/ P_2O_5	CaO/ P_2O_5	U/ CaO
1	132	20.82	44.51	6.34	2.14	2.97	24	70	27.67	46.6	2.53	1.68	1.50
2	121	28.16	45.7	4.23	1.62	2.65	25	76	15.55	29.7	4.89	1.91	2.56
3	123	32.04	48.24	3.84	1.51	2.55	26	127	30.2	50.6	4.21	1.68	2.51
4	114	32.95	48.15	3.46	1.46	2.37	27	123	30.64	47.4	4.01	1.55	2.59
5	168	29.52	48.6	5.69	1.65	3.46	28	111	31.9	47.2	3.48	1.48	2.35
6	146	29.83	47.41	4.89	1.59	3.08	39	110	32.81	50.5	3.35	1.54	2.18
7	143	27.92	47.63	5.12	1.71	3.00	30	60	20.97	49.52	2.86	2.36	1.21
8	146	29.67	49.54	5.88	1.67	2.95	31	61	26.96	55.31	2.26	2.05	1.10
9	161	30.44	44.69	5.28	1.47	3.60	32	64	30.93	49.07	2.07	1.59	1.30
10	157	30.66	50.75	5.13	1.66	3.09	33	48	25.92	46.58	1.85	1.80	1.03
11	86	21.19	51	4.06	2.41	1.69	34	190	26.95	53.06	7.05	1.97	3.58
12	165	29.52	51.75	5.59	1.75	3.19	35	39	16.31	33.01	2.39	2.02	1.18
13	158	30.66	53.72	5.15	1.75	2.94	36	63	29.02	46.13	2.17	1.59	1.37
14	160	32.95	52.93	4.86	1.61	3.02	37	83	27.3	52.9	3.04	1.94	1.57
15	160	32.95	52.18	4.86	1.58	3.07	38	57	19.42	43.67	2.94	2.25	1.31
16	168	27	54.02	6.22	2.00	3.11	39	35	18.53	53.72	1.89	2.90	0.65
17	13	31.34	50.72	4.4	1.62	2.72	40	34	22.85	53.92	1.49	2.36	0.63
18	115	30.75	50.8	3.74	1.65	2.26	41	58	25	41.09	2.32	1.64	1.41
29	120	33.98	52.23	3.52	1.54	2.30	42	113	23.92	44.73	4.72	1.87	2.53
20	111	31.72	50.71	3.5	1.60	2.19	43	49	16.59	51.75	2.95	3.12	0.95
21	95	30.21	48.6	3.15	1.61	1.95	44	79	29.86	46.2	2.65	1.55	1.71
22	106	25.6	51.46	4.14	2.01	2.06	45	52	29.74	50.8	1.75	1.71	1.02
23	73	24.44	44.6	2.99	1.82	1.64	46	67	29.8	48.5	2.25	1.63	1.38
								105	**27.46**	**48.52**	**3.81**	1.77	2.17

However, grade phosphorites are present west of Dhiban, near the village of Shgaig. The area is populated and the deposits have not been mentioned by JPMC or other workers (Abed and Khaled, 1985). Reserves are not estimated and the U contents of 14 samples is 79 ppm with a range of 4-118 ppm (Table 5)

Table 5. Uranium, P_2O_5 and CaO contents and other ratios in the phosphorites of the Mujib Area (Abed and Khaled, 1985).

	U ppm	P_2O_5%	CaO%	U/ P_2O_5	CaO/ P_2O_5	U/ CaO
1	92	22.94	52.41	4.01	2.28	1.76
2	22	16.85	44.7	1.31	2.65	0.49
3	15	14.8	47.29	1.01	3.20	0.32
4	4	16.81	47.4	0.24	2.82	0.08
5	103	13.16	51.13	7.83	3.89	2.01
6	110	18.95	52.47	5.80	2.77	2.10
7	110	23.18	53.79	4.75	2.32	2.04
8	116	29.72	51.8	3.90	1.74	2.24
9	78	26.81	50.24	2.91	1.87	1.55
10	85	23.69	52.18	3.59	2.20	1.63
11	118	30.1	51.3	3.92	1.70	2.30
12	48	17.94	54.64	2.68	3.05	0.88
13	91	24.85	57.31	3.66	2.31	1.59
14	111	22.92	50.17	4.84	2.19	2.21
Av.	**79**	**21.62**	**51.20**	**3.60**	**2.37**	**1.54**

3.2.3. Ruseifa Deposits.

During 1988, Ruseifa mines were closed and the remaining deposits south of the Amman-Zarqa highway are becoming more and more urbanized. Thus, the following lines are of historical value only. The Ruseifa phosphorites consist of four horizons (A1, A2, A3, and A4 topmost) separated by carbonates and chert beds (Fig. 5). Table 6 shows the analysis of 17 samples with an average U of 123 ppm and a range of 57-184. Uranium content increases upwards and the A4 horizon have the highest content of more than 180 ppm (Abed and Khaled, 1985).

Table 6. Uranium, P_2O_5 and CaO contents and other ratios in the phosphorites of Ruseifa (Abed and Khaled, 1985).

	U ppm	P_2O_5%	CaO%	U/ P_2O_5	CaO/ P_2O_5	U/ CaO
1	123	17.25	52.61	7.02	3.05	2.34
2	121	26.66	55.26	4.55	2.07	2.19
3	113	13.26	52.7	8.52	3.97	2.14
4	56	24.67	42.58	2.27	1.73	1.32
5	86	24.59	42.97	3.5	1.75	2.00
6	57	25.31	43.62	2.25	1.72	1.31
7	183	29.79	52.65	6.11	1.77	3.48
8	184	28.94	50.33	6.53	1.74	3.66
9	127	26.31	46.71	4.82	1.78	2.72
10	73	21.69	43.68	3.37	2.01	1.67
11	119	20.96	53.17	5.68	2.54	2.24
12	117	17.31	49.45	6.76	2.86	2.37
13	161	30.5	53.8	5.28	1.76	2.99
14	162	31.11	53.75	5.21	1.73	3.01
15	181	21.75	53.82	8.32	2.47	3.36
16	117	16.54	54.2	7.07	3.28	2.16
17	117	17.93	52.1	6.53	2.91	2.25
Av.	**123**	**23.21**	**50.20**	**5.52**	**2.16**	**2.46**

3.2.4. Al-Kora Deposits, NW Jordan

The NW Jordan phosphorites are promising future deposits for phosphorites and uranium. There are, at least, several hundred million tons of high grade phosphorites with high U content relative to other deposits discussed earlier. However, the high population (many villages and towns) and the green nature of the area (forests and agriculture) might have been behind the decision not to mine the deposits. Also, the deposits are present within a folded belt which makes open pit mining rather difficult if not impossible in certain localities (Mikbel and Abed 1985).

Table 7 shows the analysis of18 samples with an average of 153 ppm U and a range of 59-379 ppm U (Abed and Khaled, 1985; Sadaqah, 2000, Sadaqah et al., 2005). The highest U content is around 6 times more than that of Eshidiyya and might be of economic nature if extracted as a byproduct through the fertilizers industry. Detailed field and laboratory work can pinpoint the localities with the high U content.

Table 7.Uranium, P_2O_5 and CaO contents and other ratios in the phosphorites of Al-Kora Basin, NW Jordan.(Abed and Khaled, 1985; Sadaqah *et al*., 2005).

	U ppm	P_2O_5%	CaO%	U/ P_2O_5	CaO/ P_2O_5	U/ CaO
1	88	24.09	40.52	3.65	1.68	2.17
2	117	30.23	44.01	3.87	1.46	2.66
3	186	32.7	52.4	5.69	1.60	3.55
4	129	18	53.79	7.16	2.99	2.40
5	120	14.22	50.44	8.44	3.55	2.38
6	132	30.18	46.62	4.37	1.54	2.83
7	127	24.37	54.9	5.21	2.25	2.31
8	81	21.08	33.18	3.84	1.57	2.44
9	75	31.5	52.4	2.38	1.66	1.43
10	238	34.16	52.98	6.97	1.55	4.49
11	88	26.25	52.78	3.35	2.01	1.67
12	89	24.05	53.09	3.70	2.21	1.68
13	301	20.92	50.06	14.39	2.39	6.01
14	343	18.95	51.95	18.10	2.74	6.60
15	109	24.06	52.52	4.53	2.18	2.08
16	59	10.13	52.39	5.82	5.17	1.13
17	379	27.75	53.08	13.66	1.91	7.14
18	92	22	52.23	4.18	2.37	1.76
Av	**153**	**24.15**	**49.96**	**6.63**	**2.07**	**3.06**

3.2.5. Area Comparison

Absolute U content might not be the best way of comparing its abundance in the various localities. For this reason, the U/P_2O_5 ratio is used, meaning the amount of U in ppm present for each 1% P_2O_5. The average U/P_2O_5 ratio for the samples in each locality (not the ratio of averages) is shown in Table 8. It is clear from Table 8 that the ratio increases northwards. It is 2.24 in Eshidiyya; i.e. there is 2.24 ppm U in Eshidiyya deposits for each 1% P_2O_5. It increases to 6.63 in NW Jordan, which clearly shows that the NW Jordan phosphorites are three times more enriched in U compared with Eshidiyya. The other localities are intermediate between Eshidiyya and NW Jordan. The possible reasons for this northwards increasing trend are discussed further below.

Table 8The U/P_2O_5 sample averages in the phosphorite deposits of Jordan, n = number of samples averaged.

	U ppm	P_2O_5 %	CaO %	U/ P_2O_5	n
Eshidiyya	51	20.83	36.71	2.24	60
Central Jordan	105	27.46	48.52	3.81	44
Mujib	79	21.62	51.2	3.6	13
Ruseifa	123	23.21	50.2	5.52	16
NW Jordan	153	24.15	49.96	6.63	18

4. Behavior of U During Mining and Upgrading.

Mining and upgrading are the not discussed here because they are not the subject of this paper. However, mining and upgrading involve the removal of the overburden, obtaining the phosphorite ore, crushing the ore to liberate the suitable grain size, sieving to get a roughly sand-size product, washing with fresh water to get red of the fines especially clays, and finally drying. Samples from all these stages were analyzed for their U and other elements and the following conclusion was reached (Al-Huwaiti et al., 2005; Abed et al., 2008). Uranium behaves similar to the behavior of P and Ca (Fig. 8a); i.e. U stays fixed in the crystal structure of francolite, as discussed in the mineralogy section.

Environmentally, the discharged washing water has not contaminated the groundwater in Al-Hasa and Al-Abiad mines area despite the fact that the washing process has been ongoing since 1965 and 1979 respectively. Groundwater samples from wells and springs in central Jordan have a U content less than 2 ppb (parts per billion) (Jiries et al., 2004; Abed et al., 2008). See Fig.8b.

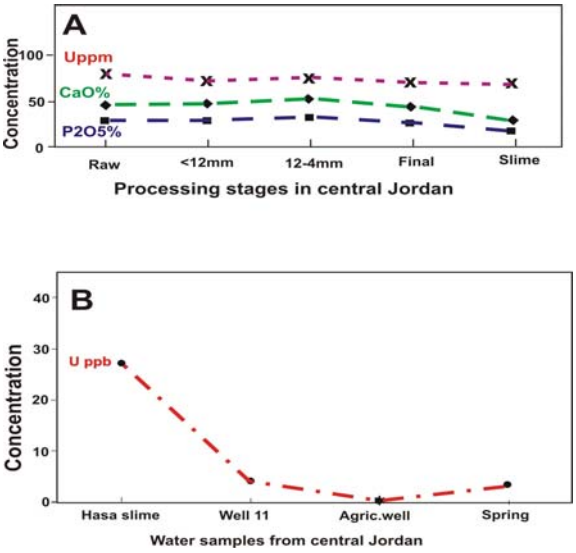

Fig. 8 shows the behavior of U during mining, crushing, sieving and washing (8a upper) and 8b shows the concentration in ppb in the groundwater in central Jordan.

5. Behavior of U in the Fertilizers Industry.

In the fertilizers industry, the upgraded phosphorite ore is reacted with sulphuric acid (H_2SO_4) to produce phosphoric acid (H_3PO_4) and phosphogypsum. The crystal structure of francolite is destroyed through this reaction, its PO_4 forms phosphoric acid, and the Ca of francolite forms the phosphogypsum. Analysis of the two products, the acid, and gypsum, clearly shows that U follows the PO_4 group and is concentrated in the phosphoric acid. The phosphogypsum has no more than 2 ppm U. The phosphoric acid is then transferred to the fertilizer, diammonium phosphate (DAP), and U is found to be concentrated in the. DAP. Through these reactions, U is found to be concentrated in the phosphoric acid and the DAP by a factor of 1.5 (Fig. 9). For more details, see Abed et al., (2008).

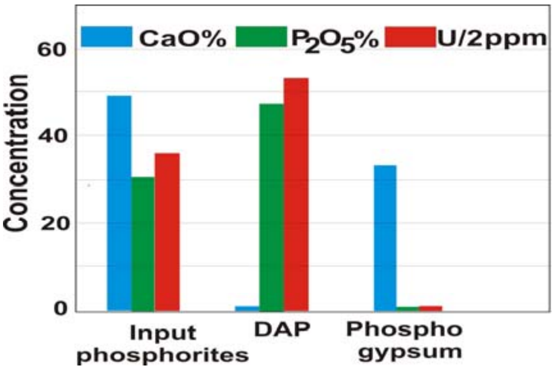

Fig. 9 Behavior of U in the fertilizers industry. Note that the U and P2O5 are enriched by a factor of 1.5 in the DAP fertilizer and the U in phosphogypsum is around 2 ppm.

6. Phosphogenesis and the Enrichment of U: Discussion

Why phosphorites have more U compared with other sedimentary rocks? Why U contents increases northwards in the Jordanian phosphorites? Following is an attempt to answer these and others related to phosphogenesis.

Phosphorite, bedded chert, porcelanite and organic-rich sediments, as an association, are known to deposit under upwelling currents regimes (Sheldon, 1987; Iijima, et al., 1994 and the papers within). This is well documented in the recent and subrecent Earth history in shallow continental shelf where upwelling currents are intense and still ongoing; e.g. the coasts of SW Africa (Birch, 1980), the western coast of South America up till California in the north (Froelich *et al*., 1988; Burnett, 1990; Kolodny and Garrison, 1994), and in the southeastern United States where the Gulf Stream causes upwelling (Riggs *et al*., 1998). Thus, the association of these facies is usually taken as due to upwelling in ancient phosphorite deposits (Baturin, 1982; Abed and Amireh, 1983; Alomogi-Labin *et al.,* 1993; Glenn *et al*., 1994; Follmi, 1996). However, some authors had explained the formation of ancient phosphorites without the need of upwelling (e.g. Heggie et al., 1990; Glenn and Arthur, 1990)

Upwelling currents spread deep, cold marine water on the surface of the relatively shallow continental shelves adjacent to the continents (Fig. 10). Deep, cold water, 1000 m or more, is usually rich in nutrients, most important of which are Si and P which are the basic food for the phytoplanktons (diatoms and dinoflagellates); the lowest step in marine food chains which inhabit the photic zone or the upper 100-200 m of the sea water column. Under such conditions, bioproductivity of the marine food chain is highly increased. Rate of death of these organisms is consequently increased to produce an oxygen minimum zone (OMZ) extending few hundred metres below the photic zone and might reach the shelf floor. The formation of the OMZ reduces the amount of the oxidized soft tissues of the descending organisms, thus giving more chances to the soft tissues (organic matter, OM) to joint the sediments accumulating at the shelf floor. A higher rate of sedimentation will ensure a higher rate of burial for the OM to escape long exposure and oxidation. Consequently, a sediment- rich OM is formed (Baturin, 1982; Salansky, 1986; Glenn et al., 1994; Lucas and Prevot-Lucas, 1995).

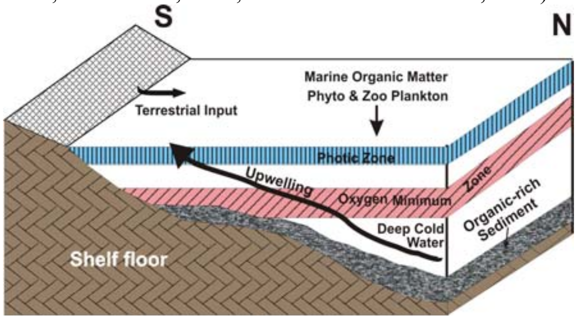

Fig. 10 A schematic model for phosphorite deposition under an upwelling regime.

Decomposition of the sediment organic matter below the water/sediment interface by bacteria and fungi liberates phosphorous to the interstitial pore fluids. Certain minerals form from these fluids like calcite, dolomite and palygorskite before the formation of apatite. This means that P, most probably as PO_4, is concentrated many folds relative to sea water before its deposition (Riggs *et al.,* 1985). Finally, apatite is either precipitated directly from these interstitial fluids (authigenic origin) or the fluids react with pre existing sediments and transform them into apatite (diagenetic origin) (Price and Calvert, 1978; Birch *et al.,* 1983; Froelich *et al.,* 1983).

Jordanian phosphorites are postulated to have deposited under upwelling cold, deep water from the Tethys Ocean in the north onto its shallow epeiric shelf where Jordan was situated during the upper most Cretaceous. This is evident from the presence of phosphorite, bedded chert, porcelanite (biogenic silica deposits), oil shale and a pronounced negative cerium anomaly indicative of deep oceanic water (Abed and Abu Murry, 1997). Furthermore, Jordanian phosphorites are dominantly authigenic, precipitated from the pore fluid solutions as phosphate mud, which was then reworked into phosphate pellets and intraclasts (Al-Agha, 1985; Abed and Al-Agha, 1989).

Recent pelletal phosphorites off the SW Africa and Peru margins are carbonate fluorapatite (Baturin, 1971; Burnett, 1977; Price and Calvert, 1978; Froelich *et al.,* 1983). The concentrations of P, C, and F in the upper few tens of centimeters of the sediment pore water are high enough to permit their direct chemical precipitation as carbonate fluor apatite. On the other hand, the bone material is made of dahlite; carbonate hydroxyapatite, with F content far less than 1% or even hydroxyapatite which is devoid of F (McConnell, 1973; Altschuler, 1973). Dahlite is readily converted into carbonate fluorapatite through the interaction with sediment pore water during early diagenesis, incorporating F and possibly CO_3 into its structure. This conversion process takes place contemporaneously with the direct precipitation of pelletal/intraclast material as carbonate fluorapatite (Froelich *et al.,* 1983; Abed and Fakhouri, 1996).

Accordingly, there should be abundant organic matter associated with the phosphorites in their depositional environment. Organic matter is well known as a good scavenger for U and many other trace metals. Most probably, the newly deposited apatite would take up U into its open crystal structure from the engulfing pore fluids which were formed after organic matter decomposition. Uranium, then, becomes part of the apatite occupying some of the positions located for Ca in the apatite structure. It should be emphasized that U in the ancient phosphorites is present within the crystal structure of apatite not adsorbed on the organic matter (Froelich *et al.,* 1983; Bernett, 1990).

In Jordan, the northwards increase of U may be due to higher organic matter associated with the phosphorites in north Jordan. The NW Jordan deposits have around 6% organic matter (Abed and Al-Agha, 1989) with much lower contents further south. The organic matter in the other localities, other than NW Jordan, is to be seen within the phosphate pellets and intraclasts. The dark colour of some of these particles is indicator of organic matter. This is evident from the leaching and oxidation of pellets/intraclasts rims by percolating oxidizing groundwater through these permeable phosphorite deposits throughout the history of these deposits.

7. Conclusions

High grade phosphorites are wide spread in Jordan. Despite the fact that Ruseifa mines were closed and the central Jordan deposits and near depletion, huge reserves are still existing in Eshidiyya Basin (in excess of 1000 million tons), Al-Kora Basin, NW Jordan (several hundred million tons), and the subsurface of the eastern desert.

The phosphorites of Jordan are the main carrier of Uranium in the country. Uranium is present within the crystal structure of francolite (carbonate flour apatite) substituting for Ca. Uranium content varies up 379 ppm in certain phosphorite horizons.

Uranium content in the various localities increases northwards. Eshidiyya deposits lower member (main deposits) has around 70 ppm U while the upper member (A0) 133 ppm, central Jordan 105 ppm, Ruseifa 123 ppm, and NW Jordan 153 ppm. It should be emphasized that certain phosphorite horizons have much more U compared with these averages. Detailed field geology can pinpoint such horizons if U is to be exploited. It is here postulated that organic matter may be one of the main reason for the northwards increase of U.

During mining and upgrading of the phosphorite ores, U sticks to the mineral francolite and thus behaves similar to Ca and P_2O_5. No groundwater contamination with U is noticed in central Jordan despite the fact that fresh water used in washing the upgraded ore has been discharged to the local environment since more than 45 years.

Throughout the fertilizers industry, U follows P, first into the phosphoric acid and then into the diammonium phosphate (DAP) where it becomes concentrated by a factor of 1.5 relative the fed ore. On the contrary, calcium leaves francolite to phosphogypsum but U does not follow suite, thus phosphogypsum is almost devoid of U with a content up to 2 ppm.

REFERENCES

[1] Abed, A. M., 1989. On the genesis of the phosphorite-chert association in the Amman Formation in Tel es Sur area, Ruseifa, Jordan. *Science Geologie Bulletin*, *Strasbourg* 42, 141-153.

[2] Abed, A. M., 1994. Shallow marine phosphorite-chert-palygorskite association, Upper Cretaceous Amman Formation, Jordan. In: A. Iijima, A. M. Abed, and R. Garrison, (Editors.), *Siliceous, Phosphatic and Glauconitic Sediments in the Tertiary and Mesozoic. Proc. 29th Intern. Geol. Congr., Part C.* VSP, The Netherlands, pp. 205-224.

[3] Abed, A. M., 2000. Geology of Jordan, Jordanian Geologists Association, Amman (In Arabic).

[4] Abed, A. M. and Amireh, B., 1983. Petrography and geochemistry of some Jordanian oil shale from north Jordan: Journal of Petroleum Geology, 5, 261-274.

[5] Abed, A. M. and Khalid, H. 1985 Uranium distribution in the Jordanian phosphorite. *Dirasat*, 12: 91-103.

[6] Abed, A. M. and Al-Agha, M. R., 1989. Petrography, geochemistry and origin of the NW Jordan phosphorites. *J. Geol. Soc. London,* 146: 499-506.

[7] Abed, A. M. & Fakhouri, K., 1996. On the chemical variability of phosphatic particles from the Jordanian phosphorites. *Chemical Geology* 131, 1-13.

[8] Abed , A. M. and Abu Murry, O., 1997. Rare earth element geochemistry of the Jordanian Upper Cretaceous phosphorites. *Arab Gulf J. Scient. Res.,* 15, 41-61.

[9] Abed, A. M. and Sadaqah, R., 1998.. Role of Upper Cretaceous oyster bioherms in the deposition and accumulation of high- grade phosphorites in central Jordan. Journal of Sedimentary Research, 68B, 1009-1020.

[10] Abed. A. M. & Amireh, B. S., 1999. Sedimentology, geochemistry, economic potential and paleogeography of an Upper Cretaceous phosphorite belt in the southeastern desert of Jordan. *Cretaceous Research,* 20, 119-133.

[11] Abed, A. M., Arouri, K. and Boreham, C., 2005. Source rock potential of the phosphorite-bituminous chalk-marl sequence in Jordan. Marine and Petroleum Geology, 22, 413-425

[12] Abed, A. m., Sadaqah, R. and Al-Jazi, M., 2007 Sequence stratigraphy and evolution of Eshidiyya phosphorite platform, southern Jordan. Sedimentary Geology, 198, 209-219.

[13] Abed, A. M., Sadaqah, R., and Kuisi, M. A., 2008. Uranium and potentially tozic metals during the mining, beneficiation and processing of phosphorite and their effects on ground water in Jordan. Mine water and the Environment, 27, 171-182.

[14] Abed, A. M., Sadaqah, R., 2011. Enrichment of uranium in the upper phosphorite horizon (A0) in Eashidiyya, south Jordan. Cretaceous Research (in press).

[15] Al-Agha, M. R., 1985. Petrography, geochemistry and origin of the NW Jordan phosphorites. Thesis. Univ. of Jordan (unpubl).

[16] Al-Hwaiti, M., Matheis, G. and Saffarini, G., 2005, Mobilization, redistribution and bioavailability of potentially toxic elements in Shidiya phosphorites, Southern Jordan. Environmental Geology 47, 431-444.

[17] Almogi-Labin, A., Bein, A. and Sass, E., 1993. Late Cretaceous upwelling system along the southern Tethys margin (Israel): Interrelationship between productivity, bottom water environments, and organic matter preservation. *Paleoceanography,* 8: 671-690.

[18] Altschuler, Z. S. 1973. The weathering of phosphatic deposits: geochemical and environmental aspects. In: G. Griffith, A. Becton, J. M. Spencer and D. T. Mitchell (Editors.). *Environmental Phosphorus Handbook.* Willey, New York, pp. 33-96.

[19] Altschuler, Z. S., 1980. The geochemistry of trace elements in marine phosphorites, Part 2: Characteristics, abundances and enrichment. SEPM Spec publ 29:19-30.

[20] Baturin, G. N. 1971. Recent authigenic phosphorite formation on the SW African shelf. In: F. M. Delany (Editor), The Geology of the East Atlantic Margin. ICSU/SCOR Working Party 31 Symp. Cambridge. *Inst. Geol. Sci. Rep*., 70/16, pp. 88-97.

[21] Baturin, G.N., 1982, Phosphorites on the sea floor.. Developments in Sedimentology 33, Elsevier, Amsterdam, 343 p.

[22] Bender, F. 1974. Geology of Jordan. Borntraeger, Berlin.

[23] Birch, G.F., 1980. A model for penecontemporaneous phosphatization by diagenetic and authigenic mechanism from the western margin of southern Africa. In *Marine phosphorites* (ed Bentor, Y.)*, Society of Economic Paleontologists and Mineralogists, Special Publications* 29, 70-100

[24] Birch, G. F., Thomson, J., McArthur, J. and Burnett, W. C., 1983. Pleistocene phosphorites off the west coast of South Africa. *Nature*, 302: 601-603.

[25] Burnett, W. C. 1977. Geochemistry and origin of phosphorites deposits from off Peru and Chile. *Geol. Soc. Amer. Bull*., 88: 813-23.

[26] Burnett, W.C., 1990. Phosphorite growth and sediment dynamics in the modern Peru shelf upwelling system, In *Phosphorite deposits of the world, v. 3, Neogene to modern phosphorites (*eds Burnett, W.C. and Riggs, S.), 62-74. Cambridge University Press, Cambridge).

[27] Capetta, H., Pfeil, F. Schmidt-Kittler, N. and Martini, E., 1996. New biostratigraphic data on the marine Upper Cretaceous and Paleogene of Jordan. Unpublished report by the, Jordan Phosphate Mining Co, Amman, Jordan.

[28] Coppens, R., Bashir, S. and Ritchard, P. 1977. Radioactivity of El-Hasa phosphates, a preliminary study. Mineral Deposita, 12, 189-196.

[29] El-Hiyari, M., 1985. The geology of Jabal Al-Mutarammil, Map sheets No 3252, III. National Mapping Project, Bulletin 1, Natural Resources Authority, Amman, Jordan.

[30] Follmi, K. B., 1996. The phosphorus cycle, phosphogenesis and marine phosphate-rich deposits. Earth Science Review 40, 55-124.

[31] Froelich, P. N., Kim, K. H., Jahnke, R., Burnett, W. C., Soutar, A. and Deakin, M. 1983. Pre water fluoride in Peru continental margin sediments: uptake from seawater. *Geochim. Cosmochim. Acta*, 47: 1905-12.

[32] Froelich, P., Arthur, M., Burnett, W., Deakin, M., Hensley, V., Jahnke, R., Kaul, L., Kim, H., Soutar, A., and Vathakanoan, C. 1988. Early diagenesis of organic matter in Peru continental margin sediments- phosphorite precipitation: Marine Geology, 80, 309-343.

[33] Glenn, C. R. and Arthur, M. A., 1990. Anatomy and origin of a Cretaceous phosphorite-green sand giant, Egypt. *Sedimentology,* 37: 123-148.

[34] Glenn, C. R.; Follmi, K. B.; Riggs, S. R.; Baturin, G. N.; Grimm, K. A. Trappe, J.; Abed, A. M.; Galli-Oliver, C.; Garrison, R. E.; Iiyin, A. V.; Jehl, C.; Rohrlich, V.; Sadaqah, R. M.; Schidlowski, M.; Sheldon, R. E. and Siegmind, H., 1994. Phosphorus and phosphorites: sedimentary and environments of formation. *Eclogae Geologicae Helvetica,* 87, 747-788.

[35] Glikson, M., Gibson, D. L. and Philp, R. P., 1985. Organic matter in Australian Cambrian oil shale and other Lower Palaeozoic shales: Chemical Geology, 51, 175-191.

[36] Hamam, K. A., 1977. Forminifera from the Maastrichtian bearing strata of Al-Hasa, Jordan. *Jour. Foram. Res.*, 7: 34-43.

[37] Heggie, D. T.; Skyring, G. W., O'Brian, G. W., Reimers, C., Herczef, A., MoriartyD. J. W., Burnett, W. C. and Milnes, A. r., 1990. Organic carbon cycling and the modern phosphorite formation on the East Australian continental margin: an overview. In: A. J. G. Notholt and I. Jarvis (Eds.) *Phosphorite Research and Development.* Geological Society Special Publication 52, 87-118.

[38] Iijima, A., Abed, A. M. and Garrison, R., (Editors.), *Siliceous, Phosphatic and Glauconitic Sediments in the Tertiary and Mesozoic.* VSP, The Netherlands.

[39] Jarvis, I., 1992. Sedimentology, geochemistry and origin of phosphatic chalk: The Upper Cretaceous of NW Europe. *Sedimentology*, 39, 55-97.

[40] Jiries, A., El-Hasan, T., Al-Hiwati, M., and and Seiler, K. P., 2004. Evaluation of the Effluent Water Quality Produced from Phosphate Mines in Central Jordan. Mine Water and the Environment. 23 (3): 133-137 Khalid, H., and Abed, A. M., 1982. Petrography and geochemistry of Esh Shidiya phosphates. *Dirasat*, 9: 81-102.

[41] Khalifa, M. Kh. And Abed, A. M., 2011. Lithostratigraphy and microfacies analysis of the Ajlun Group (Cenomanian to Turonian) in Wadi Sirhan Basin, SE Jordan. *Jordan Journal for Environmental and Earth Sciences (IN press)*

[42] Kolodny, Y. and Garrison, R., 1994. Sedimentation and diagenesis in paleo-upwelling zones of epeiric sea and basinal settings: A comparison of the Cretaceous Mishash Formation of Israel and the Miocene Monterey Formation of California. In: A. Iijima, A. M. Abed, and R. Garrison, (Editors.), *Siliceous, Phosphatic and Glauconitic Sediments in the Tertiary and Mesozoic. Proc. 29th Intern. Geol. Congr., Part C.* VSP, The Netherlands, pp. 133-158.

[43] Krauskopf, K. and Bird, D., 1995. Introduction to geochemistry, 3rd Ed. McGraw Hill, Boston.

[44] Lucas, J. and Prevot-Lucas, L., 1995. Tethyan phosphates and bioproductites. In: Nairn, A. E. et al. (eds), The ocean basins and margins - The Tethys ocean. *Plenum Press*. 8, 367-391.

[45] McArthur, J. M., Hamilton, P. J., Greensmith, J. T., Walsh, J. N., Boyce, A. B., Fallick, A. E., Birch, G., Benmore, R. A. and Coleman, M. L., 1987. Francolite geochemistry - meteoric alteration on a local scale. *Chem. Geol. (Isotope Geoscience),* 65: 415-425.

[46] McClellan, G. H. and Kauwenbergh, S. J. V., 1990. Mineralogy of sedimentary apatite. In: A. J. G. Notholt and I. Jarvis (Editors), *Phosphorite Research and Development. Geol. Soc. Lond. Specl. Publ. no. 52, 23-31.*

[47] McConnell, D., 1973. Apatite, crystal chemistry and mineralogy. Springer, Berlin. 111pp.

[48] Mikbel, Sh. and Abed, A. M., 1985. Discovery of large phosphate deposits in NW Jordan. *Dirasat,* 12, 125-124.

[49] Nathan, Y., 1984. The mineralogy and geochemistry of phosphorites. In: Nriagu, J. O. and Moore, P. O. (eds), Phosphate minerals. Springer, Berlin, 275-291.

[50] Notholt, A. J. G., Sheldon, R. P. and Davidson, D. F., 1989. Phosphate deposits of the world, Volume 2, Phosphate rock resources. Cambridge University Press, Cambridge.

[51] Powell, J. H., 1989. Stratigraphy and Sedimentation of the Phanerozoic Rocks in Central and South Jordan, Part B: Kurnub, Ajlun and Belqa Groups: Bulletin 11, NRA, Amman.

[52] Quennell, A. M., 1951. The geology and mineral rsorces of the (former) Transjordan. *Colonial Geology and Mineral Resources, London, 2, 85-115.*

[53] Prevot, L. and Lucas, J., 1980. Behavior of some trace elements in phosphatic sedimentary formations. In: Y. K. Bentor (Editor), *Marine phosphorites*. SEPM Spec. Publ., 29: 31-41.

[54] Price, N. B. and Calvert, S. E., 1978. The geochemistry of phosphorites from the Namibian shelf. *Chem. Geol*., 23: 151-178.

[55] Riggs, S, R., 1979. Petrology of the Tertiary phosphorite system of Florida., *Econ. Geol*., 74: 194-220.

[56] Riggs, S. R., 1980. Intraclast pellet phosphorite sedimentation in the Miocene of Florida. *Journal of the Geological Society, London* 137, 741-748.

[57] Riggs, S. R., Snyder, S., Hine, A., Snyder, Sc., Elligton, D. and Mallette, P., 1985. Geologic framework of phosphate resources in Onslow Bay, North Carolina continental shelf. *Econ. Geol*., 80: 716-738.

[58] Riggs, S. R., Ambrose, W. G., Cook, J. W., Snyder, S. C., & Snyder, St. W., 1998. Sediment production on sediment-straved continental margins: The interrelationship between hardbottoms, sedimentological and benthic community processes, and storm dynamics. *Journal of Sedimentary Research,* A68, 155-168.

[59] Sadaqah, R. M., 2000. Phosphogenesis, geochemistry, stable isotopes and depositional sequence of the Upper Cretaceous phosphorite formation in Jordan. Unpublished Ph. D thesis , Univ. of Jordan, Amman, 257p.

[60] Sadaqah, R. M., Abed, A.M., Grimm, K. A. and Pufahl, P. K., 2005. The geochemistry of REE , Yttrium and Scandium in some Upper Cretaceous Jordanian phosphorites, *Dirasat* 32, 32-47.

[61] Sheldon, R. P. 1981. Ancient marine phosphorites. *Ann. Rev. Earth planet. Sci.* 9: 251-84.

[62] Sheldon, R. P., 1987. Association of phosphatic and siliceous marine sedimentary deposits. In: J. R. Hein (Editor), *Siliceous sedimentary rock-hosted ores and petroleum.* Nostrand Reinhold, New York, pp. 56-79.

[63] Slansky, M., 1986. *Geology of sedimentary phosphates*, 210 pp. (Elsevier, Amsterdam).

[64] Soframines and Consortium Partners, 1987. Feasibility study of Eshidiyya phosphate project. Unpubl. Jordan Phosphate Mines Company, Amman, Jordan.

JJEES
Jordan Journal of Earth and Environmental Sciences

Volume 4 (Special Publication, Number 2), Jan. 2012
ISSN 1995-6681
Pages 47- 61

Recent Advances in the Chemistry of Nitriles and Enaminonitriles

Fathy M. Abdelrazek[a,*], Mahmoud S. Bahbouh[b]

[a] *Chemistry Department, Faculty of Science, Cairo University, 12613 Giza, Egypt*

[b] *Chemistry Department, Faculty of Science, Al-Baath University, Homs, Syria*

Abstract

Recent developments in the chemistry of nitriles and enaminonitriles are surveyed with emphasis on the most new findings of our group's work aimed at developing efficient approaches to different heterocyclic compounds as well as correcting some erroneous literature reports and reviews.

Keywords :Active Methylene Nitriles; Arylidenes, Alkylidenes; Dimethylformamide Dimethylacetal; Enaminones; Heterocyclic Compounds.

abbreviations

AcOH	Acetic acid
NH_4OAc	Ammonium acetate
NBS	N-Bromo-succinimide
DMAD	Dimethyl acetylene dicarboxylate
DMF	Dimethyl formamide
DMFDMA	Dimethyl formamide dimethyl acetal
EtOH	Ethanol
Pip.	Piperidine
NaOEt	Sodium ethoxide
DBU	1,8-Diazabicyclo[5.4.0]undec-7-ene
(Bmim)OH	1-Butyl-3-methylimidazolium hydroxide (Ionic Liquid)

1. Introduction

1.1. Synthesis of heterocycles from active nitrile and enaminonitrile intermediates

In the last decades, organic cyano compounds have found extensive utilization in the synthesis of heterocycles. The chemistry of these compounds is very rapidly developing [1] and enormous number of reports, reviews and monographs [2-9] have been recently written to cover the developments in this area. However, due to extensive literature on the subject, none of these articles could afford a complete view of the subject. In the present work, a trial to cover the utility of nitriles and enaminonitriles, especially of the systems **1, 2** and **3** (Figure 1) in the synthesis of different heterocyclic compounds and their fused derivatives will be summarized.

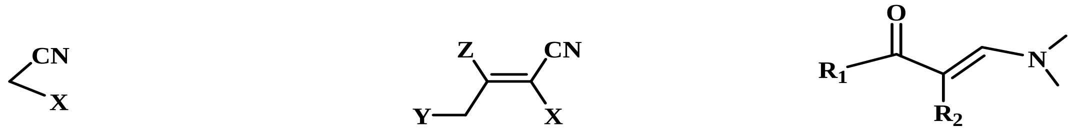

1; X=
a, CN
b, COOEt
c, $CONH_2$
d, $CSNH_2$
e, COPh
f , $CONHNH_2$

2; X	**Y**	**Z**
a, CN	**CN**	**NH_2**
b, COOEt	**COOEt**	**NH_2**
c, CN	**COOEt**	**NH_2**
d, COOEt	**CN**	**NH_2**
e, CN	**SCN**	**Ph**
f, COOEt	**SCN**	**Ph**
g, CN	**COOEt**	**Ph**
h, CN	**CN**	**Ph**
i , COOEt	**H**	**Ph**
j , CN	**H**	**Ph**
k, COPh	**CN**	**Ph**

3 R^1	**R^2**
a, Ph	**H**
b, 2-Furyl	**H**
c, 2-Thienyl	**H**
d, CH_3	**$NHCOCH_3$**
e, CH_3	**CONHPh**

Figure 1

It should be stated here that our intention is not to make an encyclopedic scan of the subject but rather to demonstrate the importance and recent advances of these derivatives in the last decade as intermediates in the synthesis of heterocyclic compounds that could be useful to researchers in this field.

---

[*] Corresponding author. e-mail: prof.fmrazek@gmail.com..

2. Five Membered Rings containing:

2.1. One heteroatom:

2.1.1. Furan derivatives:

Malononitrile **1a** reacted with 2-bromo-1-phenylpropan-1-one **4** to give 2-(1-methyl-2-oxo-2-phenylethyl) malononitrile **5**, which is cyclized in presence of trifluoro-acetic acid **6** to give 2-amino-4-methyl-5-phenylfuran-3-carbonitrile **7** [10] (Scheme 1).

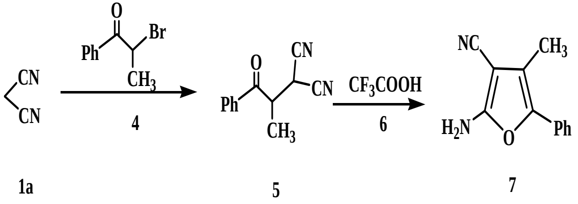

Scheme 1

2-Benzoyl-3-phenylpent-2-enedinitrile 2k underwent bromination with NBS to afford 1-Benzoyl-3-bromo-2-phenylpropenedinitrile derivative 8 [11]. This last compound reacted with potassium hydroxide to afford the furan derivatives 11 and 12 via the intermediates 9 and 10 respectively [12] (Scheme 2).

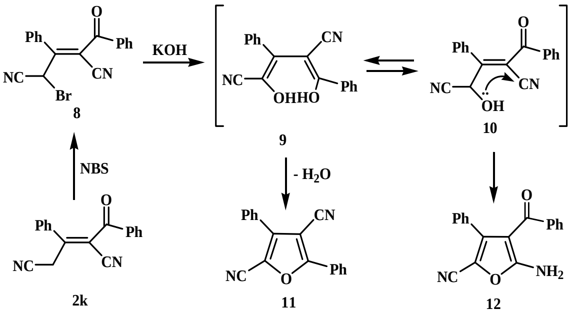

Scheme 2

Under acidic conditions the 1,4-diketone 13 was converted into the furan derivative 14 [13] (Scheme 3).

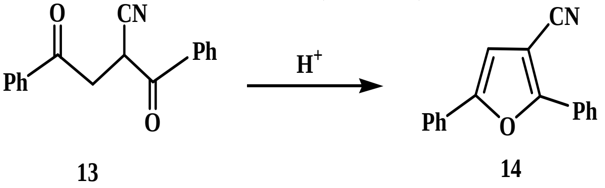

Scheme 3

p-Bromo-phenacylnitrile derivatives 15a,b afforded furan derivatives 16, 17 and 18 upon reflux in ethanol catalyzed by triethylamine. 15a afforded 16 as sole product, while 15b afforded a mixture of two furan derivatives 17 and 18 [14](Scheme4).

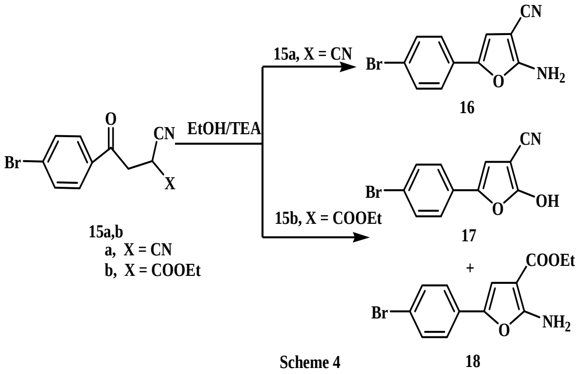

Scheme 4

2.2. Thiophene Derivatives:

Both 2-benzoyl-3-phenylpent-2-enedinitrile **2k** and 1-Benzoyl-3-bromo-2-phenylpropenedinitrile derivative **8** could be transformed into the thiophene derivative **19** upon the reaction with elemental sulfur or sodium hydrogen sulfide respectively [15] (Scheme 5).

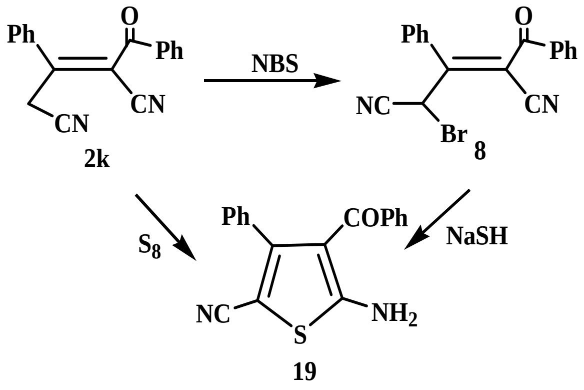

Scheme 5

Compound **2h** is reported to undergo bromination also with NBS to afford the bromo derivative **20**.

Both **2h** and **20** could be transformed into the thiophene-3,5-dicarbonitrile derivative **21** [16] (Scheme 6).

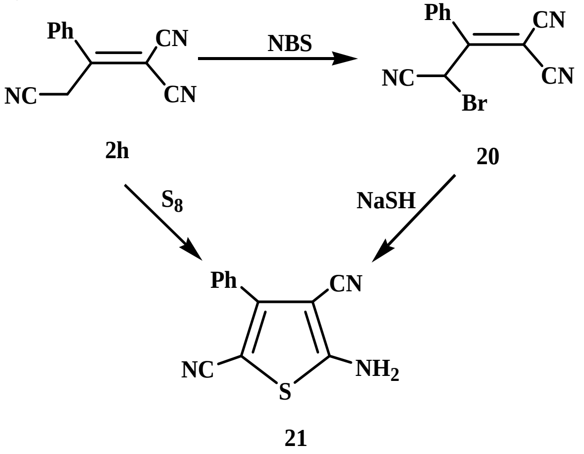

Scheme 6

2.3. Pyrrole Derivatives:

It has been also reported that compound **20** reacts with the aromatic amines **22a-d** to give the N-aryl substituted pyrrole derivatives **24a-d** presumably via the intermediates **23**; and with the urea derivatives **25a-c** to afford the pyrrole derivatives **26a-c** [16] (Scheme 7).

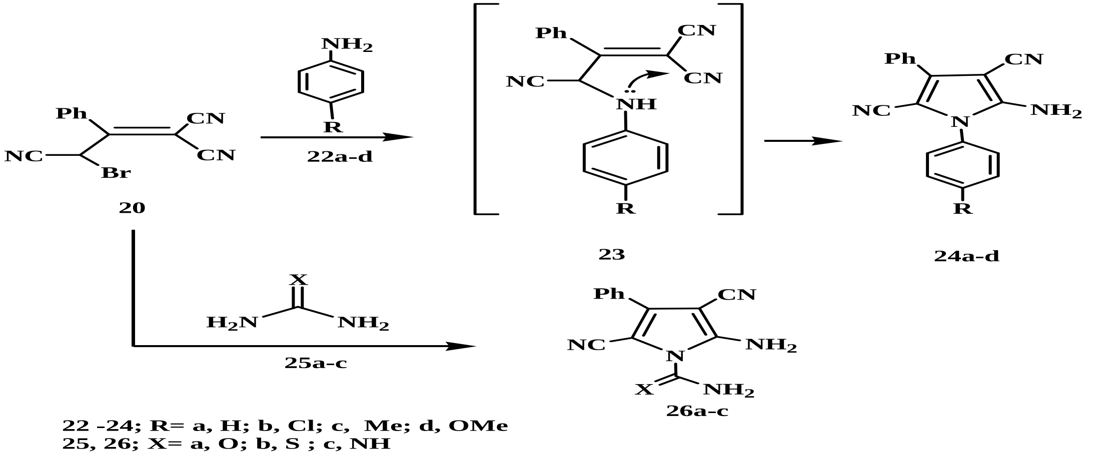

Scheme 7

1-Benzoyl-3-bromo-2-phenylpropenedinitrile derivative **8** is reported to react also with urea, thiourea and guanidine **25a-c** to afford the pyrrole derivatives **27a-c** respectively [15] (Scheme 8).

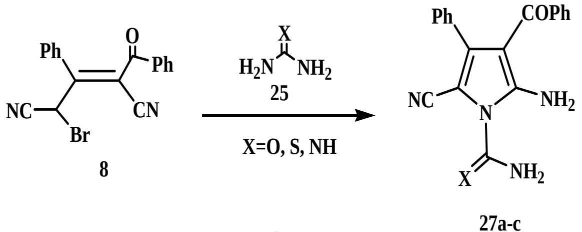

Scheme 8

The reaction of the phenacylmalononitrile derivatives 15a,c-e with aniline under reflux in absolute ethanol in the presence of catalytic amounts of conc. HCl afforded a single product in each reaction; these compounds were identified as 1,5-disubtituted 2-amino-3-cyano-pyrroles 28a–d [17] (Scheme 9).

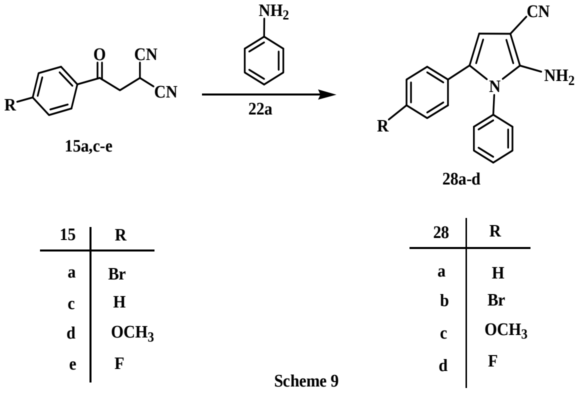

15	R
a	Br
c	H
d	OCH_3
e	F

28	R
a	H
b	Br
c	OCH_3
d	F

Scheme 9

It has been reported that phenacylmalononitrile derivatives **15c,f** react with dimethylformamide dimethylacetal (DMFDMA) in refluxing toluene to give the enaminones **29a,b** respectively**.** Compounds **29a,b** react with the aromatic amines **22a,c,d** in refluxing ethanol to afford the pyrrole derivatives **31a-f** via the intermediates 3**0a-f** [18] (Scheme 10).

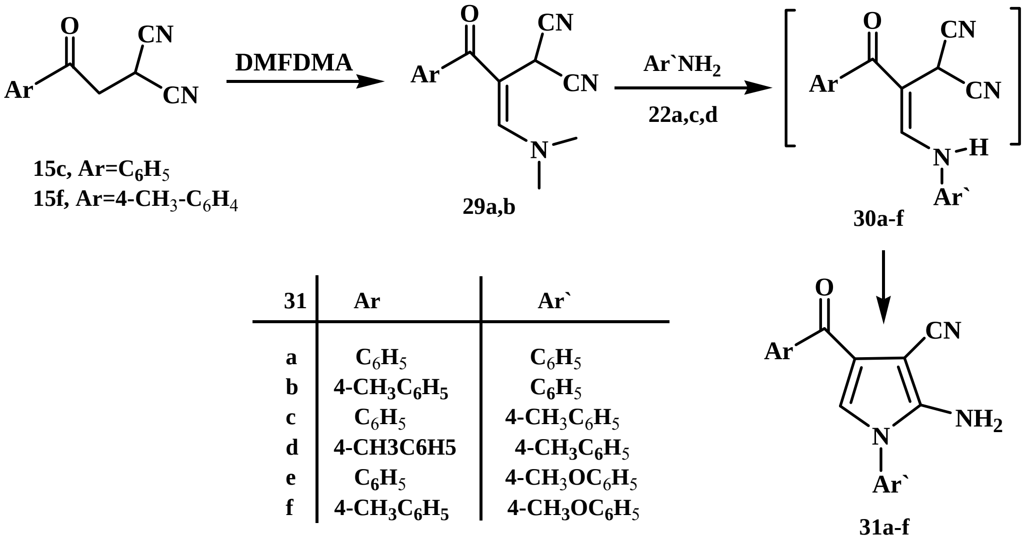

31	Ar	Ar`
a	C_6H_5	C_6H_5
b	4-$CH_3C_6H_5$	C_6H_5
c	C_6H_5	4-$CH_3C_6H_5$
d	4-CH3C6H5	4-$CH_3C_6H_5$
e	C_6H_5	4-$CH_3OC_6H_5$
f	4-$CH_3C_6H_5$	4-$CH_3OC_6H_5$

Scheme 10

3. Two Heteroatoms:

3.1. Pyrazole Derivatives:

P-Bromo-phenacyl malononitrile **15a** reacted with hydrazine derivatives at room temperature to afford the diaminopyrazoles **32a,b** while ethyl *p*-bromo-phenacyl cyanoacetate **15b** afforded the 4-phenacylpyrazole derivatives **32c,d**. Compounds **15a** and **15b** underwent the coupling reaction with the aromatic diazonium salts **33a-d** to afford the pyrazole derivatives **34a-h** respectively [14] (Scheme 11).

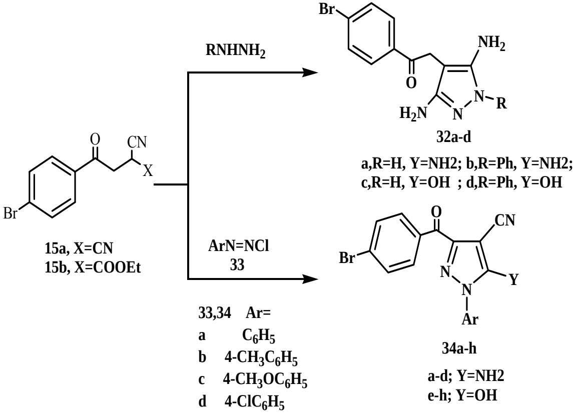

Scheme 11

The carbonyl compounds **35** condensed with DMFDMA to yield the corresponding enaminones **36**. Treatment of the enaminones **36** with hydrazine hydrate, phenyl, or alkyllhydrazines and hydroxylamine afforded the 3,4-disubstituted pyrazoles **37** [19, 20] (Scheme 12).

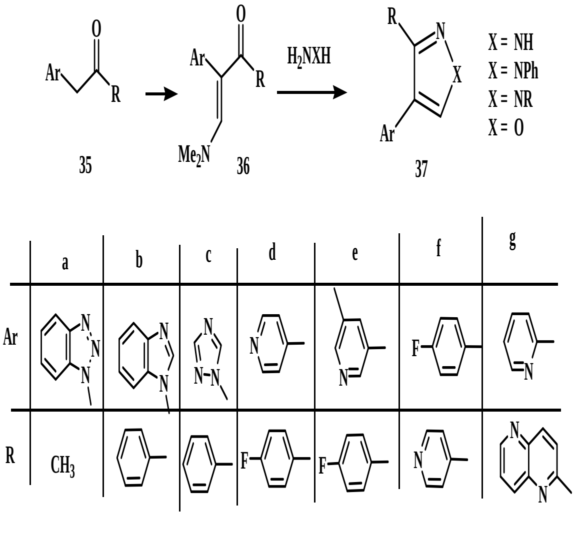

Scheme 12

Acetoacetanilide 38 is reported to react with DMFDMA to afford the enaminone 3e. Treatment of 3e with hydrazine and phenyl hydrazine afforded the respective pyrazole derivatives 39a,b [21-25] (Scheme 13).

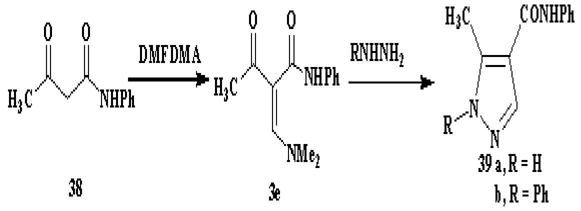

Scheme 13

The enaminone 4**1** was obtained from 3-(2-fluoro-phenyl)-3-oxo-propionic acid ethyl ester **40** with DMFDMA and converted directly to the pyrazole derivative **43** by reaction with (5-phenyl-pyridin-2-yl)-hydrazine **42** [26, 27] (Scheme 14).

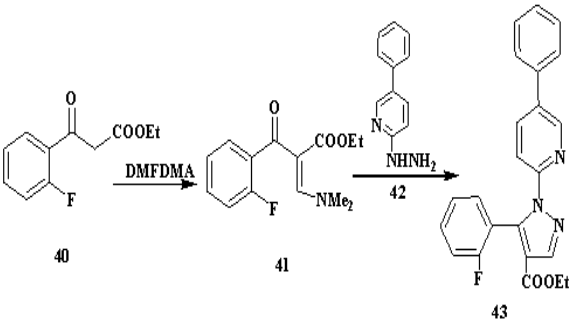

Scheme 14

4. Six Membered Rings Containing:

4.1. One Heteroatom:

4.1.1. Pyridine Derivatives:

Compound **8** is reported to react with cyanoacetamide **1c** and cyanothioacetamide **1d** to afford the pyridine derivatives **44** [15] (Scheme 15).

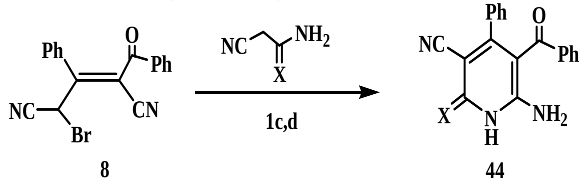

Scheme 15

The enaminone 36a reacted with cyanothioacetamide 1d to yield the polyfunctionaly substituted pyridine derivative 45 [27] (Scheme 16).

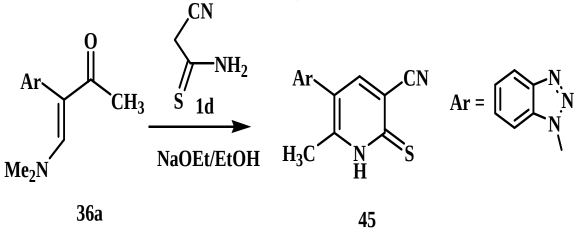

Scheme 16

The enaminone derivatives **3a-c** are reported to react with malononitrile **1a** to afford the intermediate condensation compounds **46a-c**. These compounds were claimed to undergo cyclization to afford the 2-(1*H*)-pyridone derivatives **47a-c** [28].

However, in a recent reinvestigation of this reaction it has been shown that the intermediates isolated from this reaction are the 2-cyano-5-dimethylamino-5-arylpenta-2,4-dienoic amide derivatives **48a-c** which were cyclized to the 2-(1*H*)-pyridone derivatives **49a-c**, respectively [29] (Scheme 17).

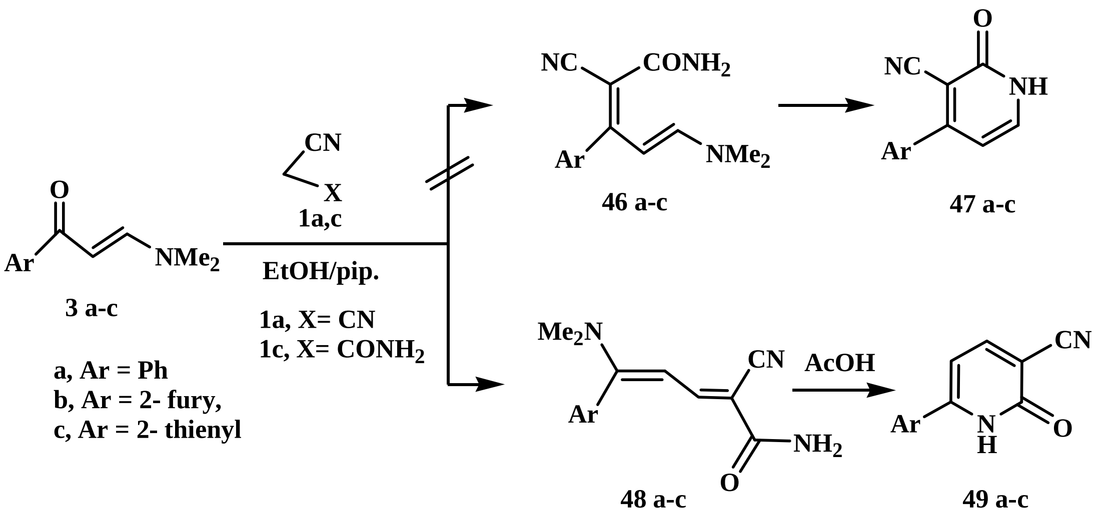

Scheme 17

The structures of the intermediate dienamides **48a-c** were confirmed through X-ray analysis of **48a** (Figure 2) and a plausible mechanism for their formation via the intermediate steps **50-52** has been suggested [29] (Scheme 18).

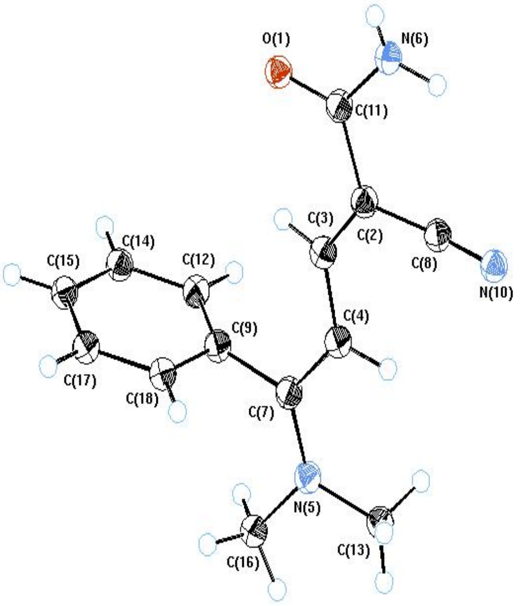

Fig 2: X-ray picture of **48a**.

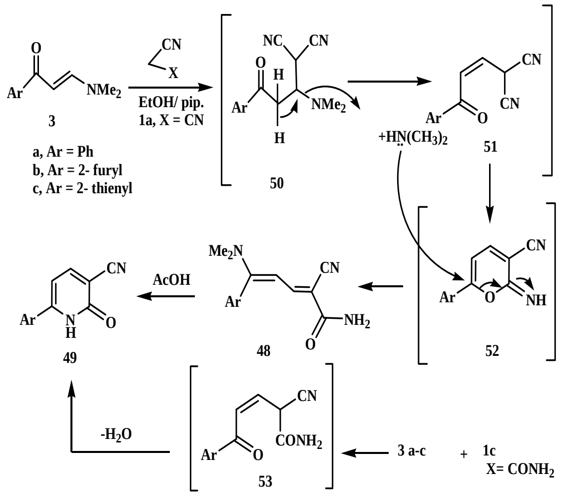

Scheme 18

The reaction of **3a-c** with cyanoacetamide **1c** afforded the same 2-(1*H*)-pyridone **49** presumably via the intermediate **53** which offers a further evidence of the suggested mechanism.

The reaction of 3-acetyl amino-4-dimethylamino-but-3-en-2-one **3d** with malononitrile **1a** was also claimed to afford the condensation intermediate **54** which was claimed to be cyclized to afford 2-(1*H*)-pyridone derivative **55** [30].

Reinvestigation of this reaction showed that it proceeds according to the sequence shown in the previous mechanism to afford the intermediates **56** and **57** which were cyclized into 2-(1*H*)-pyridone derivative **58** [29] (Scheme 19).

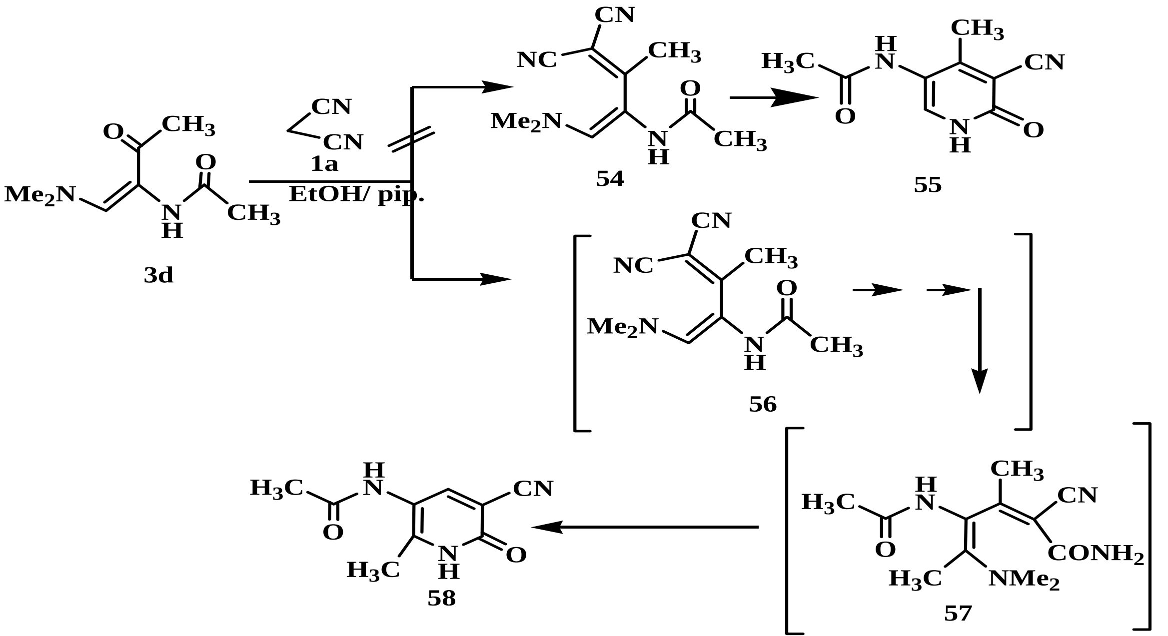

Scheme 19

The reaction of the enaminone **3d** with cyanothioacetamide **1d** was also claimed [30] to afford the 2-(1*H*)-pyridinethione **60** via the condensation intermediate **59.** Reinvestigation of this reaction has also shown that the reaction did not proceed via condensation but rather via substitution of dimethylamino group followed by cyclization of the intermediate **61** to afford **62** [31] (Scheme 20).

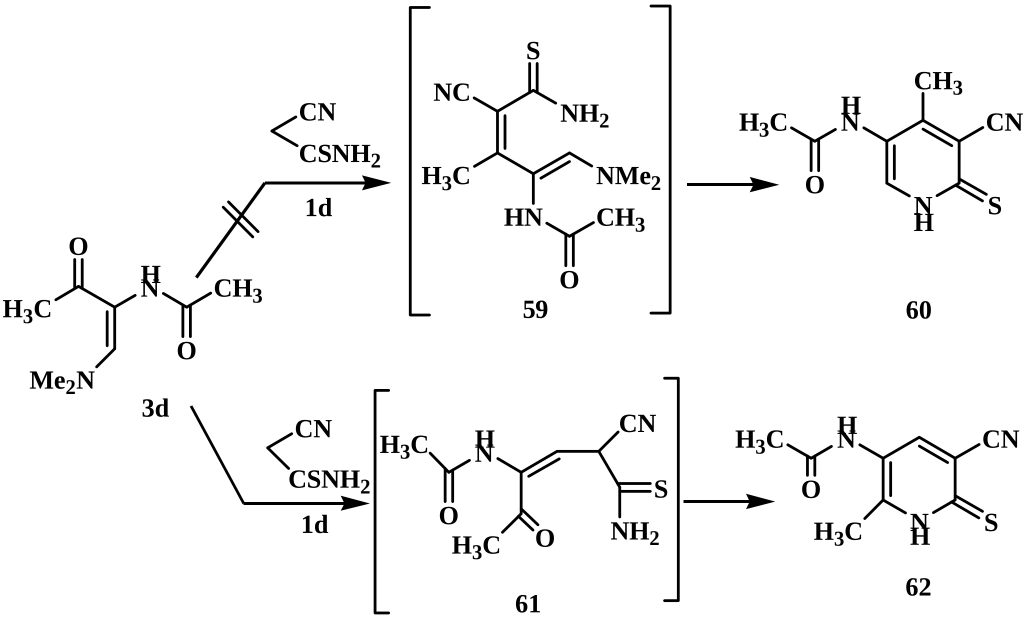

Scheme 20

The reaction of the structurally related compound 2-dimethylaminomethylene-3-oxo-*N*-phenylbutyramide **3e** with cyanoacetamide **1c** was reported to afford the 5-carboamido-3-cyano-4-methylpyridin-2(1*H*)-one derivative **64** assumingly via the condensation intermediate **63** [32, 33]. Reinvestigation of this reaction showed that the 6-methyl 2-(1*H*)-pyridone derivative **66** was obtained presumably via the intermediate **65** [31] (Scheme 21).

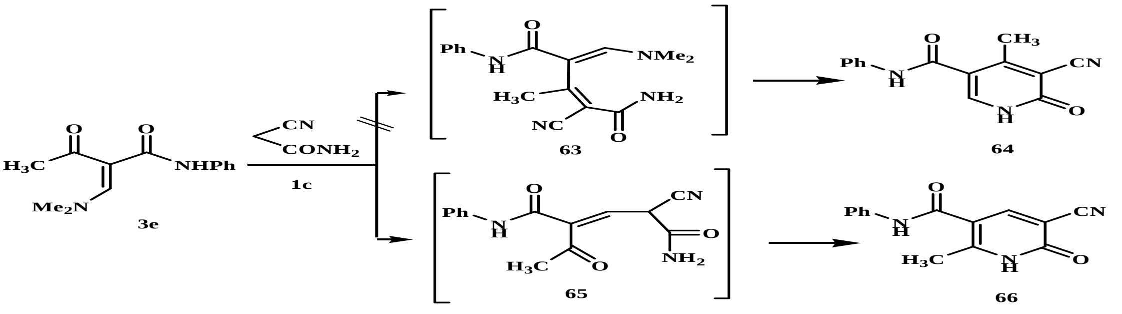

Scheme 21

The reaction of **3e** with cyanothioacetamide **1d** was claimed also to afford the pyridinethione derivative **68** via the condensation intermediate **67** [32]. Reinvestigation of this reaction has also shown that the reaction proceeds via the intermediate **69** followed by cyclization to afford the pyridinethione compound **70** [31] (Scheme 22).

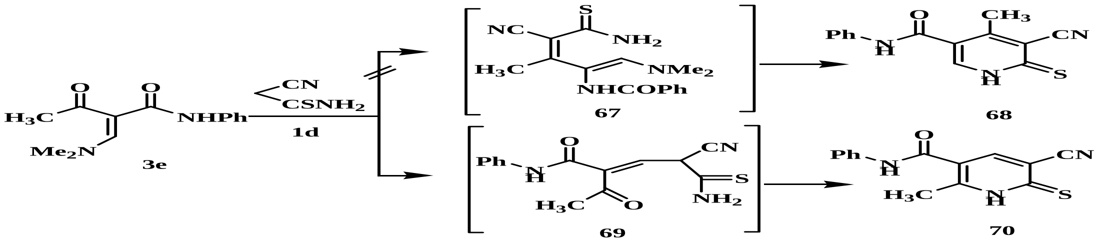

Scheme 22

\Compound 70 was allowed to react with dimethyl acetylene dicarboxylate (DMAD) to afford an addition product via the tautomerized thiol function with loss of the CONHPh group as shown by X-ray crystallography (Figure 3). The X-ray picture shows also that the methyl group is located at the 6th position of the pyridine ring as shown in our structure 70; not in the 4th position as was claimed in structure 68 [32]. \

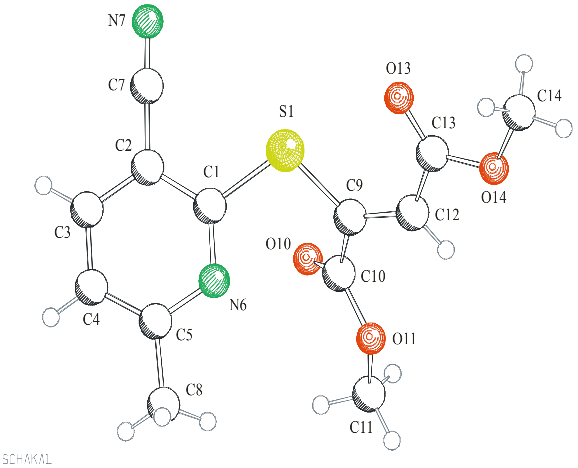

Figure 3: X-ray picture of 70-DMAD adduct

It should be mentioned that the structures of the pyridine-2-(1*H*)-ones **49**, **58**, **66** and pyridine-2-(1*H*)-thiones **62** and **70** are in complete agreement with those reported earlier and confirmed by X-ray study of the products of a related reaction between enaminones and cyanoacetamide **1c** and cyanothioacetamide **1d** [34].

It is worth also to mention here that the position of the aryl group in the erroneous structure **47** and its correct structure **49** seems to be not easily distinguishable by elemental analyses and the spectral data, this is understandable and may seem of little importance to the reader. However it is not understandable and seems of great importance when the substituent becomes a methyl group as in compounds **55** and **60** by Elnagdi et. al. [28, 30] and in compound **64** and **68** by Abu ElMaati et. al.[32, 33]. The authors further claimed that the latter compounds react with the arylidene derivatives of malononitrile to afford the isoquinoline derivatives **71;** and have cited a complete set of analyses and spectra to these imaginary products while initially there is no methyl group in position-4 (Scheme 23).

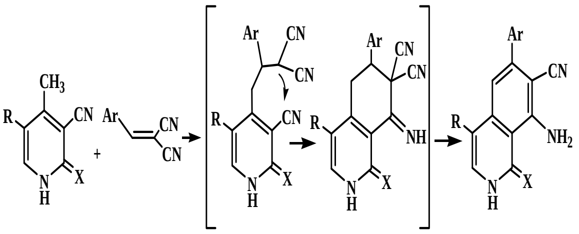

55; R=NHCOCH$_3$, X=O
60; R=NHCOCH$_3$, X=S
64; R=CONHPh, X=O
68; R=CONHPh, X=S

71

Scheme 23

2-Cyanomethylbenzylidine malononitrile **2h** reacts with trichloroacetonitrile in refluxing benzene or toluene catalyzed by piperidine to afford the pyridine **73** presumably via the intermediate **72.** The trichloromethyl moiety in **73** could be easily substituted by OH, OMe, OEt upon refluxing in water, methanol or ethanol, respectively, to afford the pyridine derivatives **74a-c** [35] (Scheme 24).

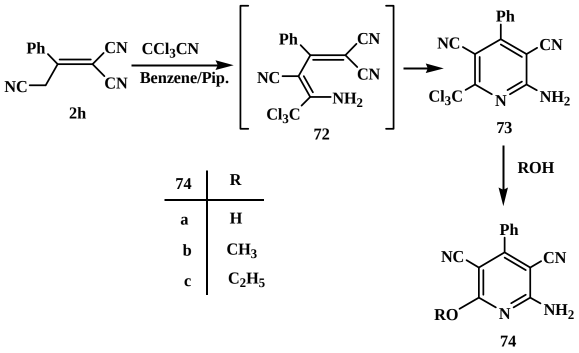

74	R
a	H
b	CH_3
c	C_2H_5

Scheme 24

We have reported a novel synthesis of the N-substituted pyridone derivatives 76a-f starting from the cyanoacetamide derivatives 1c,f and their related derivatives 1g-j with 1-benzyl-1,3-dibromo-2-phenylpropane 75 in ethanol in presence of potassium carbonate [36] (Scheme 25) .

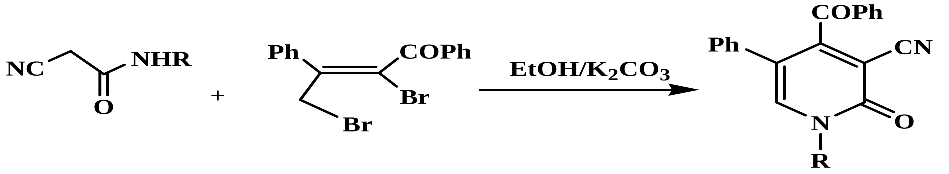

1c, f, g-j **75** **76a-f**

1	R
c	H
f	NH_2
g	N=CHPh
h	Ph
i	4-$CH_3C_6H_4$
j	4-ClC_6H_4

76	R
a	H
b	NH_2
c	N=CHPh
d	Ph
e	4-$CH_3C_6H_4$
f	4-ClC_6H_4

Scheme 25

Compound **75** could be transformed into 2-benzoyl-3-phenylpent-2-enedinitrile **2k**. This last compound could be cyclized with different reagents to afford the new pyridine derivatives **77-80** [37] (Scheme 26)

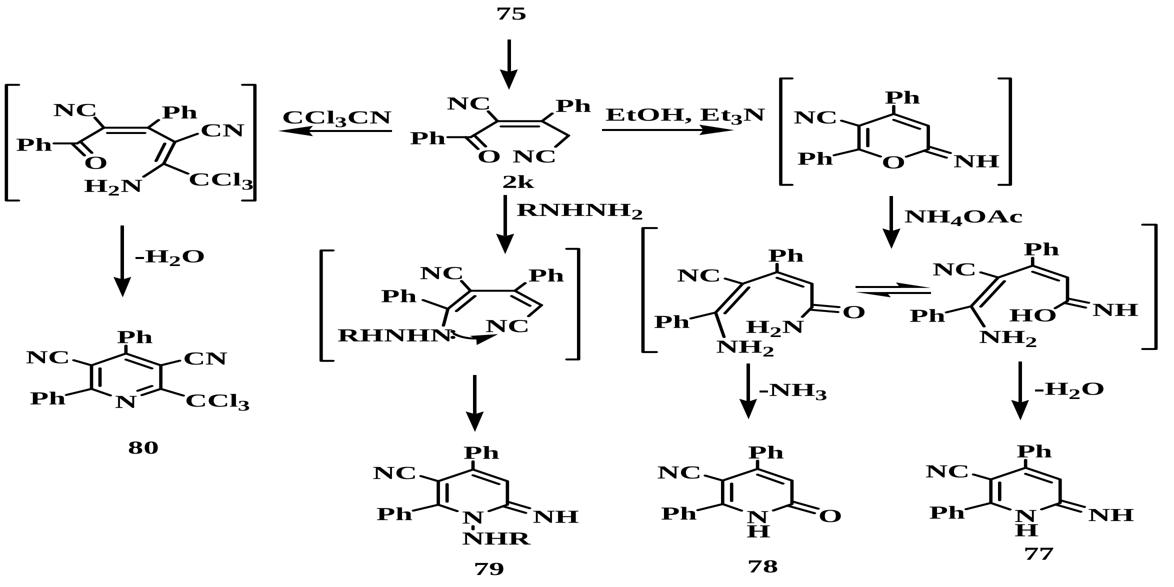

Scheme 26

Most recently 2-(1-aryl-ethylidene)-malononitriles **81a-f** are reported to undergo self dimerization in ethanol catalyzed by sodium ethoxide to afford 2-[4,6-diaryl-3-cyano-6-methyl-5,6-dihydropyridin-2(1*H*)-ylidene]-malononitrile derivatives **82a-f** respectively. The structure of the dimer was elucidated by X-ray crystallography (Figure 4); and a plausible mechanism for its formation was suggested [38, 39] (Scheme 27).

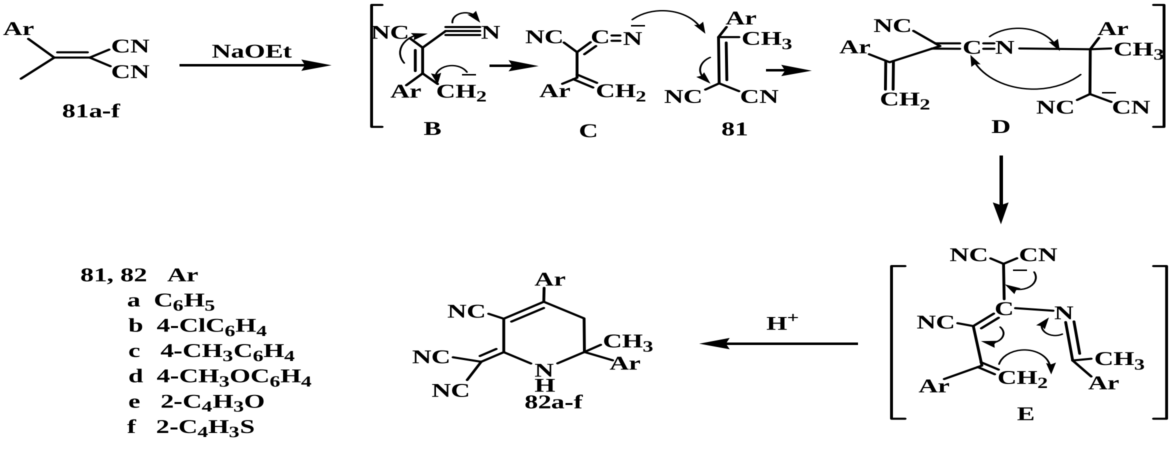

Scheme 27

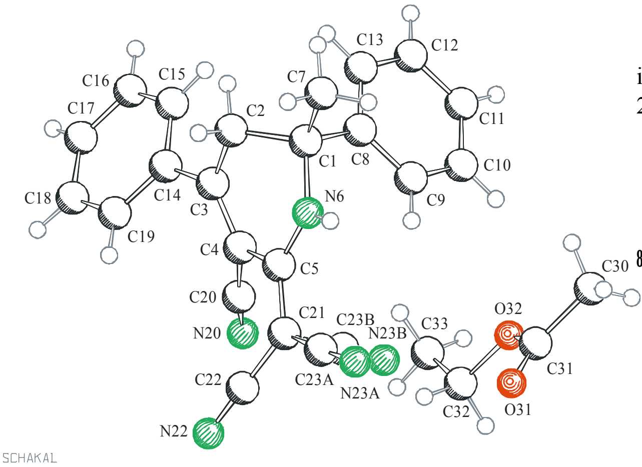

Fig 4.X-ray picture of the dimer **82a.**

4.2. Two Heteroatoms:

4.2.1. Pyridazine Derivatives:

p-Bromo-phenacyl malononitrile **15a** reacts with hydrazine derivatives in refluxing ethanol catalyzed by triethylamine to afford **83a,b.** Refluxing **83a** in ethanol/hydrochloric acid mixture furnished the pyridazine-6-one **84**. Compound **83b** under the same reaction conditions underwent ring contraction to afford the furan derivative **16** [14] (Scheme 28).

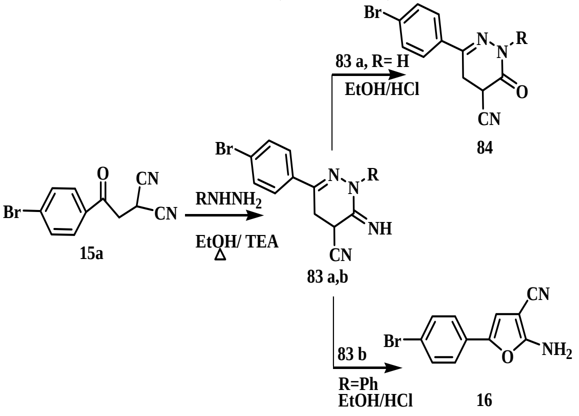

Scheme 28

A plausible mechanism for the transformation of **83b** into the furan derivative **16** was suggested [14] (scheme 29).

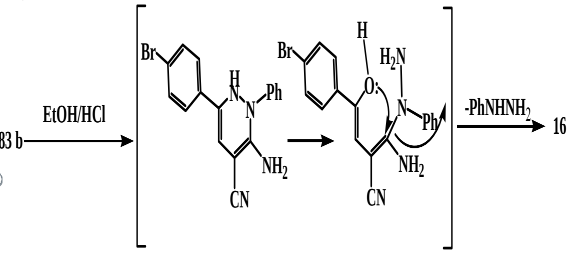

Scheme 29

We have reported that **2g** undergoes the coupling reaction with the aryl diazonium chlorides **30** to yield the hydrazo derivatives **85** which are readily cyclized into the pyridazin-imine derivatives **86** [40, 41] (Scheme 30).

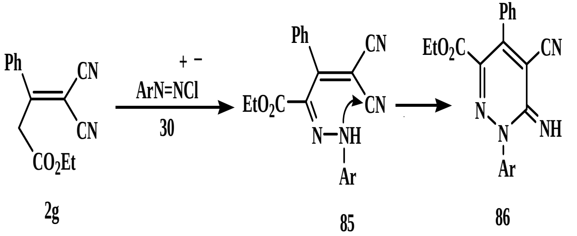

Scheme 30

It has also been reported that the arylhydrazones **87a-c** condensed with **1b** to yield the pyridazinones **88a-c** [42, 43] (Scheme 31).

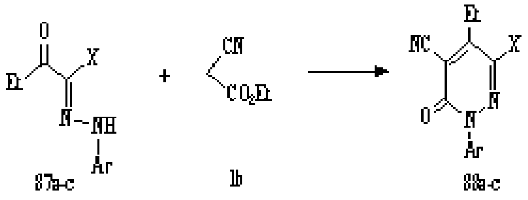

87, 88 a, X=CO2Me; b, X=CN; c X=CO2Et

Scheme31

The bromo derivative **20** reacts with hydrazines to afford **89a,b** which could be cyclized into the pyridazine derivatives **90a,b** [44] (Scheme 32).

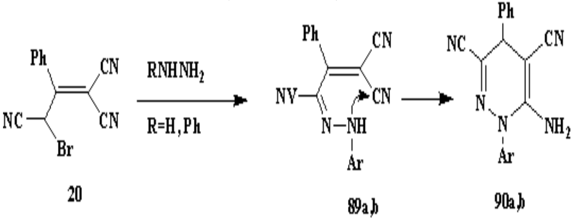

Scheme 32

Enaminones **29a,b** (in scheme 10) have been successfully transformed into the pyridazine derivatives **91a-d** through their reaction with hydrazine and phenylhydrazine. The dihydro derivatives **91a,b** could be oxidized to the fully aromatic pyridazine derivatives **92a,b** [45] (Scheme 33).

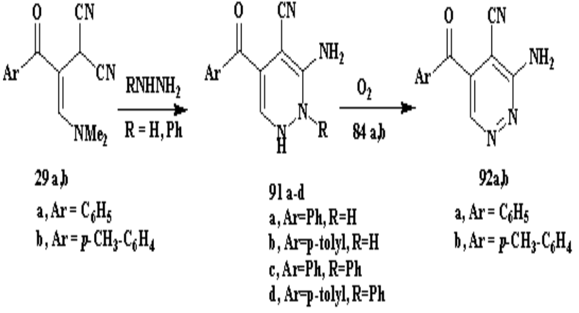

Scheme 33

4.2.2. Pyrimidine Derivatives:

Compound **75** is reported to afford the pyrimidine derivatives **93** and **94** upon reaction with mono and disubstituted urea and thiourea derivatives [36] (Scheme 34).

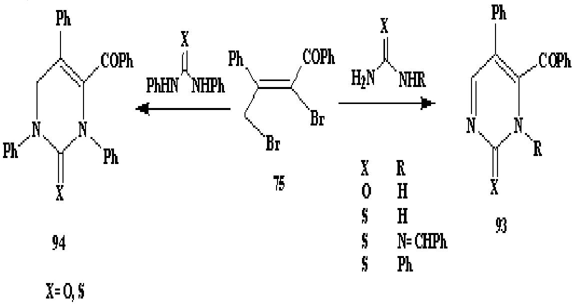

Scheme 34

Treatment of the enaminones **36** with thiourea in the presence of sodium ethoxide afforded the corresponding 4,5-disubstituted pyrimidine-2-thione derivatives **95** [46, 47] (Scheme 35).

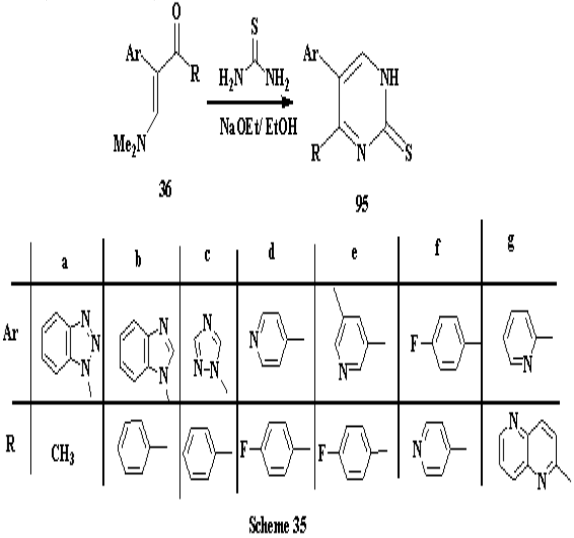

Scheme 35

Most recently it has been reported that malononitrile **1a** reacts with different aldehydes and guanidine hydrochloride in a one pot synthesis assisted by microwave in an ionic liquid to afford the pyrimidine derivatives **96** in good to excellent yields [48] (Scheme 36).

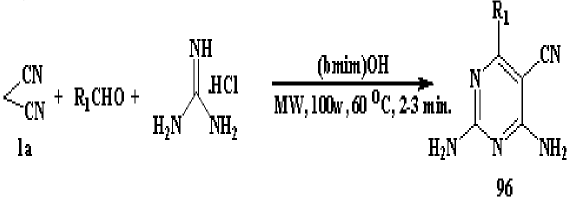

Scheme 36

4.2.3. Fused Heterocyclic Rings:

The bromo derivative **20** has been reported to react with cyanoacetohydrazide **1f** to afford the pyrrolo-pyridazine derivative **97**. Compound 20 is also reported to react with anthranilonitrile and methyl anthranilate to afford the pyrroloquinazoline derivatives **98a,b** respectively. It reacts also with the amino furan and thiophene derivatives **99a-c** to afford the imino-indacene derivatives **100a-c** which could be transformed into their –oxo derivatives **101a-c** respectively [16] (Scheme 37).

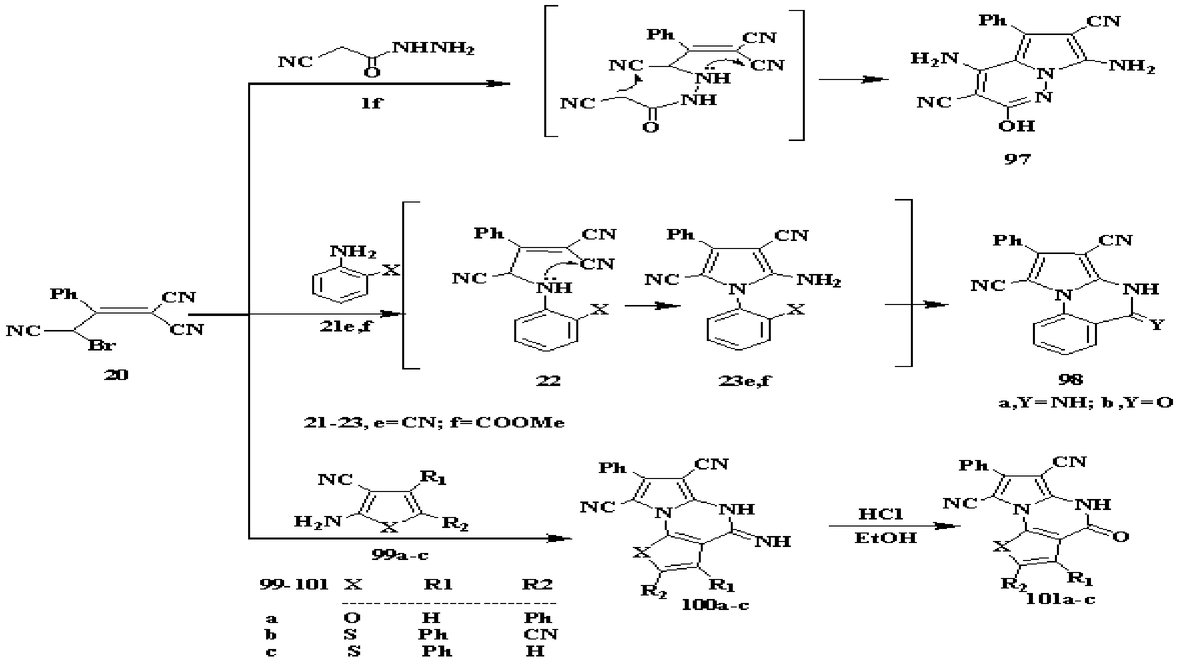

Scheme 37

The trichloromethyl group in compound **73** could be substituted by a hydrazino group upon reaction with hydrazine hydrate at room temperature to afford the pyridyl hydrazine derivatives **102a,b**. Refluxing compounds **102** in ethanol with ammonium acetate afforded the pyrazolo[3,4-b]pyridine derivatives **103a,b**. It worth to mention that **103a,b** were obtained directly upon refluxing **73** in hydrazine hydrate [35] (Scheme 38).

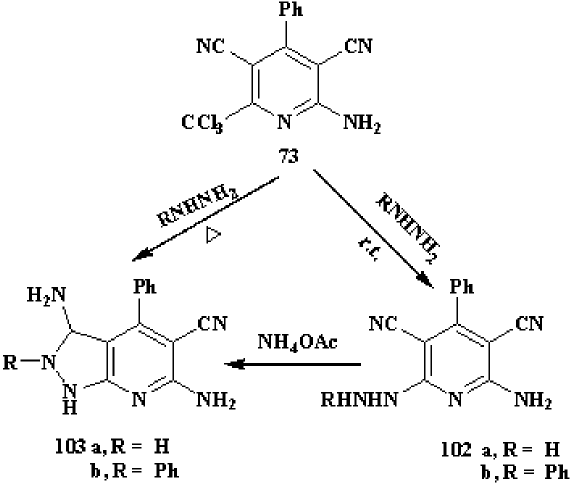

Scheme 38

The dibromo derivative **75** was reported to react with amino pyrazoles **104** and benzimidazole **105** to afford the pyrazolopyrimidine derivatives **106** and the benzimidazolopyrimidine derivative **107** respectively [36] (Scheme 39).

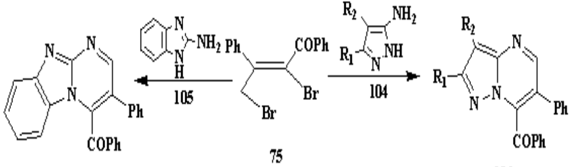

Scheme39

We have reported that cinnamonitriles derivatives **108a-f** react with the cyclic-1,3-diones **109a,b** to afford the novel chromene derivatives **110a-n** and with the NH-pyrazolones **111a,b** to afford the pyranopyrazole derivatives **112a-n** [49, 50] (Scheme 40).

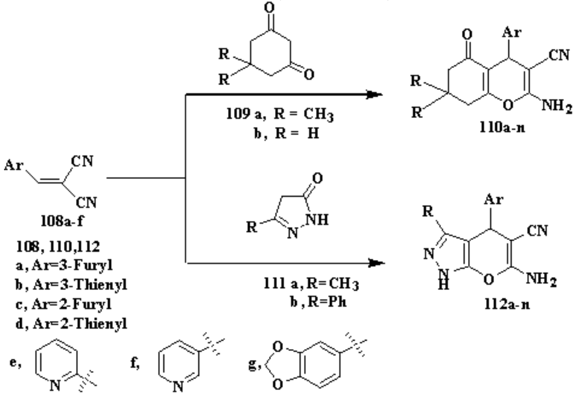

Scheme 40

The structure of these chromene derivatives was unambiguously elucidated via an x-ray crystallographic picture of the formimidate derivative of **110a** (Figure 5) [51].

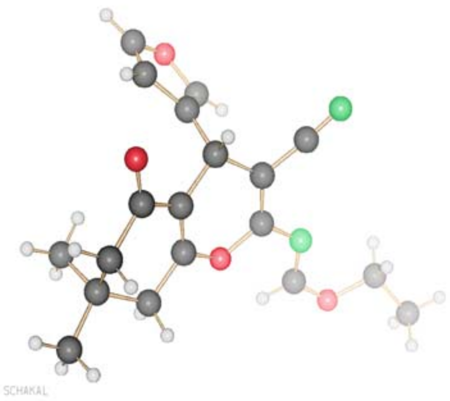

Fig 5. X-ray picture of the formimidate of **110a**

Dimedone **109b** has been reported to react with *o*-phenylenediamines to afford the imine **113** which was cyclized into the benzodiazepine derivatives **114** on reaction with cyanogen bromide [52] (Scheme 41).

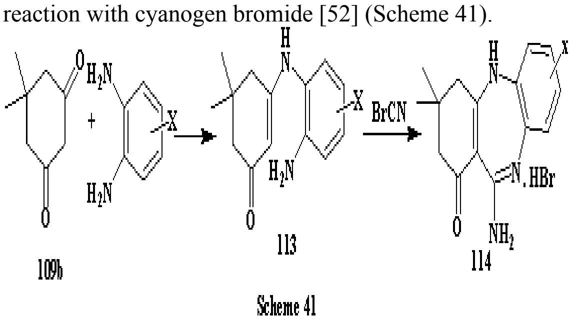

Scheme 41

The cyclic enaminoketones **115** was reported to react with benzylidenes of malononitrile **108** to afford the quinoline derivatives **116**. When a similar reaction was carried out between **117** and *p*-bromo-benzylidene malononitrile the N-anilino-quinoline derivative **118** was obtained which could be cyclized into the indolo-quinoline derivative **119**. Reacting the cyclic enamino-ketone **120** with 2,4-dichloro-benzylidene malononitrile afforded the quinolino-quinazoline **121** [53] (Scheme 42).

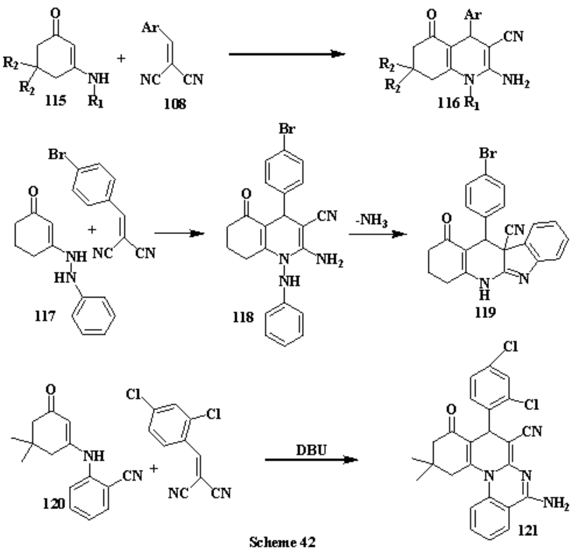

Scheme 42

Benzylidene malononitrile **108a** was reported to react with N-alkyl-2-thicarbamoylacetamide **122** and ω-bromoacetophenone **123** in presence of piperidine to afford the thiazolopyridine derivative **124** [54] (Scheme 43).

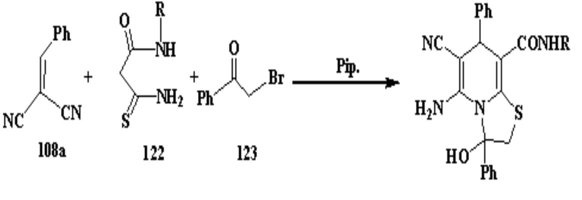

Scheme 43

On refluxing different pyrazolone derivatives **86c** with arylidene malononitriles **108a-c** in ethanol catalyzed by piperidine, the pyrano[2,3-c]pyrazolones **125a-c** and the acyclic derivatives **126a-c** were obtained. On the other hand, 1,3-disubstituted pyrazolin-5-one **86d** afforded the oxinobisprazole derivatives **127a-c** and pyrano[2,3-c]pyrazole derivatives **128a-c** [55] (Scheme 44).

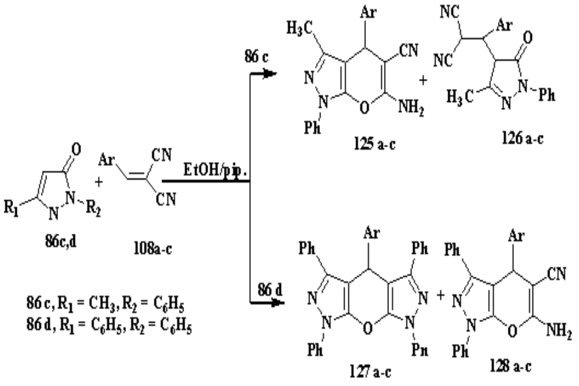

Scheme 44

The different behavior of the differently substituted pyrazoline derivatives **86** towards arylidene malononitrile derivatives is rationalized and an interesting mechanism is given in ref. [55].

It has been reported that the pyrrole derivatives **31a-f** react with hydrazine hydrate and phenyl hydrazine in refluxing ethanol to afford the pyrrolo[3,4-*d*]pyridazine derivatives **129a-f** and **130a-f,** respectively [17] (Scheme 45).

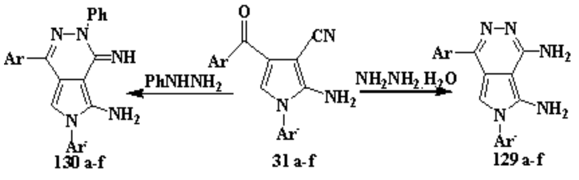

31, 129, 130:

a, Ar = C_6H_5	Ar' = C_6H_5
b, Ar = *p*-CH_3-C_6H_4	Ar' = C_6H_5
c, Ar = C_6H_5	Ar' = *p*-CH_3-C_6H_4
d, Ar = *p*-CH_3-C_6H_4	Ar' = *p*-CH_3-C_6H_4
e, Ar = C_6H_5	Ar' = *p*-CH_3O-C_6H_4
f, Ar = *p*-CH_3-C_6H_4	Ar' = *p*-CH_3O-C_6H_4

Scheme 45

The pyridazine derivatives **91a-d** and **92a,b** could be transformed into the pyridazino-pyridazine derivatives **131a-d** and **132a,b** respectively [45] (Scheme 46).

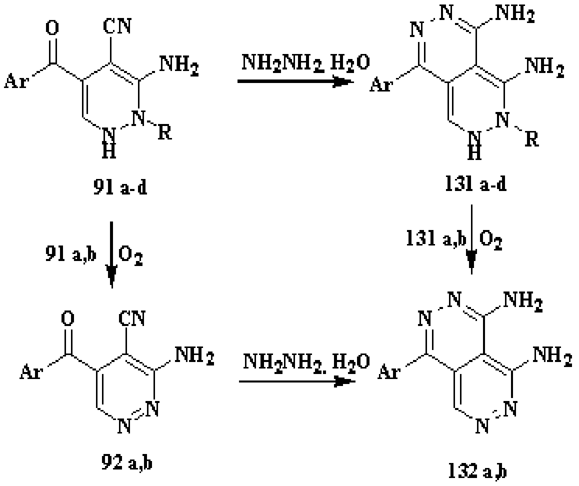

Scheme 46

The enaminones **29a,b** react with anthranilonitrile and methyl anthranilate in refluxing ethanol to afford the 5-iminopyrrolo[1,2-*a*]quinazolines **133a,b** and the oxo-analogues **134a,b** respectively. Compounds **133a,b** could be transformed into **134a,b** upon refluxing in ethanol and conc. HCl [17] (Scheme 47).

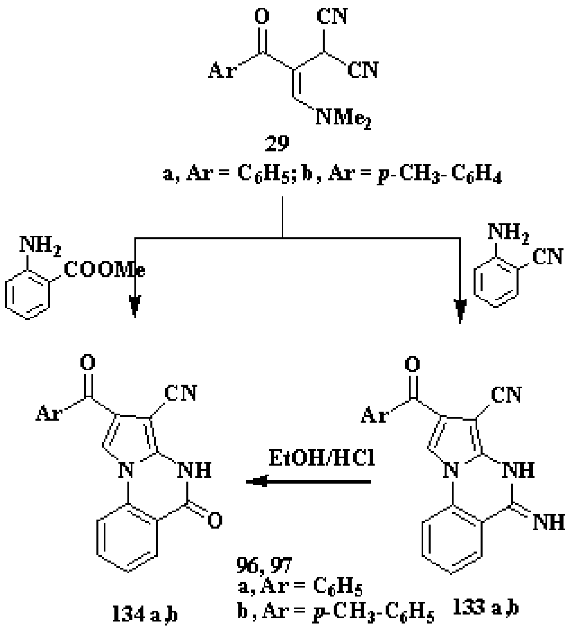

Scheme 47

Treatment of the enaminone derivatives **36** with malononitrile dimmer **2a** afforded 1,6-naphthyridine derivatives **135** [56] (Scheme 48).

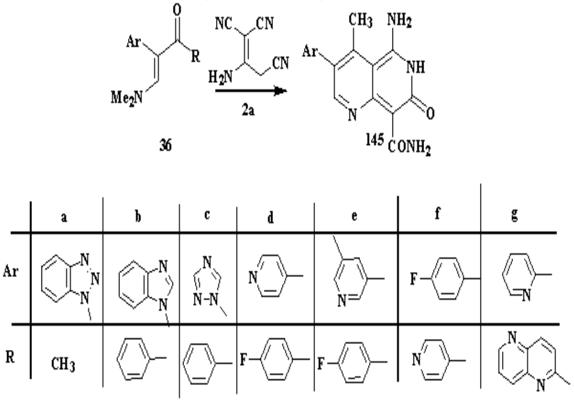

Scheme 48

Benzotriazolyl-acetonitrile **146** condenses with DMFDMA to afford the enaminonitrile derivative **147**. The reaction of **147** with 5-amino-3-methyl pyrazole afforded the pyrazolopyrimidine derivative **148** [57] (Scheme 49).

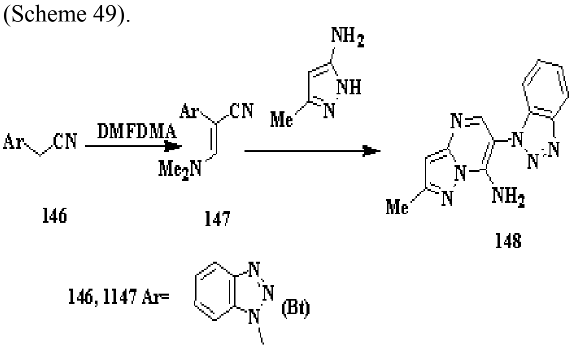

Scheme 49

Imidazo[1,2-*a*]pyridine derivative **151** could be obtained via the reaction of **149** with DMFDMA through the intermediate enamine derivative **150** [58] (Scheme 50).

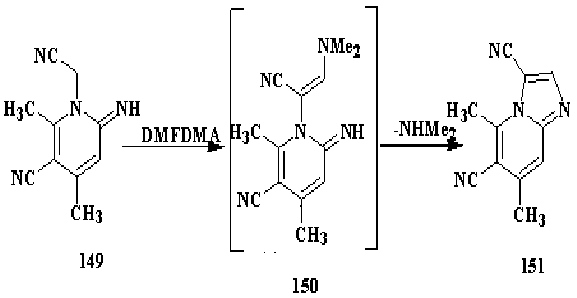

Scheme 50

Refluxing of compounds **152** with DMFDMA provided the enaminones **153**, which were directly allowed to react with bi-nucleophiles such as substituted guanidine and amino azoles (3-aminopyrazoles, 3-amino-1,2,4-triazole) to give the fused ring systems **154a,b** and **155a–d** respectively [59] (Scheme 51).

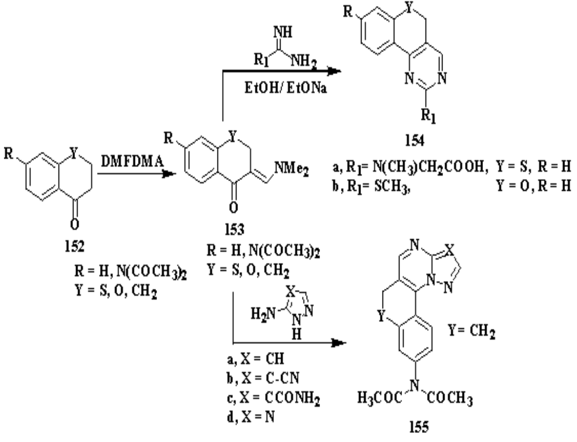

Scheme 51

The enaminone **3e** reacted with pyrazoles **156,** 1,2,4-triazole **157**, 2-aminobenzimidazole **158** and (1*H*-benzimidazol-2-yl)-acetonitrile **159** to produce pyrazolo[1,5-*a*]pyrimidines **160**, triazolo[1,5-*a*]pyrimidine **161**, the pyrimido[1,2-*a*]benzimidazole **162** and 1-methylbenzo[4,5]imidazo[1,2-*a*]pyridine-4-carbonitrile **163** respectively [23] (Scheme 52).

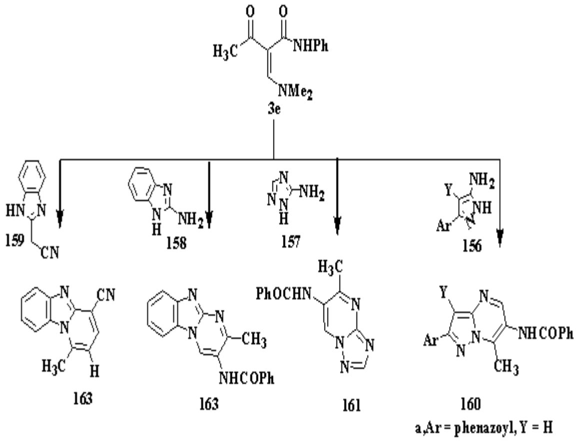

Scheme 52

Anthranilonitrile **164** is reported to react with malononitrile **1a**, ethyl cyanoacetate **1b**, cyanothioacetamide **1d**, β-ketoesters **165a,b**, arylidenes of cyanoacetohydrazide **1g** to afford the fused ring systems **166-171** respectively [60] (Scheme 53).

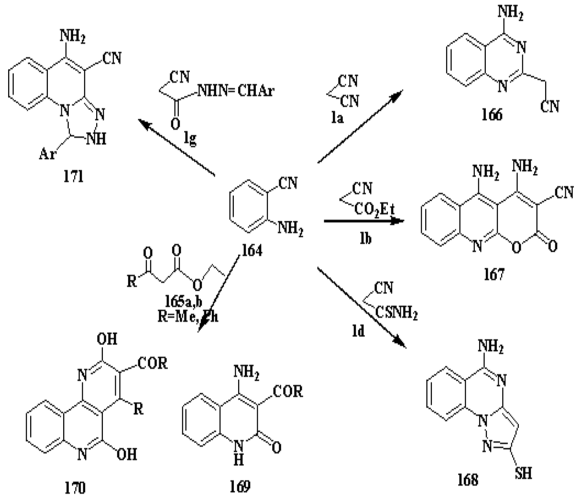

Scheme 53

2-Aminonicotinonitrile **172** is also reported to react similarly with the above mentioned reagents to afford the fused heterocyclic systems **173-178** respectively [61] (Scheme 54).

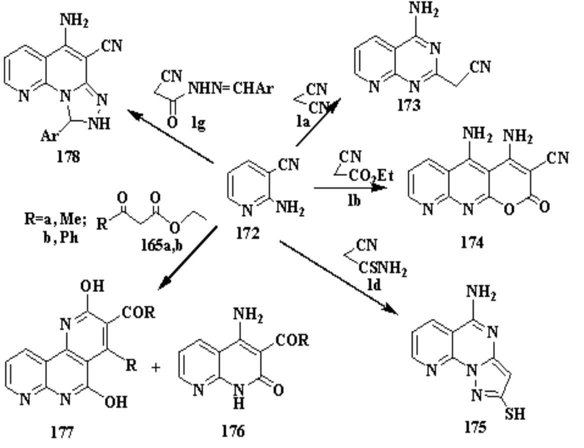

Scheme 54

References

[1] Freeman, F. *Chem. Rev.* **1969**, 69, 591.

[2] Katritzky, R.; Boulton, A. J. “Advances in Heterocyclic chemistry” Academic Press; New York **1976**.

[3] Freeman, F. *Chem. Rev.* **1980**, 80, 329.

[4] Freeman, F. *Synthesis* **1981**, 925.

[5] Meyers, I.; Sircard, J. C. “The chemistry of cyano group”., Ed. Rappoport, Z.; J. Wiley & Sons, London, New York, Chapter 1, **1970.**

[6] Fatiadi, J. *Synthesis* **1978**, 165.

[7] Fatiadi, J. *Synthesis* **1978**, 241.

[8] Freeman, F. Ed. “The Chemistry of malononitrile” California University press, Loss Angeles **1982.**

[9] Fatiadi, J. “Preparation and synthetic applications of cyano compounds, Chapter 26 in “Chemistryof cyano compounds” Supplement C to “The chemistry of functional groups” Ed. Patai, S. andRappoport, Z; J. Wiley & Sons, London, New York **1980**.

[10] Harada, H.; Watanuki, S.; Shin, S.; Hirano, Y. Jpn. Kokai Tokkyo Koho JP 2000 351,773 (Cl. C07D307/68), 19 Dec 2000, Appl. 1999/161,573, 8 Jun **1999**, 16 pp.(Japan).; *Chem. Abstr.*, 134, 29302w, **2001**.

[11] Abdelrazek, F. M.; Mohamed, A. M.; Elsayed, A. N. *Afinidad* **2008**, *65 (536)*, 322.

[12] Abdelrazek, F. M.; Michael, F. A.; El-Mahrouky, S. F. *International J. Phys. Sci*. **2007**, *2*, 212.

[13] Miyashita, Y. M.; Numata, A.; Higashino, T. *Chem. Pharm. Bull.* **1996**, *44 (2)*, 448.

[14] Abdallah, T. A.; Metwally, N. H.; Abdelrazek, F. M. *Afinidad* **2008**, *65*(*537)*, 393.

[15] Abdelrazek, F. M.; Ghozlan, S. A.; Michael, F. A. *J. Heterocycl. Chem.* **2007**, *44*, 63-67.

[16] Abdelrazek, F. M.; Metwally, N. H. *Synth. Commun.* **2006**, *36*, 83-89.

[17] Hilmy, K. M. *Arch. Pharm. Pharm. Med. Chem.* **2004**, *337*, 15.

[18] Abdelrazek, F. M.; Metwally, N. H. *Synth. Commun.* **2009**, *39*, 4088.

[19] Al-Omran, F.; Mohareb, R. M.; Abou El-Khair, A. *J. Heterocycl. Chem*. **2002**, *39*, 877.

[20] Laufer, S. A.; Wagner, G. K. *J. Med. Chem*. **2002**, *45*, 2733.

[21] (a) Kim, G. C.; Kim, M. H.; Park, Y. J.; Lee, H. S. *Repub. Korean Kongkae Taeho Kongbo KR* **2002**, *56*, 672.; (b) Kim, G. C.; Kim, M. H.; Park, Y. J.; Lee, H. S. *Chem. Abstr.* **2002**, *137*, 169544p.

[22] (a) Fraley, M. E.; Peckham, J. P.; Arrington, K. L.; Hoffman, W. F.; Hartman, G. D. US PCT IntAppl WO 03 11,837, **2003**; (b) Fraley, M. E.; Peckham, J. P.; Arrington, K. L.; Hoffman, W. F.;Hartman, G. D. *Chem. Abstr.* **2003**, *138*, 153548c.

[23] Abu Elmaati, T. A.; Said, S.; Elenein, N. A.; Sofan, M.; Khodeir, N. *Pol. J. Chem.* **2002**, *76*, 945.

[24] Stochley, M.; Clegg, W.; Fontana, G.; Golding, B. T.; Martin, N.; Rigoreau, L. J. M.; Smith, G.C. M.; Griffin, R. *J. Bioorg. Med. Chem. Lett.* **2001**, *11*, 2837.

[25] (a) Lambert, J. F.; Norris, T. US PCT *Int. Appl.* WO 02 44, 133, **2002**; (b) Lambert, J. F.; Norris, T. *Chem. Abstr.* **2002**, *137*, 20372y.

[26] Davies, G. M.; Jeffery, J. C.; Ward, M. D. *New J. Chem.* **2003**, *27*, 1550.

[27] Finke, P. E.; Meurer, L. C.; Debenham, J. S.; Toupence, R. B.; Walsh, T. F. US PCT *Int. Appl.*WO 03 82,191 **2003**; *Chem. Abstr.* **2003**, *139*, 307686f. [27] (a) Merck Patent G.m.b.H. GerOffen DE **10**, 149, 370 (**2003**); (b) Merck Patent G.m.b.H; *Chem. Abstr.***2003**, *138*, 304276r.

[28] Al-Omran, F.; Al-Awadhi, N.; Abdelkhalik, M. M.; Kaul, K.; Abu El-Khair, A.; Elnagdi, M. H. *J. Chem. Res.* **1997,** *(S)*, 84, *(M)* 601.

[29] Abdelrazek, F. M.; Elsayed, A. N. *J. Heterocycl. Chem.* **2009**, *46*, 949.

[30] Al-Omran, F.; Abu El-Khair, A.; Elnagdi, M. H. *J. Chem. Res.* **1998**, *(S)*, 798.

[31] Abdelrazek, F. M.; Sharaf, M. F.; Metz, P.; Jaeger, A. *J. Heterocycl. Chem.* **2010**, *47*, 528.

[32] Abu Elmaati, T. M. *J. Heterocycl. Chem.* **2004**, *41*, 947.

[33] Abu Elmaati, T. M.; El-Taweel F. M. A. *J. Chin. Chem. Soc.* **2002**, *49*, 1045-1050.

[34] Abu-Shanab, F. A.; Redhouse, A. D.; Thompson, J. R.; Wakefield, B. J. *Synthesis* **1995**, 557.

[35] Abdelrazek, F. M.; Metwally, N. H.; Sobhy, N. A. *Afinidad* **2006**, *63 (522)*, 149.

[36] Abdelrazek, F. M.; Metwally, N. H. *Afinidad* **2003**, *60 (508)*, 554.

[37] Abdelrazek, F. M.; Michael, F. A. *Afinidad* **2006**, *63(524)*, 335.

[38] Abdelrazek, F. M.; Metwally, N. H.; Kassab, N. A.; Sobhy, N. A.; Metz, P.; Jaeger, A. *J. Heterocycl. Chem.* **2010**, *47*, 384.

[39] Abdelrazek, F. M.; Kassab, N. A.; Metwally, N. H.; Sobhy, N. A. *Eur. J. Chem.* **2010**, *1(4)*, 368.

[40] Abdelrazek, F. M.; El-Din, A. M. S.; Mekky, A. E. *Tetrahedron* **2001**, *57*, 1813.

[41] Abdelrazek, F. M.; El-Din, A. M. S.; Mekky, A. E. *Tetrahedron* **2001**, *57*, 6787.

[42] Laufer, S. A.; Wagner, G. K. *J. Med. Chem.* **2002**, *45*, 2733.

[43] Wang, S.; Meades, C.; Wood, G.; Osnowski, A.; Anderson, S.; Yuill, R.; Thomas, M.; Mezna, M.; Jackson, W.; Midgley, C.; Griffiths, G.; Fleming, I.; Green, S.; McNae, I.; Wu, S.; McInnes, C.; Zheleva, D.; Walkinshaw, M. D.;Fischer, P. M. *J. Med. Chem.* **2004**, *47*, 1662.

[44] Abdelrazek, F. M. *Synth. Commun.* **2005**, *35*, 2251.

[45] Abdelrazek, F. M.; Fadda, A. A.; El-Sayed, A. N. *Synth. Commun.* **2011**, *41*, 1119-1126.

[46] (a) Gellibert, F. J.; Hartley, C. D.; Mathews, N.; Woolven, J.M. GB PCT Int Appl WO 02 62,794, 2002; (b) Gellibert, F. J.; Hartley, C. D.; Mathews, N.; Woolven, J. M. Chem Abstr 2002,137, 169515e.

[47] Abdel-Megid, M.; Elnagdi, M. H.; Negm, A. M. *J. Heterocycl. Chem.* **2002**, *39*, 105.

[48] Raghuvanshi, D. S.; Singh, K. N. *J. Heterocycl. Chem.* **2011**, *48(3)*, 582-585.

[49] Abdelrazek, F. M.; Metz, P.; Farrag, E. K. *Arch. Pharm. Pharm. Med. Chem.* **2004**, *337*, 482.

[50] Abdelrazek, F. M.; Metwally, N. H.; Sobhy, N. A. *Afinidad* **2008**, *65(538)*, 482.

[51] Abdelrazek, F. M.; Metz, P.; Kataeva, O.; Jaeger, A.; El-Mahrouky, S. F. *Arch. Pharm. Chem. Life Sci.* **2007**, *340*, 543.

[52] Bennamane, N.; Kaoua, R.; Hammal, L.; Nedjar-Kolli, B. *Org. Commun*. **2008**, *1:3*, 62-68.

[53] Litchitsky, B. V.; Dudinov, A. A.; Krayushkin, M. M. *Arkivoc* **2001**, *ix*, 73-79.

[54] Krauze, A.; Vilums, M.; Sile, L.; Duburs, G. *Chem. Heterocyclic Compds*. **2007**, *43 (5)*, 653-675.

[55] Abdelrazek, F. M.; Metwally, N. H.; Sobhy, N. A. *Afinidad* **2005**, *62 (520)*, 616.

[56] Al-Omran, F.; Mohareb, R. M.; Abou El-Khair A. *J. Heterocycl. Chem.* **2002**, *39*, 877.

[57] Al-Omran, F.; Abd El-Hay, O. Y.; Abou El-Khair A. *J. Heterocycl. Chem.* **2000**, *37*, 1617.

[58] Mustazza, C.; Del Giudice, M. R.; Borioni, A.; Gatta, F. *J. Heterocycl. Chem.* **2001**, *38*, 1119.

[59] Yermolayev, S. A.; Gorobets, N. Yu.; Lukinova, E. V.; Shishkin, O. V.; Shishkina, S. V.; Desenko, S. M. *Tetrahedron* **2008**, *64*, 4649.

[60] Metwally, N. H.; Abdelrazek, F. M. *Synth. Commun.* **2005**, *35*, 2481-2487.

[61] Abdelrazek, F. M.; Michael, F. A. *Afinidad* **2006**, *63(523)*, 229.

JJEES

Jordan Journal of Earth and Environmental Sciences

Volume 4 (Special Publication, Number 2), Jan. 2012
ISSN 1995-6681
Pages 63- 66

Characterization and Possible Industrial Applications of Tripoli Outcrops at Al-Karak Province.

Tayel El-Hasan[a],Husam Al-Hamaideh[b]

[a]*Department of Geology, Faculty of Science, Taibah University, Al-Madinah Al-Munawarah; KSA.*

[b]*Faculty of Engineering, Civil Engineering Department, King Abdel-Aziz University, Jeddah, KSA.*

Abstract

Tripoli layers outcropping at the old village of Aynun, 10 km south of Al-Karak city is embedded within Wadi Um Ghudran Formation of lower Cretaceous age. The area has the richest deposits in Al-Karak province and is minable because of the uninhibited possible mining sites and low overburden thickness.

Tripoli layers varied in thickness from 3-12m.It is composed mainly of high SiO_2 (up to 93 wt%). Quartz is the essential component. The physical properties of tripoli (bulk density, specific gravity, water adsorption and size distribution) are suitable for its use as a filler and filter. The whiteness (82%) makes tripoli suitable for us in manufacturing external paint.

The effect of partial replacement of the components of ordinary Portland cement by tripoli on the compressive strength, setting time, soundness and normal consistency has decreased the compressive strength. Replacement of cement by tripoli in mass ratios of 10%, 20%, and 30% has decreased the 28-days compressive strength of mortar cubes by 6.2%, 14.7%, and 32.1% respectively. The volume of mix water required to produce a paste of normal consistency has increased with increasing the ratio of tripoli in the paste. The increasing ratio of tripoli in the paste did not affect the setting time nor the soundness of the paste.

Keywords: Tripoli;Al-Karak;Cement Paste; Compressive Strength; Soundness.

1. Introduction

The government of Jordan is encouraging the foreign investment in the sector of mining and natural products industry, because it is the type of investment that can generates large number of employments and increases the country export yields. Within this frame The main concern of this study is to investigate tripoli as a natural raw materials for possible use in various industries.

Tripoli is a soft, very fine grained, earthy material that is nearly pure silica. It is known in trade market as (soft silica) (Wileborn, 1994). The annual World production is about 30 million tons, 30-50% is used as an abrasive (Kogel et al., 2006). The largest deposits in the world are in USA at Missouri, Oklahoma and Illinois (Gensen & Bateman, 1981). Tripoli is also found in Europe such as France, Germany, and UK. Tripoli in Jordan is crypto-crystalline silica; white, very fine, soft powdery form, light-friable (Khoury, 2006). It is found as permeable and highly porous beds with some chert nodules (El-Hasan & Al-Hamaidah, 2011). Jeresat & Bashir, (1972), studied the tripoli occurrences in Madaba and Tafila. Al-Omari (1975), described the Tripoli deposits in El-Shahabiyah and Aynun at Al-Karak area. He found the SiO_2 content is more than 92%. Khoury (1986) analyzed samples from Al-Karak and Amman and reported the presence of amorphous silica phase. The adsorption capacities of Tripoli in removing heavy metal from aqueous solutions were studied by (Al-Omari, 2003; El-Hasan et al., 2009, and Al-Ghezawi et al., 2010). Khoury (1987) discussed the origin of Tripoli and concluded that tripolization of chert is another process associated with tripolization of limestone. Khoury (1990), explains the nomenclature overlap between tripoli and porcelanite, and concluded that tripoli is different from porcelanite in composition and texture. Alden, 2011 has mentioned that tripoli is high purity silica (SiO_2) that readily breaks and is easily reduced to fine powder. He the origin of tripoli as a result of leaching of calcium carbonate from the Upper Division of the Arkansas Novaculite leaving residual re-crystalline silica. Triploi is classified in the USA under the the natural abrasives sector based on a hardness less than 5.5 (Wileborn, 1994).

Tripoli outcrops at Al-Karak province bears economic quantities (Khoury, 2006, El-Hasan and Al-hamaideh, 2011). Tripoli reserves in central Jordan were estimated 1 million m^3 in the sheet area of Al-Karak alone (Technostone, 1983). However, they found that exploitation was not economic due to higher production cost comparing with revenues at that time. While according to (Kogel et al., 2006), the USA is the world number one in tripoli production of 68,800 ton/year this figures were in the year (2003), at an average price equal to 257$/tone. Therefore, under this World prices Al-Karak tripoli seems to be much feasible.

The following work aims to carry out geochemical and mineralogical characterization of the tripoli in at Aynun area. Tripoli was added as a cement paste replacing agent. The concrete was tested for engineering properties such as compressive strength, soundness, consistency, soundness and setting time.

2. Study Area Settings:

The investigated area of Aynun is located 10 km to south-southwest of Al-Karak city (Fig. 1). The geological map of Al-Karak area (map sheet No. 3152 III) indicates four main sites of tripoli deposits; El-Shahabiyah, Aynun, Rakeen and Tafilah road (Wadi Falqa) (Powell, 1987),. Aynun area was chosen as potential production area because it has higher outcropped thicknesses, lower overburden and relatively uninhibited areas.. The investigated site belongs to the upper Cretaceous Period and namely Wadi Ghudran Formation (WG) (Coniacian age) and Amman Silicified Limestone (ASL) of Coniacian – Santonaian age.

The detailed lithology of WG formation shows that it is composed of sequence of white-buff chalk; its thickness reaches up to 84m and composed of chalk, dolomitic and phosphatic siliceous sandstone, grey chert, chalky-laminated tripoli, and chalk with thin chert beds. The thickness of ASL Formation is 80 m and is composed of thick auto-brecciated chert, inter-bedded with phosphatic limestone, coquina limestone and phosphatic chert (Powell, 1987).

Tripoli outcrops (12 m thick) are bedded, finely laminated soft deposits with relicts or nodules of pale chert (Fig. 2). The soft tripoli spreads laterally and become bedded chert within few hundred meters. It is most likely to be of late diagenetic origin resulted after the alteration of chert with high proportion of carbonate, which might be due to slightly acidic groundwater flow (Khoury, 2006 and Alden, 2011).

3. Materials, Analyses and Experimental Design

Tripoli rock samples were collected from Aynun area and were analyzed geochemically using XRF instrument model (S4 Pioneer / Minibruker) at the Natural Resources Authority (NRA). The physical properties of tripoli were tested for size distribution, density, , specific gravity, water and oil absorption capacity Whiteness test was done using the instrument (Pincher PN-488) available at the NRA.

The mineralogical investigation was done to three tripoli samples from Aynun area by using XRD instrument model (XPERT MPD) available at the NRA.

The Ordinary Portland Cement (OPC= obtained from the Jordan cement industry company of Lafarge) was used. The cement is classified as CEM-1 42.50 N according to the specification of the European Committee for Standardization (CEN).

Sand filler used in the experiments is the same that is used for testing in Jordan cement industry. It is a natural sand standard, consisting of rounded particles and with silica content not less than 98%. The sand particle size distribution limits are defined according to the British Standards. The sand sample was delivered in plastics bags weight of (1350±5) grams. Tap water was used.

4. Experimental set up and procedure:

Cement paste was partially replaced by tripoli in three mixture ratios of 10, 20, and 30% by weight. Mortar cubes were made and their compressive strength and other parameters were determined with setting time of 2 and 28 days. OPC mortar cubes were made as reference samples. Each mortar mix was prepared from 1350 grams of standard sand and 450 grams of binder (cement and tripoli) as shown in Table (3). The mortar was mixed for 4 minutes in a laboratory ELE mixer. The weight ratios of (water: binder: sand) were (0.5: 1: 3) were kept constant for all samples. A total number of twelve mortar cubes, three cubes from each binder mixture were tested at each setting time to study the effect of tripoli addition and curing time on compressive strength and other parameters. The compressive strength of the mortar cubes was measured using ELE testing machine. The recorded value is the average of three values for each age. Before determining the setting time of the binders, the normal consistency for each binder paste was determined. Twelve binder paste samples (three samples from each mixture) were tested for setting time using vicat apparatus.

5. Results and Discussion

The results have indicated that the tripoli of Aynun has a very high SiO_2 % content which is above 92 wt%, with Al_2O_3, Fe_2O_3 and TiO_2 impurities. Moreover, the average CaO% is 2.57wt% (Table 1). The physical properties results have indicated that the bulk density of tripoli equals to 0.6 g/cm^3, the specific gravity equals 2.3-2.5, the water absorption capacity 48% - 61% and the oil absorption medium was good (30%), which makes it suitable to be used as a filler and filter.

Table 1. XRF analytical results for selected tripoli samples from Aynun area. (all are in weight %)

	Aynun-1	Aynun-1	Aynun-1	Max	Min	Mean
SiO_2	92.79	92.88	92.88	92.88	92.79	92.84
Al_2O_3	1.04	0.94	0.93	1.04	0.93	0.98
Fe_2O_3	0.06	0.08	0.10	0.06	0.10	0.08
TiO_2	0.006	0.006	0.006	0.006	0.006	0.006
Na_2O	0.21	0.23	0.25	0.25	0.23	0.24
K_2O	0.48	0.47	0.48	0.48	0.47	0.48
MgO	0.40	0.37	0.40	0.40	0.37	0.39
CaO	2.61	2.52	2.57	2.61	2.52	2.57
MnO	0.001	0.001	0.001	0.001	0.001	0.001
P_2O_5	0.06	0.06	0.06	0.06	0.06	0.06
LOI	2.38	2.42	2.40	2.43	2.38	2.41

The sieve analysis shows that the lower than 0.074 mm size fraction is 98.2%, the less than 0.01 mm is 76.1%. The size distribution makes tripoli suitable as abrasive material, ceramic and paint industries.

Tripoli of Aynun is not very white Table (2), but it has relatively high whiteness degree with an average of 81.77%, The high whiteness degree makes tripoli powder suitable for paint manufacturing, The higher bulk density makes it also suitable for the outdoor paints because of its high resistant to weathering. The XRD results have indicated that tripoli is composed of quartz as shown in (Fig. 3).

Table 2. Whiteness analysis for a selected tripoli samples from Aynun area.

Sample Name	Whiteness %
Aynun-Tripoli-1	82.6
Aynun-Tripoli-2	81.3
Aynun-Trpoli-3	81.4

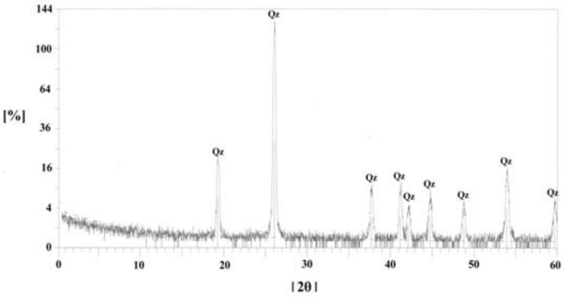

Fig. 3. XRD chart for a selected tripoli sample from Aynun study area.

The chemistry is quite different from OPC mainly in SiO_2, Al_2O_3 and CaO contents as shown in Table (4).

Table 4: Chemical composition of tripoli and Ordinary Portland Cement.

Component	SiO_2	Al_2O_3	Fe_2O_3	CaO	MgO	K_2O	Na_2O
Cement	19.94	5.37	3.18	63.65	2.59	0.82	0.1
Tripoli	92.84	0.98	0.08	2.57	0.39	0.48	0.21

The addition of tripoli to the mixture will deviate its chemical composition from normal OPC. The estimated volume of water required to produce pastes of normal consistency for binders containing tripoli ratios of 10, 20, and 30% has increased by 2, 3.3, and 6.3 ml respectively compared with binders containing 0% tripoli (Fig. 4).

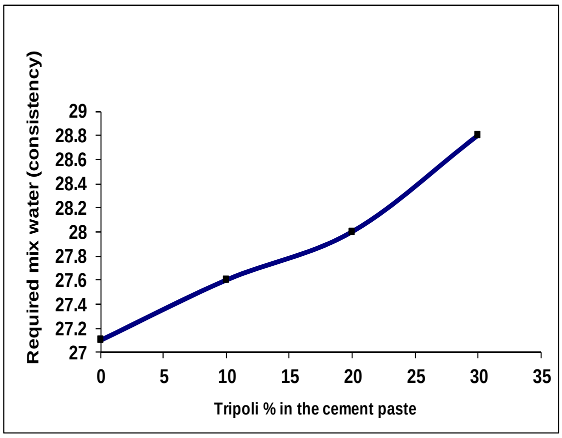

Fig. 4. The relation between tripoli % in cement paste and water consistency.

This is related to the presence of excessive quartz which is not soluble and not reactive as lime in the hydrated OPC. The effect of partial replacement of cement by tripoli on the compressive strength of the concrete can be established by comparing the measured values for a given curing time and ratios as indicated in (Fig. 5).

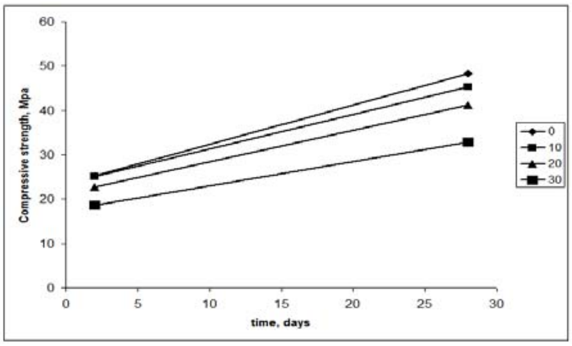

Fig. (5): Effect of replacing cement by tripoli on the compressive strength of mortar cubes

One can observe that the compressive strength increases with increasing curing time and decreases with increasing tripoli mix ratio. The increase of compressive strength with time is due to the continuous hydration reactions of cement. The addition of tripoli increases the silica content at the expense of lime which is responsible for the cementing and strength properties (Table 5).

Table 5: Chemical composition of binder containing different ratios of tripoli

TRIPOLI % In Cement paste	Components						
	SiO_2	Al_2O_3	Fe_2O_3	CaO	MgO	K_2O	Na_2O
0	19.94	5.37	3.18	63.65	2.59	0.82	0.10
10	27.23	4.93	2.87	57.54	2.37	0.79	0.11
20	34.52	4.49	2.56	51.43	2.15	0.75	0.12
30	41.81	4.05	2.25	45.33	1.93	0.72	0.13

Therefore, the replacement of cement by tripoli in mass ratios of 10, 20, and 30% has decreased the 28-days compressive strength of the concrete cubes by 6.2, 14.7, and 32.1% respectively. These results are in good agreement with previous results for oil shale ash replacing the OPC obtained by (Al-Hamaiedeh et al., 2010), where the compressive strength has decreased by 7.4, 11.7, and 23% due to replacement of cement by oil shale ash in ratios of 10, 20, and 30% respectively.

The reduction in the compressive strength caused by the addition of tripoli decreases with setting time. The compressive strength gaining of concrete with tripoli is slower than that of mortars without tripoli. The low development of compressive strength is probably related to the increase of silica content at the expense of lime. It is expected that an increase of compressive strength with tripoli might occur with longer curing time.

The presence of tripoli in the binder in ratios of 10, 20, and 30% did not increase the setting time (Fig. 6).

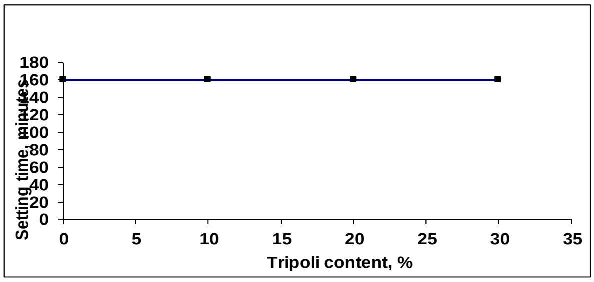

Fig. 6.The relationship between tripoli content in cement past and the setting time

This situation is related to the absence of reaction of water with tripoli in comparison lime. However, the increase of tripoli ratio decreases the amount of reactive CaO in binders (Table 5) that causes some negative effects on formation of calcium-silicate-hydrate (C-S-H). The Le Chatelier experiment was made to study the expansion of binder pastes (soundness) containing different ratios of tripoli. The results of the Le Chatelier experiment shows that the expansion of concrete containing tripoli was not significant and do not exceed the standard value of 10 mm stated by British Standards (BS, 1995) (Fig. 7).

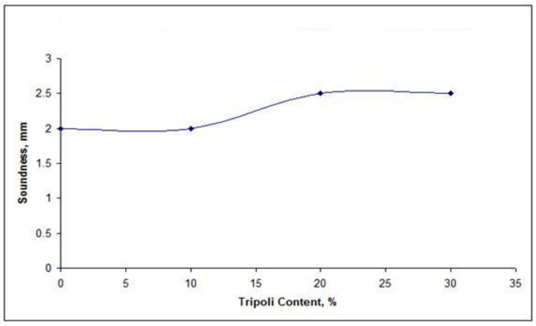

Fig. 7. The relationship between tripoli % in cement past and the soundness.

6. Conclusions

The results of the conducted experiments have indicated that the higher is the level of OPC replacement by tripoli, the lower is the compressive strength. The longer is the curing period, the higher is the compressive strength. Replacing cement by tripoli, did not affect the setting time of concrete. The increase of the tripoli cement ratio has slightly increased the soundness and did not exceed the allowable limits with tripoli content up to 30%. Therefore, the results of the conducted experiment proved the possibility of replacement of OPC by tripoli in ratios up to 20% without causing significant effects on the studied properties of cement. Comparing with oil shale ash, tripoli shows better compressive strength, setting time and good soundness, due to its lower sulfur content. The investigation showed that tripoli deposits at Al-Karak province and particularly Aynun area are feasible to undergo further mining and manufacturing for use as a filler and abrasive material due to its quantity, availability at surface (lower overburden), beside its preferable mineralogical and geochemical properties.

Acknowledgment:

The authors are deeply thankful for Jordan cement industry company (Lafarge) for their help in the analysis and experimental part.

References

[1] Alden, A. (2011): Abrasive minerals, http://geologz.about.com/bio/Andrew-Alden-453.html.

[2] AL-Ghezawi, N., Al-Anber, M., Al-Anber, Z., El-Hasan, T. And Al-Momani, I. (2010): Decontamination and adsorption modeling of aqueous Pb+2 and Co+2 ions using natural inorganic materials: Tripoli (NT) and Bentonite (NB), Desalination and Water Treatment 24 (2010) 336–343.

[3] Al-Hamaidh, H., Maaitah, O. and Mahadin, S. (2010): Using Oil Shale in Concrete Binder. EJGE, 15:601-608.

[4] Al-Omari, H. (2003): Study of the Adsorption of (Ni) and Cu(II) by Tripol, Mutah
Lil-Buhuth wad-Dirasat, Vol. 18, No. 1, 77-94.

[5] Al-Omari, K. (1975): The Triploi prospects of Ainun and El-Sh-habiyeh, NRA, Internal Report, Amman. Saadi , T.(1968): Tripoli, NRA, Internal report, Amman.

[6] El-Hasan, T., Al-Anbar, Z., Batarseh, M., Al-Naser, F., Al-Anbar, M, Ziadat, A.., Kato, Y. and Jiries, A (2009): Removal of Zn^{+2} Cu^{+2} and N^{+2} ions from aqueous solutions via Tripoli: Simple component with single phase model. Current World Environment. 3(1): 1-14.

[7] El-Hasan, T. & Al-Hamaidah, H. (2011): Occurrences, characteristics and possible industrial applications of Tripoli rock outcropping at Al-Karak province. 2nd International Conference In Materials On Jordan, Abstract Book, Page 62.

[8] Gensen, M.L. and Bateman, A.M. (1981): Economic Mineral deposits Network. John Wiley & Sons.

[9] Jeresat, K. & Bashir, S. (1972): The Tripoli occurrences between Madaba and Tafila, NRA, Internal Report, Amman.

[10] Khoury, H (1990): The discovery of diatomite in Jordan, Unpublished Report, University of Jordan (in Arabic).

[11] Khoury, H. (2006): Industrial rocks and minerals in Jordan, Publication of the University of Jordan (in Arabic).

[12] Khoury, H. (1987): Tripolization of chert in Jordan, Sediment. Geol. 53:305-310.

[13] Khoury, H. N., (1986): The origin of tripoli in Jordan. Sediment. Geol., 48, 223-235.

[14] Kogel, J. E., Trivedi, N.C., Barker, J. M. and Krukowski, S.T. (2006): Industrial Minerals and Rocks, commodities, markets and uses. 7th edition. SME, pp. 1570.

[15] Powell, J. (1987): The geology of the Karak map sheet area, NRA. Amman. Unpublished report.

[16] Technostone SpA, Carrara (MS) (1983): Project for the development of no-metallic minerals industry in Jordan – Italian Foreign Affairs Ministry Project.

[17] Wileborn, W.W., (1994): Abrasives. In: Industrial Minerals and Rocks, 6th Ed. Edited bz D.D. Carr Littleton, Co, SEM. 497-507.

المملكة الأردنية الهاشمية

الجامعة الهاشمية

المجلة الأردنية
لعلوم الأرض والبيئة

JJEES

مجلة علمية عالمية محكمة

العدد الخاص ٢

http:// jjees.hu.edu.jo/

ISSN 1995-6681

المجلة الأردنية لعلوم الأرض والبيئة

مجلة علمية عالمية محكمة

المجلة الأردنية لعلوم الأرض والبيئة : مجلة علمية عالمية محكمة أسستها اللجنة العليا للبحث العلمي في وزارة التعليم العالي والبحث العلمي، الأردن، وتصدر عن عمادة البحث العلمي والدراسات العليا، الجامعة الهاشمية، الزرقاء، الأردن.

ترسل البحوث إلى العنوان التالي:
رئيس تحرير المجلة الأردنية لعلوم الأرض والبيئة
عمادة البحث العلمي والدراسات العليا
الجامعة الهاشمية
الزرقاء ١٣١٣٣ - الأردن
فرعي: 4147 هاتف : 3903333 (5) 962+
Email: jjees@hu.edu.jo
Website: www.jjees.hu.edu.jo